Nickel complexes of 1,2,4-triazole derived amido-functionalized N-heterocyclic carbene ligands: Synthesis, theoretical studies and catalytic application

Anuj Kumar, Linus Paulin Bheeter, Manoj Kumar Gangwar, Jean-Baptiste Sortais, Christophe Darcel, Prasenjit Ghosh

Nickel Complexes of 1,2,4-Triazole Derived Amido-functionalized N-heterocyclic Carbene Ligands: Synthesis, Theoretical Studies and Catalytic Application

Anuj Kumar,[†] Linus Paulin Bheeter,[‡] Manoj Kumar Gangwar,[†] Jean-Baptiste Sortais,[‡] Christophe Darcel*,[‡] and Prasenjit Ghosh*,[†]

[†]Department of Chemistry

Indian Institute of Technology Bombay,

Powai, Mumbai 400 076.

[‡]Université de Rennes 1,

UMR CNRS-UR1 6226 Institut des Sciences chimiques de Rennes,

Team "Organometallics: Materials and Catalysis" - Centre for Catalysis and Green Chemistry

Campus de Beaulieu, 35042 – Rennes, France

Email: pghosh@chem.iitb.ac.in, christophe.darcel@univ-rennes1.fr,

Fax: +91 22 2572 3480, +33 2 23 23 69 39

Keywords: nickel; *N*-heterocyclic carbene; borylation; aryl bromide; DFT studies

Abstract: A series of nickel complexes (**1**−**3**)**b** of 1,2,4-triazole derived amido-functionalized *N*-heterocyclic carbene ligands were synthesized and structurally characterized. In particular, the [1-(R)-4-*N*-(furan-2-ylmethyl)acetamido-1,2,4-triazol-5-ylidene]$_2$Ni [R = Et (**1b**), *i*-Pr (**2b**) and Bn (**3b**)] complexes were obtained by the direct reaction of the corresponding triazolium chloride salts (**1**−**3**)**a** by the treatment with $NiCl_2$•$6H_2O$ in presence of K_2CO_3 as a base. The density functional theory studies performed on these complexes reveal highly polar character of the NHC−Ni σ-bonding interaction with corresponding molecular orbital having a maximum contribution (59−69 %) from the NHC ligand fragments while that of a minimum contribution (4 %) from the central nickel atom. The (**1**−**3**)**b** complexes were found to be moderately active for the catalytic borylation reactions of bromoaryl derivatives by *bis*(pinacolato)diboron reagent (B_2pin_2) in the presence of Cs_2CO_3 as a base at 70 °C.

Introduction

Recent increase in interest in nickel catalysis has led to the discovery of many interesting catalytic transformations and has thrown open exciting possibilities for this metal [1]. In comparison to its immediate congener, palladium, [2] that has seen phenomenal success in catalysis in recent times, nickel has surprisingly maintained a low profile all throughout. As a matter of fact, nickel, as a metal, is quite attractive for catalysis mainly for its high nucleophilicity that arise out of its small size as a 1st row transition metal, and for its several accessible oxidation states,[3] that make it flexible towards various catalytic cycles [4]. In addition to these favorable catalytic attributes, nickel is inexpensive and thus, as a whole, is ideally suited for catalysis.

One of our interests [5] lies on exploring the catalytic potential of nickel, and towards this goal, we intended to use the now popular *N*-heterocyclic carbene ligands that are widely recognized for their success in homogeneous catalysis [6]. In this context, we have recently observed the superiority of the nickel *N*-heterocyclic carbene complexes over their palladium analogs in the hydroamination reactions of the activated olefins [7]. We have also designed nickel *N*-heterocyclic carbene complexes for the bifunctional catalysis of the Michael addition reaction under base-free conditions by employing suitably tailored chelating amido-functionalized *N*-heterocyclic carbene ligands of the imidazole scaffold [8,9]. Meanwhile, some of us were also interested in the reactivity of half-sandwich *N*-heterocyclic carbene (NHC) nickel complexes in efficient and chemoselective catalytic hydrosilylation of aldehydes, ketones and imines under mild conditions [10].

Extending even further, we sought to explore the utility of the nickel complexes of the related amido-functionalized *N*-heterocyclic carbene ligands of the 1,2,4-triazole scaffold in various other catalytic transformations like in the catalytic borylation reactions of bromoaryl derivatives by *bis*(pinacolato)diboron. The borylation reaction [11] is important for providing convenient access to the high value intermediates of the day-to-day organic synthesis, mainly for the Suzuki-Miyaura Cross-Coupling reaction. In this context it is noteworthy that the nickel catalysts, despite being among the pioneering ones for the C−C cross coupling reaction, as observed from the early report of the Corriu-Kumada coupling with Grignard reagents [12], they remained less popular till date than their palladium counterparts in various C−C cross coupling reactions including the Suzuki-Miyaura reaction [13]. From this perspective, quite importantly, the recent reports of the nickel catalysis for the borylation reactions of the organohalide derivatives providing convenient access to the borylated synthons [14], would ignite interest on the metal. In addition to the nickel, our other interest in the 1,2,4-triazole based *N*-heterocyclic carbene ligands arises from the fact that these ligands are less explored as compared to their imidazole analogues [15,16].

Hence, in this contribution, we report a series of nickel complexes namely [1-(R)-4-*N*-(furan-2-ylmethyl)acetamido-1,2,4-triazol-5-ylidene]$_2$Ni [R = Et (**1b**), *i*-Pr (**2b**) and Bn (**3b**)] of the 1,2,4-triazole derived *N*-heterocyclic carbene ligands that show low to moderate activity in the catalytic borylation reactions of bromoaryl derivatives by bis(pinacolato)diboron.

Results and Discussions

A series of amido-functionalized *N*-heterocyclic carbene precursors namely, 1-(R)-4-*N*-(furan-2-ylmethyl)acetamido-1,2,4-triazolium chloride [R = Et (**1a**), *i*-Pr (**2a**), Bn (**3a**)] were synthesized from the respective 1-(R)-1,2,4-triazoles by the direct reaction of 2-chloro-*N*-(furan-2-ylmethyl)acetamide in 52−66 % yield (Scheme 1). The formation of the 1,2,4-triazolium chloride salts (**1**−**3**)**a** was very much evident from the appearances of the characteristic (NC*H*N) resonances at a highly downfield region at 10.8−10.2 ppm in the ^{1}H NMR spectrum and at 146.1−145.8 ppm in the ^{13}C{^{1}H} NMR spectrum and were further confirmed by High Resolution Mass Spectrometry (HRMS) studies that showed the $[NHC+H]^{+}$ peaks at *m/z* 235.1206 (**1a**), *m/z* 249.1356 (**2a**) and *m/z* 297.1350 (**3a**) against the corresponding calculated values of *m/z* 235.1195 (**1a**), *m/z* 249.1352 (**2a**) and *m/z* 297.1352 (**3a**).

The nickel complexes (**1**−**3**)**b** were then synthesized from the respective triazolium chloride salts (**1**−**3**)**a** by the treatment with $NiCl_2$•$6H_2O$ in CH_3CN in presence of K_2CO_3 (4.4 equiv.) as a base (Scheme 1 and Figure 1). The diamagnetic nature of the (**1**−**3**)**b** complexes indicated a square planar geometry at the metal center in these complexes. The ^{1}H NMR spectrum showed the absence of the NC*H*N and amido-N*H* resonances, consistent with the formation of a carbene center on the triazolium ring along with the chelation of the anionic amido-functionalized side arm to the metal center in these complexes. Quite interestingly, the two methylene moieties of the (**1**−**2**)**b** complexes were diastereotopic in nature and exhibited four sets of resonances for the **1b** and the **2b** complexes while displaying a $^{2}J_{HH}$ coupling constant of 15 Hz. In contrast, all of the three methylene groups of the **3b** complex were also

diastereotopic in nature displaying six sets of resonances while exhibiting a $^{2}J_{HH}$ coupling constant of 15 Hz in the ^{1}H NMR spectrum. Lastly, the characteristic Ni−$C_{carbene}$ resonance appeared at 171.6−171.0 ppm region in $^{13}C\{^{1}H\}$ NMR spectrum of the (**1**−**3**)**b** complexes.

The single crystals of (**1-3**)**b** were duly obtained from an acetonitrile solution for the X-ray single crystal diffraction analysis. The molecular structure of the (**1**−**3**)**b** complexes determined by the X-ray diffraction studies showed the metal center in a square-planar geometry (Figure 2−4 and Table 1). The nickel in the (**1**−**3**)**b** complexes is linked to two chelated *N*-heterocyclic carbene ligands, which were arranged in a *cis*-disposition to each other and were bound to the metal center through the carbene-C and an amido-N atoms. The Ni−$C_{carbene}$ bond distances in the **1b** [1.860(3) Å and 1.859(3) Å], **2b** [1.853(2) Å and 1.853(2) Å] and **3b** [1.871(4) Å and 1.871(4) Å] complexes compare well with the average *d*(Ni−$C_{carbene}$) distance [1.864 Å] observed for the related structurally characterized nickel(II) complexes of chelated amido-functionalized *N*-heterocyclic carbene ligands that are present in the Cambridge Structural Database [17]. Similarly, the Ni−N_{amido} bond distances in **1b** [1.9230(2) Å and 1.9220(2) Å], **2b** [1.9260(18) Å and 1.9211(18) Å] and **3b** [1.927(3) Å and 1.931(3) Å] are also comparable to the average *d*(Ni−N_{amido}) [1.932 Å] observed for the related structurally characterized complexes in the Cambridge Structural Database [17].

Further, insights into the electronic structures of these (**1**−**3**)**b** complexes were obtained with the aid of the density functional theory (DFT) study. Specifically, the geometry optimized structures were computed for the (**1**−**3**)**b** complexes at the

B3LYP/LANL2DZ, 6-31G(d) level of theory by using the atomic coordinates obtained from the X-ray diffraction studies (Supporting Information Figure S34−S36 and Table S7−S9). The computed structures are in good agreement with the experimental ones (Supporting Information Table S10−S12). Subsequently, the single-point calculations along with the post-wave function analysis using the natural bond order (NBO) method were performed on the geometry optimized structures at the same level of theory for a detailed understanding of the electronic properties of these complexes.

Corroborating the view of a strong electron-donation from the anionic amido-functionalized *N*-heterocyclic carbene (NHC) ligands to the metal center in the (**1**−**3**)**b** complexes, the natural and the Mulliken charge analyses indeed showed significant increase in the electron density at the nickel center in the (**1**−**3**)**b** complexes relative to that of the free Ni^{2+} ion (Supporting Information Table S1−S3). Along the same line, a scrutiny of the electronic configuration of the metal center in the (**1**−**3**)**b** complexes further revealed that the electron donation from the carbene lone pair occurred onto the *3d* and *4s* orbitals of the nickel center (Supporting Information Table S4).

Of particular interest are the Ni−$C_{carbene}$ bonding interaction in the (**1**−**3**)**b** complexes. The NBO analysis showed that the Ni−$C_{carbene}$ bonds in the (**1**−**3**)**b** complexes comprised of an interaction between a sp^2 hybridized $C_{carbene}$ orbital with a dsp^2 hybridized Ni orbital, and this is in agreement with the square-planar geometry of the central metal atom (Supporting Information Table S5). Additional understanding of the Ni−$C_{carbene}$ interaction were obtained by the Charge Decomposition Analysis (CDA) that estimated the NHC ligand to the nickel σ−donation, as denoted by *d*, and

the nickel to the NHC ligand π−back-donation, as denoted by *b*, occurring in these (**1**−**3**)**b** complexes. As expected of the anionic amido-functionalized *N*-heterocyclic carbene ligands in the (**1**−**3**)**b** complexes to be strongly σ-donating, very high *d/b* ratio of 10.95 (**1b**), 11.30 (**2b**), and 11.25 (**3b**) were observed in these complexes (Supporting Information Table S6). It is worth noting that the forward σ-donation (*d*) and the backward π- donation (*b*) values of the (**1**−**3**)**b** complexes represent the interactions between the metal center and the two amido functionalized NHC-ligand fragments, and which individually is composed of two interactions namely, a $C_{carbene}$–Ni interaction and a N_{amido}–Ni interaction.

The molecular orbital (MO) correlation diagrams were constructed for the (**1**−**3**)**b** complexes from the interaction of the individual fragment molecular orbitals (FMOs) of the free NHC ligand fragments with that of the free Ni^{2+} ion. The molecular orbital (MO) representing the NHC−Ni σ-interactions in the (**1**−**3**)**b** complexes *i.e.* the HOMO-36 (**1b**), HOMO-43 (**2b**) and the HOMO-42 (**3b**) is formed from the interaction between the carbene lone pairs of the two NHC ligand fragments with the 4*s* atomic orbital of the Ni^{2+} ion (Figure 5 and Supporting Information Figure S37 and S38). The NHC−Ni σ-bonding molecular orbital in the (**1**−**3**)**b** complexes are primarily ligand based exhibiting significant contribution [69 % (**1b**), 69 % (**2b**) and 59 % (**3b**)] from the two NHC ligand fragments and marginal contribution [4 % (**1b**), 4 % (**2b**) and 4 % (**3b**)] from the central nickel atom and this point towards a substantial ionic character of the NHC−Ni σ-interaction. Additionally, these NHC−Ni σ-bonding molecular orbitals namely, the HOMO-36 (**1b**), HOMO-43 (**2b**) and the HOMO-42 (**3b**) were all found to be deeply buried thereby suggesting highly stable nature of these Ni−NHC σ-interactions and further indicating that these

Ni−NHC σ-bonds in the (**1**−**3**)**b** complexes are less susceptible to the attacks by incoming nucleophiles and electrophiles.

The recent interest on nickel as catalysts in borylation of halogeno derivatives leading to the corresponding borylated compounds useful in Suzuki-Miyaura cross-coupling reactions prompted us to examine (**1**−**3**)**b** as potential catalysts for the coupling of bis(pinacolato)diboron with aryl bromides. In particular, in the presence of the 3 equiv. of Cs_2CO_3, the nickel complexes (**1**−**3**)**b** catalyzed the reaction between the *bis*(pinacolato)diboron reagent (B_2pin_2) (1.5 equiv.) with the 1 equiv. of arylbromide substrates exhibiting moderate conversions (61−90 %) and yielding the corresponding borylated compounds in 13 % , 10 % and 8 %, respectively along with the dehalogenated arenes (Table 2, entries 1−3). It must be noticed that except the formation of the borylated derivatives, and the unreacted starting reagents, only dehalogenated arenes were obtained as side products. The formation of the reduced arene derivatives can be explained by the oxidative addition of the haloarene leading to an Ni(Ar)(X) intermediate which was then hydrolyzed.

Subsequently, the most active catalyst, **1b**, was used in the borylation reactions of various other arylbromide substrates. (Table 2, Entries 4−9) The *ortho*- and the *meta*-tolylbromide displayed 88 % and 91 % conversions respectively along with low amount of borylated tolyl derivatives of 12 % and 14 % respectively (Table 2, Entries 4 and 5). However, with the *p*-anisylbromide and *p-tert*-butylphenylbromide substrates, the better yields (20 % and 18%, respectively) were observed at 73 % and 71 % conversions (Table 2, Entries 6 and 7). Notably, the electron-donating substituted aryl bromide substrates seem to be more reactive than the phenylbromide

substrate (83% conv., 10% yield, entry 8). For the 2-naphtylbromide substrate, the formation of the 20% of the corresponding borylated arene was observed (Table 2, entry 9).

Conclusion

In summary, a series of nickel complexes (**1**−**3**)**b** of the chelating anionic amido-functionalized N-heterocyclic carbene ligands have been synthesized and structurally characterized. The density functional theory studies performed on the (**1**−**3**)**b** complexes point toward highly stable NHC−Ni interactions that are predominantly σ-bonding in nature. The (**1**−**3**)**b** complexes were found to be moderately active for the catalytic borylation reactions of bromoaryl derivatives by the *bis*(pinacolato)diboron reagent (B_2pin_2) in the presence of Cs_2CO_3 as a stoichiometric base at 70 °C, mainly due to a competitive dehalogenation reaction.

Experimental Section

General Procedures. All manipulations were carried out using a combination of a glovebox and standard Schlenk techniques. $NiCl_2 \bullet 6H_2O$ was purchased from SD-fine Chemicals (India) and used without any further purification. 1-(ethyl)-1,2,4-triazole [18], 1-(*i*-propyl)-1,2,4-triazole [19], 1-(benzyl)-1,2,4-triazole [20] and 2-chloro-N-(furan-2-ylmethyl)acetamide[21] were synthesized according to modified literature procedures. ^{1}H and $^{13}C\{^{1}H\}$ NMR spectra were recorded on a Bruker 400 MHz NMR spectrometer. ^{1}H NMR peaks are labeled as singlet (s), doublet (d), triplet (t), quartet (q), quartet of doublets (qd), doublet of doublets (dd) septet (sept) and broad (br). Infrared spectra were recorded on a Perkin Elmer Spectrum One FT-IR spectrometer. Mass spectrometry measurements were done on a Micromass Q-Tof spectrometer and Bruker maxis impact spectrometer. Elemental Analysis was carried out on Thermo Finnigan FLASH EA 1112 SERIES (CHNS) Elemental Analyzer. X-ray diffraction data for compounds **1b**, **2b** and **3b** were collected on an Oxford Diffraction XCALIBUR-S diffractometer and Rigaku Hg 724+ diffractometer. Crystal data collection and refinement parameters are summarized in Table 1. The structures were solved using direct method and standard difference map techniques, and refined by full-matrix least-squares procedures on F^2. CCDC-855783 (for **1b**), CCDC-844351 (for **2b**) and CCDC-1003751 (for **3b**) contain the supplementary crystallographic data for this paper. These data can be obtained free of charge from the Cambridge Crystallographic Data center via www.ccdc.cam.ac.uk/data_request/cif.

Synthesis of 1-(ethyl)-4-N-(furan-2-ylmethyl)acetamido-1,2,4-triazolium chloride (1a)

A mixture of ethyl triazole (1.25 g, 12.9 mmol) and 2-chloro-N-(furan-2-ylmethyl)acetamide (2.21 g, 12.8 mmol) was refluxed in toluene (*ca*. 40 mL) for 16 hours during which a black viscous precipitate was formed. After decanting off the solvent, the precipitate was washed with hot petroleum ether (*ca*. 3 × 10 mL) and then dissolved in minimum amount of dichloromethane (*ca.* 4 mL). The product was precipitated out by addition of diethyl ether (*ca.* 15 mL). The product was isolated by decantation and was vacuum dried to give the product (**1a**) as a hygroscopic black solid (2.29 g, 66 %). ^{1}H NMR ($CDCl_3$, 400 MHz, 25 °C): δ 10.8 (s, 1H, N-C(5)*H*-N), 9.40 (br, 1H, N*H*CO), 9.39 (s, 1H, N-C(3)*H*-N), 7.28 (br, 1H, C_4H_3O), 6.26 (br, 1H, C_4H_3O), 6.23 (br, 1H, C_4H_3O), 5.54 (s, 2H, CH_2), 4.45 (q, 2H, $^{3}J_{HH}$ = 7 Hz, CH_2CH_3), 4.37 (d, 2H, $^{3}J_{HH}$ = 5 Hz, CH_2NH), 1.57 (t, 3H, $^{3}J_{HH}$ = 7 Hz, CH_2CH_3). $^{13}C\{^{1}H\}$ NMR (DMSO-d_6, 100 MHz, 25 °C): δ 164.5 (*C*=O), 151.4 (C_4H_3O), 145.8 (N-*C*(5)-N), 143.2 (N-*C*(3)-N), 142.7 (C_4H_3O), 110.9 (C_4H_3O), 107.9 (C_4H_3O), 49.0 (CH_2), 47.5 (CH_2CH_3), 36.1 (CH_2), 13.9 (CH_2CH_3). IR data (KBr pellet) cm^{-1}: 1686 (s) ($\nu_{c=o}$). HRMS (ES): *m/z* 235.1206 $[NHC+H]^{+}$, calcd. 235.1195. Anal. Calcd. for $C_{11}H_{15}N_4O_2Cl•H_2O$: C, 45.76; H, 5.93; N, 19.40. Found: C, 46.58; H, 6.13; N, 19.42 %.

Synthesis of [1-(ethyl)-4-N-(furan-2-ylmethyl)acetamido-1,2,4-triazol-5-ylidene]$_2$Ni (1b)

A mixture of 1-ethyl-4-N-(furan-2-ylmethyl)acetamido-1,2,4-triazolium chloride (**1a**) (0.640 g, 2.37 mmol), K_2CO_3 (1.64 g, 11.8 mmol) and $NiCl_2•6H_2O$ (0.280 g, 1.18 mmol) was refluxed in acetonitrile (*ca.* 40 mL) for 24 hours. The reaction mixture

was filtered and filtrate was reduced in vaccum up to 10 mL. The filtrate was kept at room temperature for overnight, during which yellow crystals were formed. Finally, the crystals were separated by filtration and vacuum dried to give the product (**1b**) as a yellow crystalline solid (0.135 g, 22 %). ^{1}H NMR ($CDCl_3$, 400 MHz, 25 °C): δ 8.02 (s, 2H, N-C(3)*H*-N), 7.31 (dd, 2H, $^{3}J_{HH}$ = 2 Hz, $^{4}J_{HH}$ = 1 Hz, C_4H_3O), 6.34 (dd, 2H, $^{3}J_{HH}$ = 3 Hz, $^{3}J_{HH}$ = 3 Hz, C_4H_3O), 6.12 (d, 2H, $^{3}J_{HH}$ = 3 Hz, C_4H_3O), 5.13 (d, 2H, $^{2}J_{HH}$ = 15 Hz, CH_2), 4.84 (d, 2H, $^{2}J_{HH}$ = 15 Hz, CH_2), 4.50 (d, 2H, $^{2}J_{HH}$ = 15 Hz, CH_2), 3.61 (d, 2H, $^{2}J_{HH}$ = 15 Hz, CH_2), 3.54 (qd, 2H, $^{3}J_{HH}$ =7 Hz, CH_2CH_3), 3.16 (qd, 2H, $^{3}J_{HH}$ = 7 Hz, CH_2CH_3), 1.23 (t, 6H, $^{3}J_{HH}$ =7 Hz, CH_2CH_3). $^{13}C\{^{1}H\}$ NMR ($CDCl_3$, 100 MHz, 25 °C): δ 171.0 (Ni-N*C*N), 168.3 (*C*=O), 156.6 (C_4H_3O), 142.4 (N-*C*(3)-N), 141.1 (C_4H_3O), 110.9 (C_4H_3O), 106.3 (C_4H_3O), 54.3 (CH_2), 46.9 (CH_2CH_3), 41.8 (CH_2), 15.1 (CH_2CH_3). IR data (KBr pellet) cm^{-1}: 1590 (s) ($\nu_{c=o}$). HRMS (ES): *m/z* 525.1506 $[M+H]^+$, calcd. 525.1503. Anal. Calcd. for $C_{22}H_{26}NiN_8O_4\bullet H_2O$: C, 48.64; H, 5.20; N, 20.63. Found: C, 48.42; H, 5.45; N, 20.30 %.

Synthesis of 1-(*i*-propyl)-4-N-(furan-2-ylmethyl)acetamido-1,2,4-triazolium chloride (2a)

A mixture of *i*-propyl triazole (1.96 g, 17.7 mmol) and 2-chloro-N-(furan-2-ylmethyl)acetamide (3.06 g, 17.6 mmol) was refluxed in toluene (*ca*. 30 mL) for 14 hours during which a black viscous precipitate was formed. After decanting off the solvent, the precipitate was washed with hot petroleum ether (3 × 10 mL) and then dissolved in minimum amount of dichloromethane (*ca.* 3 mL). The product was precipitated out by addition of diethyl ether (*ca.* 15 mL). The product was isolated by decantation and was vacuum dried to give the product (**2a**) as a hygroscopic black

solid (2.65 g, 53 %). ^{1}H NMR (DMSO-d_6, 400 MHz, 25 °C): δ 10.2 (s, 1H, N-C(5)$\underline{H}$-N), 9.14 (s, 1H, N-C(3)$\underline{H}$-N), 9.09 (br, 1H, N$\underline{H}$CO), 7.58 (br, 1H, $C_4\underline{H}_3O$), 6.40 (dd, 1H, $^{3}J_{HH}$ = 3 Hz, $^{3}J_{HH}$ = 3 Hz, $C_4\underline{H}_3O$), 6.31 (d, 1H, $^{3}J_{HH}$ = 3 Hz, $C_4\underline{H}_3O$), 5.11 (s, 2H, C$\underline{H}_2$), 4.86 (sept, 1H, $^{3}J_{HH}$ = 7 Hz, C$\underline{H}$(CH$_3$)$_2$), 4.34 (d, 2H, $^{3}J_{HH}$ = 5 Hz, C$\underline{H}_2$NH), 1.50 (d, 6H, $^{3}J_{HH}$ = 7 Hz, CH(C$\underline{H}_3$)$_2$). ^{13}C{^{1}H} NMR (DMSO-d_6, 100 MHz, 25 °C): δ 164.4 ($\underline{C}$=O), 151.4 ($\underline{C}_4$H$_3$O), 145.8 (N-$\underline{C}$(5)-N), 142.7 (N-$\underline{C}$(3)-N), 142.4 ($\underline{C}_4$H$_3$O), 110.8 ($\underline{C}_4$H$_3$O), 107.9 ($\underline{C}_4$H$_3$O), 55.5 ($\underline{C}$H(CH$_3$)$_2$), 49.0 ($\underline{C}$H$_2$), 36.1 ($\underline{C}$H$_2$), 21.4 (CH($\underline{C}$H$_3$)$_2$). IR data (KBr pellet) cm^{-1}: 1689 (s) ($\nu_{c=o}$). HRMS (ES): *m/z* 249.1356 [NHC+H]$^{+}$, calcd. 249.1352. Anal. Calcd. for $C_{12}H_{17}N_4O_2Cl\bullet0.5H_2O$: C, 49.07; H, 6.18; N, 19.07. Found: C, 48.63; H, 6.74; N, 17.97 %.

Synthesis of [1-(*i*-propyl)-4-N-(furan-2-ylmethyl)acetamido-1,2,4-triazol-5-ylidene]$_2$Ni (2b)

A mixture of 1-(*i*-propyl)-4-N-(furan-2-ylmethyl)acetamido-1,2,4-triazolium chloride (**2a**) (2.33 g, 8.20 mmol), K_2CO_3 (5.65 g, 40.9 mmol) and $NiCl_2\bullet6H_2O$ (0.974 g, 4.09 mmol) was refluxed in acetonitrile (*ca.* 70 mL) for 24 hours. The reaction mixture was filtered and filtrate was reduced in vacuum up to 15 mL. The filtrate was kept at room temperature for overnight, during which brown crystals were formed. Finally the crystals were separated by filtration and vacuum dried to give the product (**2b**) as a yellow crystalline solid (0.684 g, 30 %). ^{1}H NMR ($CDCl_3$, 400 MHz, 25 °C): δ 8.07 (s, 2H, N-C(3)$\underline{H}$-N), 7.29 (br, 2H, $C_4\underline{H}_3O$), 6.31 (dd, 2H, $^{3}J_{HH}$ = 3 Hz, $^{3}J_{HH}$ = 3 Hz, $C_4\underline{H}_3O$), 6.13 (d, 2H, $^{3}J_{HH}$ = 3 Hz, $C_4\underline{H}_3O$), 5.24 (d, 2H, $^{2}J_{HH}$ = 15 Hz, C$\underline{H}_2$), 4.83 (d, 2H, $^{2}J_{HH}$ = 15 Hz, C$\underline{H}_2$), 4.57 (d, 2H, $^{2}J_{HH}$ = 15 Hz, C$\underline{H}_2$), 3.59 (d, 2H, $^{2}J_{HH}$ = 15 Hz, C$\underline{H}_2$), 3.54 (sept, 2H, $^{3}J_{HH}$ = 7 Hz, C$\underline{H}$(CH$_3$)$_2$), 1.24 (d, 6H, $^{3}J_{HH}$ = 7 Hz, CH(C$\underline{H}_3$)$_2$), 1.14 (d, 6H, $^{3}J_{HH}$ = 7 Hz, CH(C$\underline{H}_3$)$_2$). ^{13}C{^{1}H} NMR ($CDCl_3$, 100 MHz, 25 °C): δ

171.2 (Ni-N<u>C</u>N), 168.5 (<u>C</u>=O), 156.2 (<u>C</u>$_4$H$_3$O), 142.3 (N-<u>C</u>(3)-N), 141.1 (<u>C</u>$_4$H$_3$O), 110.7 (<u>C</u>$_4$H$_3$O), 106.7 (<u>C</u>$_4$H$_3$O), 54.3 (<u>C</u>H(CH$_3$)$_2$), 54.2 (<u>C</u>H$_2$), 41.8 (<u>C</u>H$_2$), 24.3 (CH(<u>C</u>H$_3$)$_2$), 20.3 (CH(<u>C</u>H$_3$)$_2$). IR data (KBr pellet) cm^{-1}: 1596 (s) ($\nu_{c=o}$). HRMS (ES): *m/z* 553.1817 [M+H]$^+$, calcd. 553.1816. Anal. Calcd. for $C_{24}H_{30}NiN_8O_4$: C, 52.10; H, 5.47; N, 20.25. Found: C, 51.44; H, 6.04; N, 20.28 %.

Synthesis of 1-(benzyl)-4-N-(furan-2-ylmethyl)acetamido-1,2,4-triazolium chloride (3a)

A mixture of benzyl triazole (2.05 g, 12.9 mmol) and 2-chloro-N-(furan-2-ylmethyl)acetamide (2.21 g, 12.8 mmol) was refluxed in toluene (*ca*. 40 mL) for 32 hours during which a black precipitate was formed. After decanting off the solvent, the precipitate was washed with hot petroleum ether (*ca.* 3 × 10 mL) and then dissolved in minimum amount of dichloromethane (*ca.* 4 mL). The product was precipitated out by addition of diethyl ether (2 × 15 mL). The product was finally isolated by decantation and was vacuum dried to give the product (**3a**) as a black solid (2.20 g, 52 %). ^{1}H NMR (DMSO-d_6, 400 MHz, 25 °C): δ 10.3 (s, 1H, N-C(5)<u>H</u>-N), 9.20 (br, 1H, N-C(3)<u>H</u>-N), 9.16 (s, 1H, N<u>H</u>CO), 7.60 (br, 1H, C$_4$<u>H</u>$_3$O), 7.43 (br, 5H, C$_6$<u>H</u>$_5$), 6.41 (dd, 1H, $^3J_{HH}$ = 3 Hz, $^3J_{HH}$ = 3 Hz, C$_4$<u>H</u>$_3$O), 6.32 (d, 1H, $^3J_{HH}$ = 3 Hz, C$_4$<u>H</u>$_3$O), 5.70 (s, 2H, C<u>H</u>$_2$), 5.17 (s, 2H, C<u>H</u>$_2$), 4.34 (d, 2H, $^3J_{HH}$ = 6 Hz, C<u>H</u>$_2$NH). ^{13}C{^{1}H} NMR (DMSO-d_6, 100 MHz, 25 °C): δ 164.3 (<u>C</u>=O), 151.3 (<u>C</u>$_4$H$_3$O), 146.1 (N-<u>C</u>(5)-N), 143.8 (<u>C</u>$_6$H$_5$), 142.4 (N-<u>C</u>(3)-N), 142.4 (<u>C</u>$_4$H$_3$O), 133.4 (<u>C</u>$_6$H$_5$), 128.9 (<u>C</u>$_6$H$_5$) 128.8 (<u>C</u>$_6$H$_5$), 110.5 (<u>C</u>$_4$H$_3$O), 107.5 (<u>C</u>$_4$H$_3$O), 54.7 (<u>C</u>H$_2$), 49.1 (<u>C</u>H$_2$), 35.9 (<u>C</u>H$_2$). IR data (KBr pellet) cm^{-1}: 1669 (s) ($\nu_{c=o}$). HRMS (ES): *m/z* 297.1350 [NHC+H]$^+$, calcd. 297.1352. Anal. Calcd. for $C_{16}H_{17}N_4O_2Cl\bullet0.5H_2O$: C, 56.22; H, 5.31; N, 16.39. Found: C, 55.93; H, 5.83; N, 15.37 %.

Synthesis of [1-(benzyl)-4-N-(furan-2-ylmethyl)acetamido-1,2,4-triazol-5-ylidene]$_2$Ni (3b)

A mixture of 1-benzyl-4-N-(furan-2-ylmethyl)acetamido-1,2,4-triazolium chloride (**3a**) (1.20g, 3.60 mmol), K_2CO_3 (2.48 g, 18.0 mmol) and $NiCl_2$•$6H_2O$ (0.428 g, 1.80 mmol) was refluxed in acetonitrile (*ca.* 50 mL) for 24 hours. The reaction mixture was filtered and the filtrate reduced in vacuum up to 10 mL. The filtrate was kept at 0°C for 3 hours, during which yellow crystals were formed. Finally the crystals were quickly separated by filtration and vacuum dried to give the product (**3b**) as a yellow solid (0.163 g, 14 %). ^{1}H NMR ($CDCl_3$, 400 MHz, 25 °C): δ 8.12 (s, 2H, N-C(3)*H*-N), 7.31 (m, 6H, C_6H_5), 7.19 (br, 2H, C_4H_3O), 6.91 (d, 4H, $^3J_{HH}$ = 7 Hz, C_6H_5), 6.29 (br, 2H, C_4H_3O), 6.05 (d, 2H, $^3J_{HH}$ = 2 Hz, C_4H_3O), 4.97 (d, 2H, $^2J_{HH}$ = 15 Hz, CH_2), 4.79 (d, 2H, $^2J_{HH}$ = 15 Hz, CH_2), 4.50 (d, 2H, $^2J_{HH}$ = 15 Hz, CH_2), 4.42 (d, 2H, $^2J_{HH}$ = 15 Hz, CH_2), 4.39 (d, 2H, $^2J_{HH}$ = 15 Hz, CH_2), 3.62 (d, 2H, $^2J_{HH}$ = 15 Hz, CH_2). ^{13}C{^{1}H} NMR ($CDCl_3$, 100 MHz, 25 °C): δ 171.6 (Ni-N*C*N), 168.4 (*C*=O), 156.0 (C_4H_3O), 142.7 (N-*C*(3)-N), 141.2 (C_4H_3O), 133.6 (C_6H_5), 129.3 (C_6H_5), 129.0 (C_6H_5), 127.6 (C_6H_5), 110.7 (C_4H_3O), 106.3 (C_4H_3O), 55.4 (CH_2), 54.0 (CH_2), 42.3 (CH_2). IR data (KBr pellet) cm^{-1}: 1595 (s) ($\nu_{c=o}$). HRMS (ES): *m/z* 649.1813 $[M+H]^+$, calcd. 649.1816. Anal. Calcd. for $C_{32}H_{30}NiN_8O_4$●H_2O: C, 57.59; H, 4.83; N, 16.79. Found: C, 57.71; H, 5.05; N, 16.74 %.

Computational Methods

Density functional theory (DFT) calculations were performed on the metal complexes (**1**−**3**)**b** using GAUSSIAN 09 [22] suite of quantum chemical programs. The Becke three parameter exchange functional in conjunction with Lee-Yang-Parr correlation

functional (B3LYP) has been employed in the study [23]. The polarized basis set 6-31G(d) [24] was used to describe oxygen, carbon, nitrogen and hydrogen atoms. The Stuttgart–Dresden effective core potential (ECP) along with valence basis sets (LANL2DZ) was used for the nickel [25]. Natural bond orbital (NBO) analysis [26] was performed using NBO 3.1 program implemented in the GAUSSIAN 09 package. Frequency calculations were performed for all the optimized structures to characterize the stationary points as minima.

The metal-ligand *donor–acceptor* interaction were inspected by using the Charge Decomposition Analysis (CDA) [27] which is a valuable tool for analyzing the interactions between molecular fragments on a quantitative basis with an emphasis on the electron donation [28]. The orbital interaction between *donor* NHC and *acceptor* fragment Ni^{2+} ion in (**1**−**3**)**b** can be divided into three parts;

(i) σ-donation from two *mono*−anionic NHC ligand fragments to a nickel(II) ion $\{2[NHC]^{-}\rightarrow Ni^{2+}\}$ and designated by (*d*),

(ii) π- back donation from a nickel(II) in to two *mono*−anionic NHC ligand fragments $\{2[NHC]^{-}\leftarrow Ni^{2+}\}$ and designated by (*b*) and

(iii) A repulsive interaction (*r*) between the occupied FMOs of these two fragments.

The CDA calculations were performed using the *AOMix* [29,30] program with the B3LYP/ LANL2DZ, 6-31G(d) wave function. Molecular orbital (MO) compositions and the overlap populations were calculated using the *AOMix* program. Analysis of the MO compositions in terms of occupied and unoccupied fragment orbitals (OFOs

and UFOs, respectively), construction of orbital interaction diagrams, the charge decomposition analysis (CDA) were performed using the *AOMix-CDA* [31].

Catalysis studies

General procedure: In a Schlenk tube, under argon atmosphere, was introduced the arylbromide (0.25 mmol, 1 equiv.), Cs_2CO_3 (261 mg, 0.80 mmol, 3 equiv.), bis(pinacolato)diboron (102 mg, 0.40 mmol, 1.5 equiv.), the nickel complex **1b** (7 mg, 1.3 mmol, 5 mol%) and 1 mL of dry THF. The reaction mixture was then stirred at 70 °C for 20 h. The THF was carefully evaporated. The conversion of the arylbromide and the yield of the borylated arene were determinated by ^{1}H-NMR using 1,3,5-trimethoxybenzene (22 mg, 0.13 mmol, 0.5 equiv.) as an internal standard.

Acknowledgements

We thank Indo-French Centre for the Promotion of Advanced Research – IFCPAR (Project No: 4605-1), New Delhi, for the financial support of this research. PG is grateful to the Sophisticated Analytical Instrument Facility at IIT Bombay for the characterization data and to the National Single Crystal X-ray Diffraction Facility, IIT Bombay, and the Single Crystal X-ray Diffraction Facility at the Chemistry Department, IIT Bombay, for the crystallographic data. The computational facilities at the Computer Center, IIT Bombay, and at the Chemistry Department, IIT Bombay, are gratefully acknowledged. AK thanks CSIR, New Delhi, for research fellowship. CD and JBS thank the French "Ministère de l'Enseignement Supérieur et de la Recherche" and the CNRS for financial support. LPB thanks IFCPAR for a PhD grant.

Electronic supplementary information (ESI) available: The characterization data of the (**1**−**3**)**b** complexes (Supporting Information Figure S1−S33), the B3LYP coordinates of the optimized geometries for (**1**−**3**)**b,** NBO tables and CDA table along with orbital interaction diagrams of **2b** and **3b**. This material is available free of charge *via* the internet at http:www.xxxxxxxxx

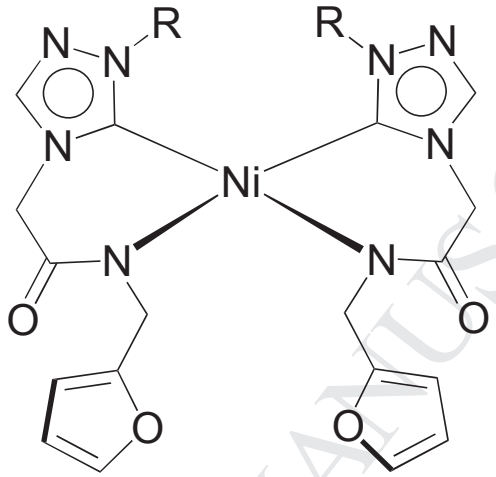

R = Et (**1b**), *i*-Pr (**2b**), Bn (**3b**)

Figure 1.

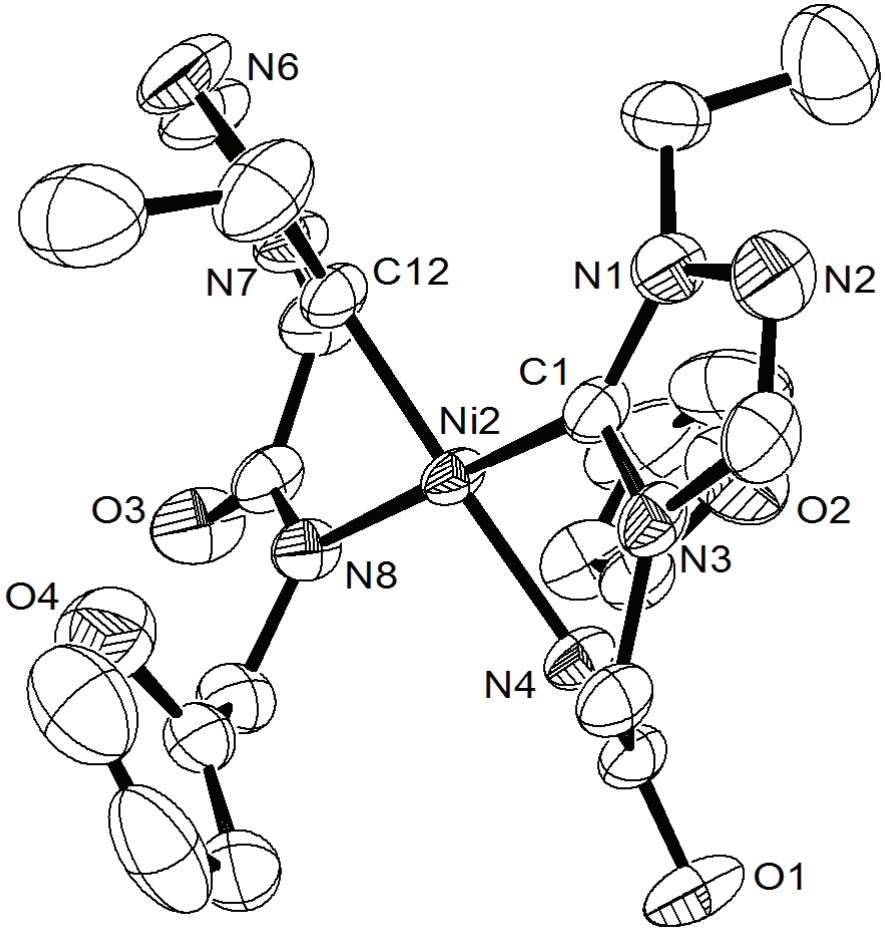

Figure 2. ORTEP view of **1b** with thermal ellipsoids are shown at the 50 % probability level. Selected bond lengths (Å) and angles (°): Ni(2)−C(1) 1.860(3), Ni(2)−C(34) 1.859(3), Ni(2)−N(4) 1.9230(2), Ni(2)−N(8) 1.9220(2), C(1)−Ni(2)−N(4) 87.54(10), C(12)−Ni(2)−N(8) 85.82(10), C(1)−Ni(2)−C(12) 94.64(11), N(4)−Ni(2)−N(8) 92.43(9).

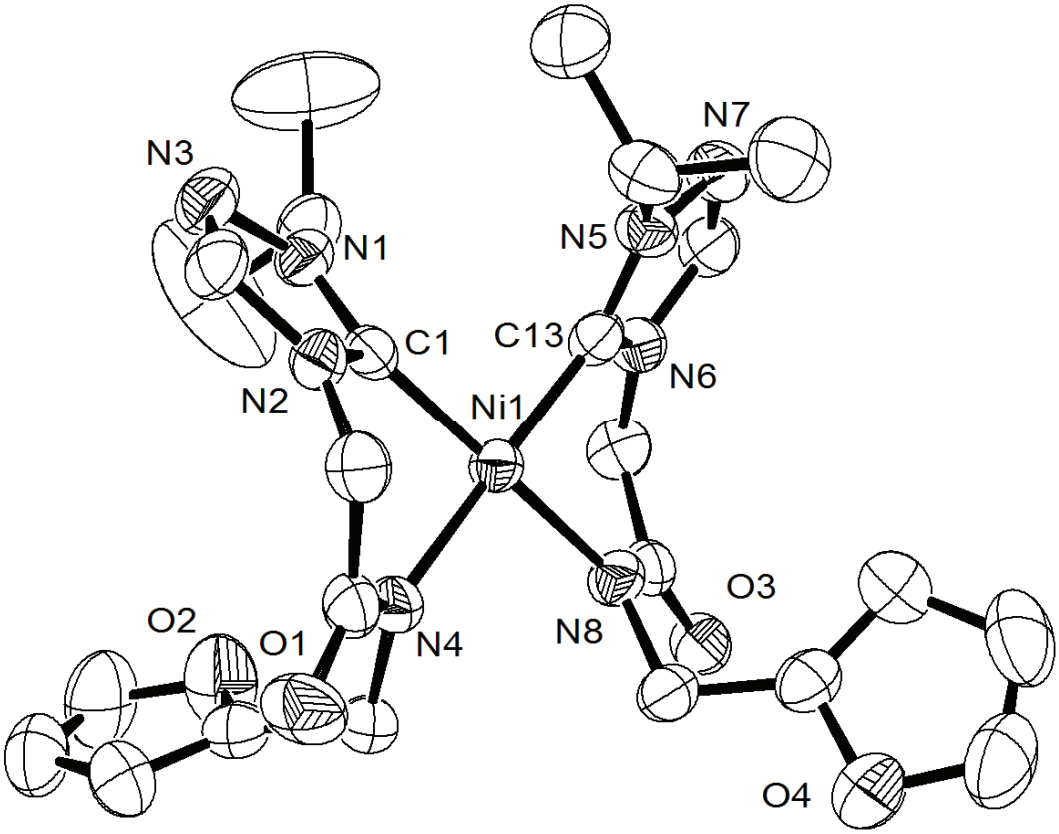

Figure 3. ORTEP view of **2b** with thermal ellipsoids are shown at the 50 % probability level. Selected bond lengths (Å) and angles (°): Ni(1)−C(1) 1.853(2), Ni(1)−C(13) 1.853(2), Ni(1)−N(4) 1.9260(18), Ni(1)−N(8) 1.9211(18), C(1)−Ni(1)−N(4) 86.67(8), C(13)−Ni(1)−N(8) 86.21(9), C(1)−Ni(1)−C(13) 92.83(8), N(4)−Ni(1)−N(8) 94.61(7).

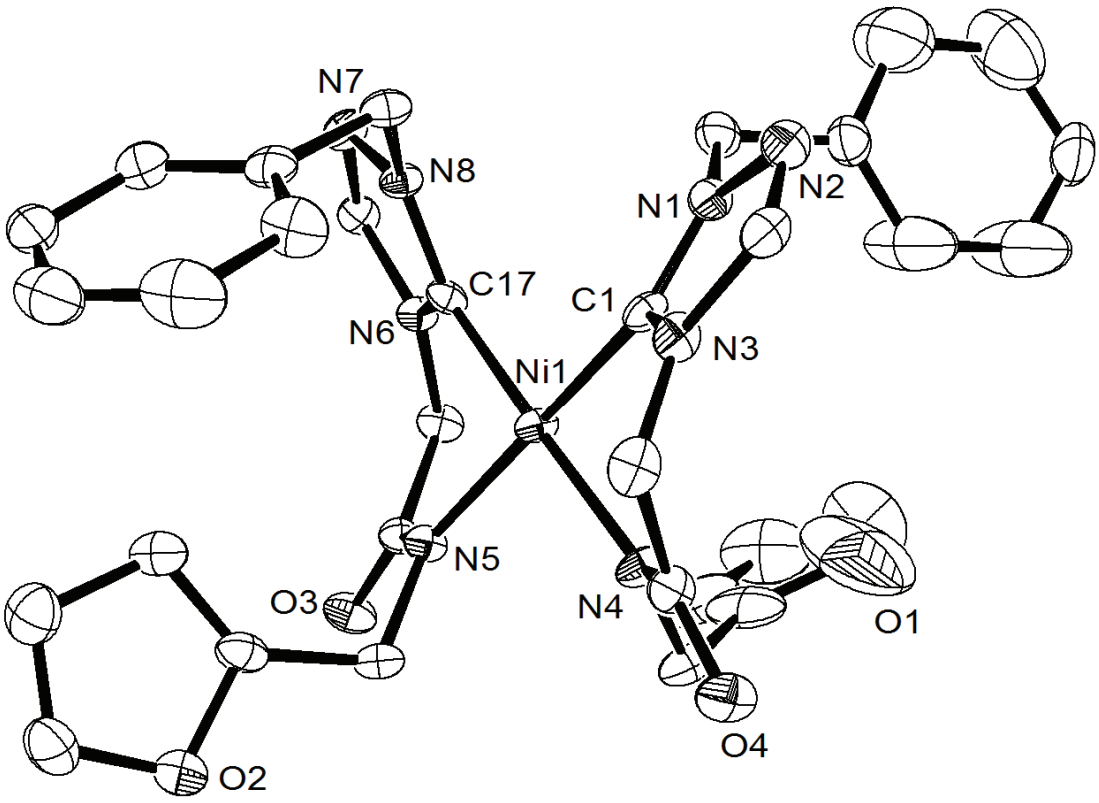

Figure 4. ORTEP view of **3b** with thermal ellipsoids are shown at the 50 % probability level. Selected bond lengths (Å) and angles (°): Ni(1)−C(1) 1.871(4), Ni(1)−C(17) 1.871(4), Ni(1)−N(4) 1.927(3), Ni(1)−N(5) 1.931(3), C(1)−Ni(1)−N(4) 86.25(14), C(17)−Ni(1)−N(5) 88.09(14), C(1)−Ni(1)−C(17) 94.40(15), N(4)−Ni(1)−N(5) 91.57(13).

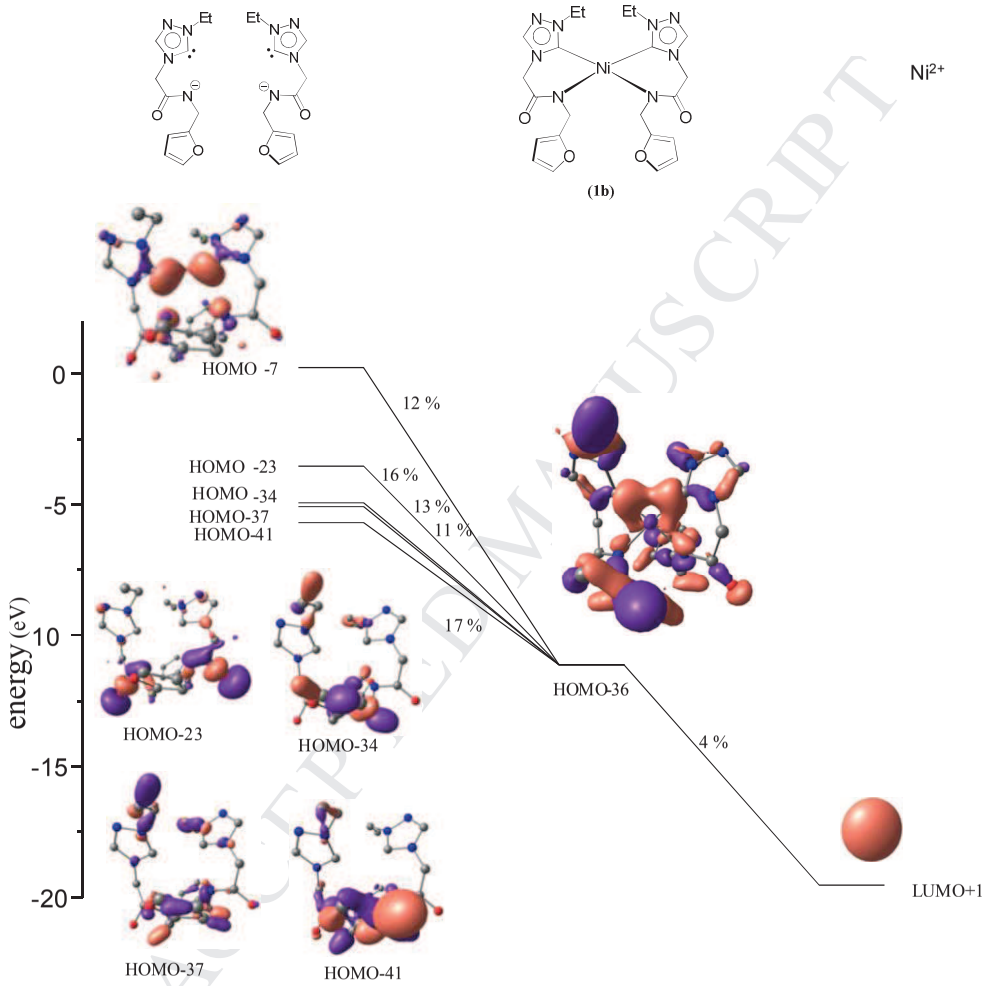

Figure 5. Simplified orbital interaction diagram showing the major contributions of the NHC–Ni bond in **1b**.

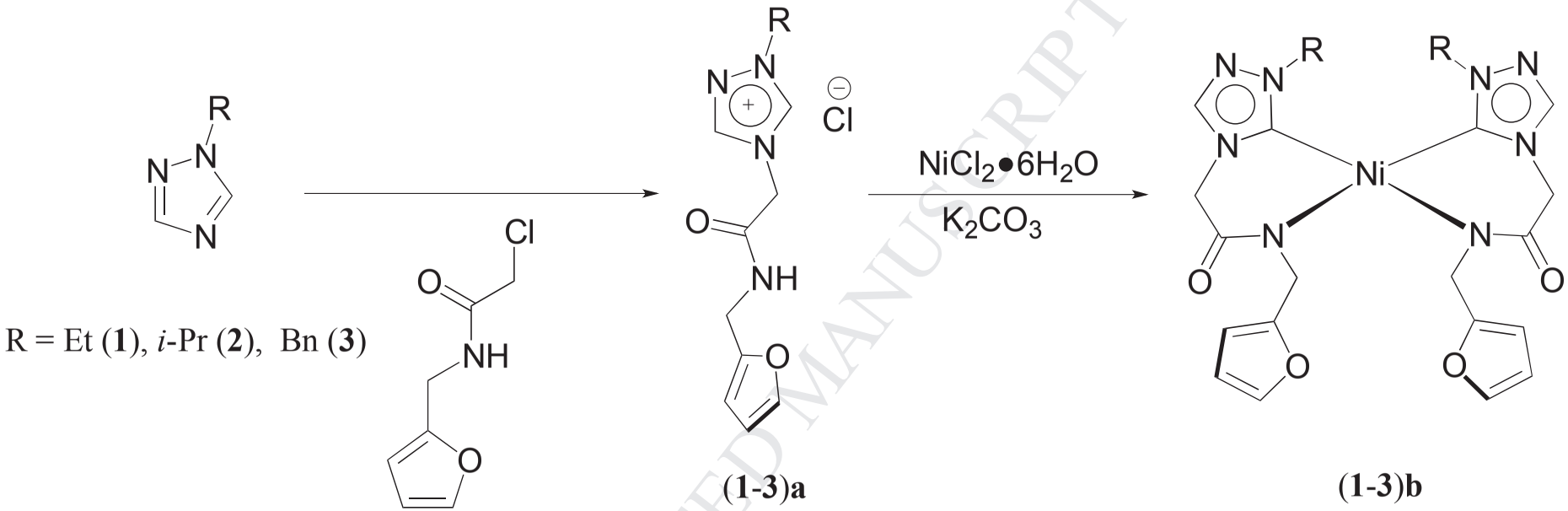

Scheme 1.

Table 1. X-ray crystallographic data for **1b**, **2b** and **3b**.

Compound	**1b**	**2b**	**3b**
Lattice	Monoclinic	Orthorhombic	Monoclinic
Formula	$C_{45}H_{53}Cl_3N_{16}Ni_2O_{8.5}$	$C_{24}H_{30}N_8NiO_4$	$C_{32}H_{30}N_8NiO_4$
Formula weight	1177.80	553.27	649.35
Space group	$P2_1/n$	$P2_12_12_1$	$P2_1/c$
a/Å	18.8306(3)	10.5000(2)	18.590(5)
b/Å	9.25340(10)	13.9266(4)	9.104(2)
c/Å	30.7706(4)	17.9794(4)	18.316(5)
α/°	90	90	90
β/°	94.472(2)	90	109.49(4)
γ/°	90	90	90
V/Å^3	5345.36(12)	2629.11(11)	2922.2(13)
Z	4	4	4
Temperature (K)	293(2)	293(2)	100(2)
Radiation (λ,Å)	0.71073	0.71073	0.71073
ρ (calcd.), g cm^{-3}	1.464	1.398	1.476
θ max, deg.	25.00	25.00	25.00
No. of data	9372	4620	7789
No. of parameters	677	338	406
R_1 [I>2sigma(I)]	0.0419	0.0277	0.0816
wR_2 [I>2sigma(I)]	0.1149	0.0689	0.204
GOF	1.038	1.034	1.109

Table 2. Selected results for catalytic borylation reactions of arylbromide by *bis*(pinacolato)diboron catalyzed by (**1**−**3**)**b**.

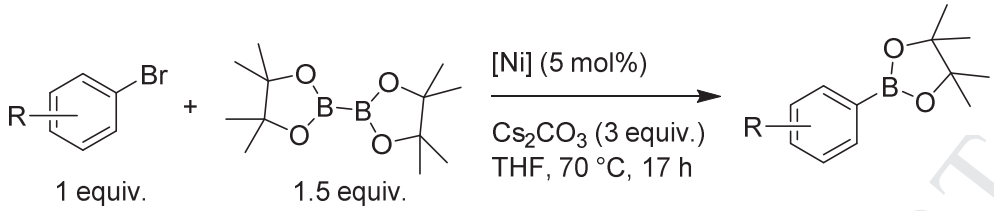

Entry	[Ni] (5 mol%)	Ar-Br	Conversion (%)[(b)]	Yield (%)[(c)]
1	**1b**	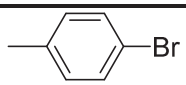	90	13
2	**2b**		75	10
3	**3b**		61	8
4	**1b**	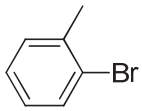	88	12
5	**1b**	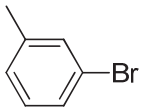	91	14
6	**1b**	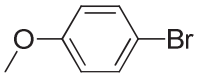	73	20
7	**1b**	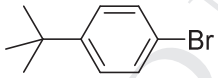	71	18
8	**1b**	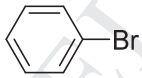	83	10
9	**1b**	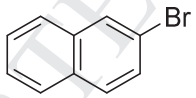	70	21

(a) Ar-Br (50 mg, 0.25 mmol, 1 equiv.), Cs_2CO_3 (261 mg, 0.80 mmol, 3 equiv.), bis(pinacolato)diboron (102 mg, 0.40 mmol, 1.5 equiv.), THF (1 mL), Ni complex (7 mg, 1.3 mmol, 5 mol%), 70 °C for 20 h. (b) Conversion of the arylbromide determinated by ^{1}H-NMR using 1,3,5-trimethoxybenzene (22 mg, 0.13 mmol, 0.5 equiv.) as an internal standard. (c) NMR yield determined with1,3,5-trimethoxybenzene as an internal standard.

Graphics for Table of Contents

Nickel Complexes of 1,2,4-Triazole Derived Amido-functionalized N-heterocyclic Carbene Ligands: Synthesis, Theoretical Studies and Catalytic Application

Anuj Kumar, Linus Paulin Bheeter, Manoj Kumar Gangwar, Jean-Baptiste Sortais, Christophe Darcel and Prasenjit Ghosh**

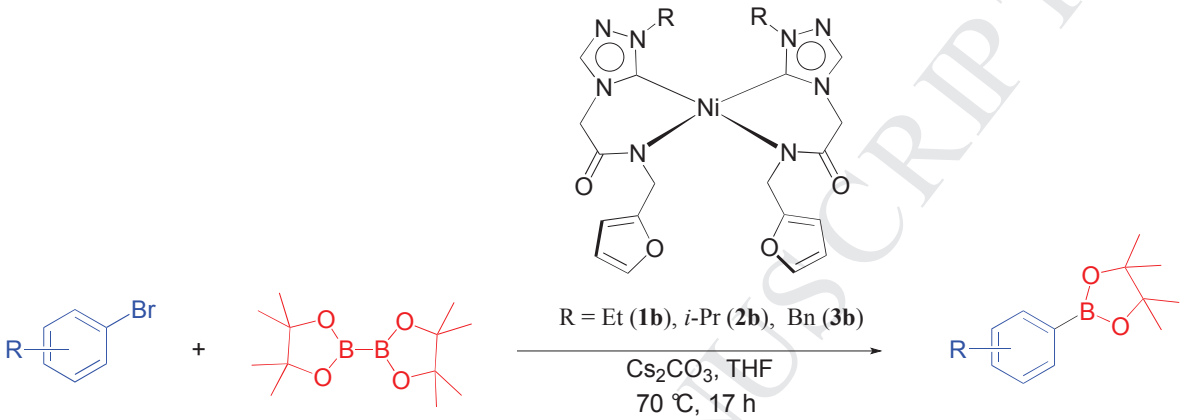

A series of nickel complexes of 1,2,4-triazole derived amido-functionalized N-heterocyclic carbene ligands were prepared, characterized and explored for their activity in the borylation reaction of arylbromides.

References

[1]. (a). A.P. Prakasham, P. Ghosh, Inorg. Chim. Acta (2014) http://dx.doi.org/10.1016/j.ica.2014.11.005

(b). S.Z. Tasker, E.A. Standley, T.F. Jamison, Nature 509 (2014) 299−309.

(c). S.Wang, W.H. Sun, C. Redshaw, J. Organomet. Chem. 751 (2014) 717−741.

(d). R. Gao, W.H. Sun, C. Redshaw, Catal. Sci. Technol. 3 (2013) 1172−1179.

(e). A. Correa, J. Cornella, R. Martin, Angew. Chem. Int. Ed. 52 (2013) 1878−1880.

(f). J. Yamaguchi, K. Muto, K. Itami, Eur. J. Org. Chem. (2013) 19–30.

[2]. (a). R. Chinchilla, C. Nájera, Chem. Soc. Rev. 114 (2014) 1783−1826.

(b). C. Valente, M. Pompeo, M. Sayah, M.G. Organ, Org. Proc. Res. Dev. 18 (2014) 180−190.

(c). Q.A. Chen, Z.S. Ye, Y. Duan, Y.G. Zhou, Chem. Soc. Rev. 42 (2013) 497−511.

(d). S.I. Gorelsky, Coord. Chem. Rev. 257 (2013)153−164.

(e). T. Vlaar, E. Ruijter, B.U.W. Maes, R.V.A. Orru, Angew. Chem. Int. Ed. 52 (2013) 7084−7097.

(f). K. Muñiz, C. Martínez, J. Org. Chem. 78 (2013) 2168−2174.

[3]. G.A. Foulds, Coord. Chem. Rev. 146 (1995) 1–90.

[4]. A. Arévalo, J.J. García, Eur. J. Inorg. Chem. (2010) 4063–4074..

[5]. (a). A. Kumar, P. Ghosh, Eur. J. Inorg. Chem. (2012) 3955–3969.

(b). A. John, P. Ghosh, Dalton Trans. 39 (2010) 7183–7206.

[6]. (a). C.C. J. Loh, D. Enders, Chem. Eur. J. 18 (2012) 10212−10225.

(b). T. Kçsterke, J. Kçsters, E-Ulrich Würthwein, C. Mück-Lichtenfeld, C. S. Brinke, F. Lahoz, F. E. Hahn, Chem. Eur. J. 18 (2012) 14594–14598.

(c). T. Kösterke, T. Pape, F. E. Hahn, Chem. Commun. 47 (2011) 10773–10775.

(d). G.C. Fortman, S.P. Nolan, Chem. Soc. Rev. 40 (2011) 5151−5169.

(e). C. Radloff, F. E. Hahn, T. Pape, R. Fröhlich, Dalton Trans. (2009) 7215–7222.

(f). F. E. Hahn, C. Radloff, T. Pape, A. Hepp, Organometallics 27 (2008) 6408–6410.

(g). F. Boeda, S.P. Nolan, Annu. Rep. Prog. Chem. Sect. B 104 (2008) 184–210.

(h). N. Marion, S.P. Nolan, Chem. Soc. Rev. 37 (2008) 1776–1782.

(i). F.E. Hahn, B. Heidrich, A. Hepp, T. Pape, J. Organomet. Chem. 692 (2007) 4630–4638.

(j). H. V. Huynh, C. Holtgrewe, T. Pape, L. L. Koh, E. Hahn, Organometallics 25 (2006) 245–249 .

(k). R. Singh, S.P. Nolan, Annu. Rep. Prog. Chem. Sect. B 102 (2006) 168–196.

(l). T. Weskamp, V.P.W. Böhm, W.A. Herrmann, J. Organomet. Chem. 600 (2000) 12–22.

[7]. C. Dash, M.M. Shaikh, R.J. Butcher, P. Ghosh, Dalton Trans. 39 (2010) 2515–2524.

[8]. (a). S. Kumar, A. Narayanan, M.N. Rao, M.M. Shaikh, P. Ghosh, J. Organomet. Chem. 696 (2012) 4159–4165.

(b). M.K. Samantaray, M.M. Shaikh, P. Ghosh, Organometallics 28 (2009) 2267–2275.

(c). S. Ray, M.M. Shaikh, P. Ghosh, Eur. J. Inorg. Chem. (2009) 1932–1941.

[9]. M. Katari, G. Rajaraman, and P. Ghosh, J. Organomet. Chem. (2014) http://dx.doi.org/10.1016/j.jorganchem.2014.02.012.

[10]. (a). L.P. Bheeter, M. Henrion, L. Brelot, C. Darcel, M.J. Chetcuti, J.-B. Sortais, V. Ritleng, Adv. Synth. Catal. 354 (2012) 2619–2624.

(b). L.P. Bheeter, M. Henrion, M.J. Chetcuti, C. Darcel, V. Ritleng, J.-B. Sortais, Catal. Sci. Technol. 3 (2013) 3111–3116.

[11]. (a). P. Li, C. Fu, S. Ma, Org. Biomol. Chem. 12 (2014) 3604–3610.

(b). W.K. Chow, O.Y. Yuen, P.Y. Choy, C.M. So, C.P. Lau, W.T. Wong, F.Y. Kwong, RSC Adv. 3 (2013) 12518–12539.

(c). J. Takaya, N. Iwasawa, ACS Catal. 2 (2012) 1993–2006.

(d). M.J. Ingleson, Synlett 23 (2012) 1411–1415.

(e). J.F. Hartwig, Chem. Soc. Rev. 40 (2011) 1992–2002.

[12]. (a). R.J.P. Corriu, J.P. Masse, J. Chem. Soc. Chem. Commun. (1972) 144.

(b). K. Tamao, K. Sumitani, M. Kumada, J. Am. Chem. Soc. 94 (1972) 4374–4376.

[13]. For a representative review, see, F.-S. Han, Chem. Soc. Rev. 42 (2013) 5270–5298.

For representative recent examples, see,

(a). S.D**.** Ramgren, L. Hie, Y. Ye, N.K. Garg, Org. Lett. 15 (2013) 3950–3953.

(b). A.M. Oertel, V. Ritleng, M.J. Chetcuti, Organometallics 31 (2012) 2829–2840.

(c). Y.-L. Zhao, Y. Li, S.-M. Li, Y.-G. Zhou, F.-Y. Sun, L.-X. Gao, F.-S. Han, Adv. Synth. Cat. 353 (2011) 1543–1550.

(d). S. Ge, J.F. Hartwig, Angew. Chem. Int. Ed. 51 (2012) 12837–12841.

(e). V. Ritleng, A.M. Oertel, M.J. Chetcuti, Dalton Trans. 39 (2010) 8153–8160.

(f). K. Inamoto, J.-i. Kuroda, E. Kwon, K. Hiroya, T. Doi, J. Organomet. Chem. 694 (2009) 389–396.

(g). J.-i. Kuroda, K. Inamoto, K. Hiroya, T. Doi, Eur. J. Org. Chem. (2009) 2251–2261.

(h). Y. Zhou, Z. Xi, W. Chen, D. Wang, Organometallics 27 (2008) 5911–5920.

(i). Z. Xi, X. Zhang, W. Chen, S. Fu, D. Wang, Organometallics 26 (2007) 6636–6642.

(j). C.-Y. Liao, K.-T. Chan, Y.-C. Chang, C.-Y. Chen, C.-Y. Tu, C.-H. Hu, H.M. Lee, Organometallics 26 (2007) 5826–5833.

(k). C.-C. Lee, W.-C. Ke, K.-T. Chan, C.-L. Lai, C.-H. Hu, H.M. Lee, Chem. Eur. J. 13 (2007) 582–591.

(l). K. Inamoto, J.-i. Kuroda, T. Sakamoto, K. Hiroya, Synthesis (2007) 2853–2861.

(m). P.L. Chiu, C.-L. Lai, C.-F. Chang, C.-H. Hu, H.M. Lee, Organometallics 24 (2005) 6169–6178.

(n). D.S. McGuinness, K.J. Cavell, B.W. Skelton, A.H. White, Organometallics 18 (1999) 1596–1605.

[14]. For selected recent examples, see,

(a). P. Leowanawat, A.-M. Resmerita, C. Moldoveanu, C. Liu, N. Zhang, D.A. Wilson, L.M. Hoang, B.M. Rosen, V. Percec, J. Org. Chem. 75 (2010) 7822–7828.

(b). T. Yamamoto, T. Morita, J. Takagi, T. Yamakawa, Org. Lett. 13 (2011) 5766–5769.

(c). J. Yi, J.-H. Liu, J. Liang, J.-J. Dai, C.-T. Yang, Y. Fu, L. Liu, Adv. Synth. Catal. 354 (2012) 1685–1691.

(d). M. Murata, Y. Sogabe, T. Namikoshi, S. Watanabe, Heterocycles 86 (2012) 133–138.

(e). G.A. Molander, L.N. Cavalcanti, C. Garcia-Garcia, J. Org. Chem. 78 (2013) 6427–6439.

(f). A.S. Dudnik, G.C. Fu, J. Am. Chem. Soc. 134 (2012) 10693−10697.

[15]. For example, the literature searchable by Scifinder Scholar provided 55 number of references for the transition metal complexes of any amido-functionalized imidazole based N-heterocyclic carbene (NHC) ligands while the similar search for the transition metal complexes of any amido-functionalized 1,2,4 triazole based N-heterocyclic carbene (NHC) ligands provided only 1 reference. See, SciFinder Scholar. https://scifinder.cas.org. Accessed August 30 (2014).

[16]. Analogous search in the Cambridge Structural database for the structurally characterized transition metal complexes likewise yielded 31 references for the amido-functionalized imidazole based N-heterocyclic carbene (NHC) complexes and only 1 reference for the transition metal the amido-functionalized 1,2,4 triazole based N-heterocyclic carbene (NHC) complexes. See, Cambridge Structural database Version 5.35, November 2013.

[17]. Cambridge Structural database Version 5.35, November (2013).

[18]. P.G. Bulger, I.F. Cottrell, C.J. Cowden, A.J. Davies, U-H. Dolling, Tetrahedron Lett. 41 (2000) 1297–1301.

[19]. F. Dallacker, K. Minn, Chemiker-Zeitung 110 (1986) 101–108.

[20]. B.A. Astleford, G.L. Goe, J.G. Keay, E.F.V. Scriven, J. Org.Chem, 54 (1989**)** 731−732.

[21]. M. Bayrakcı, Ş. Yiğiter, Tetrahedron 69 (2013) 3218−3224.

[22]. Gaussian 09, Revision **A.1**, M.J. Frisch, G.W. Trucks, H.B. Schlegel, G.E. Scuseria, M.A. Robb, J.R. Cheeseman, G. Scalmani, V. Barone, B. Mennucci, G.A. Petersson, H. Nakatsuji, M. Caricato, X. Li, H.P. Hratchian, A.F. Izmaylov, J. Bloino, G. Zheng, J.L. Sonnenberg, M. Hada, M. Ehara, K. Toyota, R. Fukuda, J. Hasegawa, M. Ishida, T. Nakajima, Y. Honda, O. Kitao, H. Nakai, T. Vreven, J.A. Montgomery,

J.E. Peralta, F. Ogliaro, M. Bearpark, J.J. Heyd, E. Brothers, K.N. Kudin, V.N. Staroverov, R. Kobayashi, J. Normand, K. Raghavachari, A. Rendell, J.C. Burant, S.S. Iyengar, J. Tomasi, M. Cossi, N. Rega, J.M. Millam, M. Klene, J.E. Knox, J.B. Cross, V. Bakken, C. Adamo, J. Jaramillo, R. Gomperts, R.E. Stratmann, O. Yazyev, A.J. Austin, R. Cammi, C. Pomelli, J.W. Ochterski, R.L. Martin, K. Morokuma, V.G. Zakrzewski, G. A. Voth, P. Salvador, J.J. Dannenberg, S. Dapprich, A.D. Daniels, O. Farkas, J. B. Foresman, J.V. Ortiz, J. Cioslowski, D.J. Fox, Gaussian, Inc., Wallingford CT, (2009).

[23]. (a). A.D. Becke, Phys. Rev. A 38 (1998) 3098−3100.

(b). C. Lee, W. Yang, R.G. Parr, Phys. Rev. B 37 (1998) 785−789.

[24]. (a). W.J. Herre, R. Dditcrfield, J.A. Pople, J. Chem. Phys. 56 (1972) 2257−2261.

(b). G.A. Petersson, A. Bennett, T.G. Tensfeldt, M.A. AI-Laham, W.A. Shirley, J. Chem. Phys. 89 (1988) 2193−2218.

(c). G. A. Petersson, M. A. AI-Laham, J. Chem. Phys. 94 (1991) 6081−6090.

[25]. (a). O. Das, N.N. Adarsh, A. Paul, T.K. Paine, Inorg. Chem. 49 (2010) 541–551.

(b). O. Gutierrez, D.J. Tantillo, Organometallics 29 (2010) 3541−3545.

(c). M. Ishida, Y. Naruta, F. Tani, Dalton Trans. 39 (2010) 2651−2659.

(d). E.B. Kadossov, K.J. Gaskell, M.A. Langell, J. Comput. Chem. 28 (2007) 1240−1251.

(e). D. C. Graham, K. J. Cavell, B. F. Yates, Dalton Trans. (2007) 4650−4658.

(f). Q.Z. Han, Y.H. Zhao, H. Wen, Data Sci. J. 6 (2007) S837−S846.

[26]. A.E. Reed, L.A. Curtiss, F. Weinhold, Chem. Rev. 88 (1988) 899−926.

[27]. S. Dapprich, G. Frenking, J. Phys. Chem. 99 (1995) 9352−9362.

[28]. (a). D. Nemcsok, K. Wichmann, G. Frenking, Organometallics 23 (2004) 3640−3646.

(b). S.F. Vyboishchikov, G. Frenking, Chem. Eur. J. 4 (1998) 1439−1448.

(c). C. Boehme, G. Frenking, Organometallics 17 (1998) 5801–5809.

(d). G. Frenking, U. Pidun, J. Chem. Soc. Dalton Trans. (1997) 1653–1662.

[29]. S.I. Gorelsky, AOMix: Program for Molecular Orbital Analysis, version 6.87d; University of Ottawa: Ottawa, Canada, 2014.; http://www.sg-chem.net/ (accessed June 18, 2014).

[30]. (a). S.I. Gorelsky, J. Chem. Theory Comput., 8 (2012) 908−914.

(b). D.R. Denomme, S.M. Dumbris, I.F.D. Hyatt, K.A. Abboud, I. Ghiviriga, L. McElwee-White, Organometallics 29 (2010) 5252–5256.

(c). N. Dimakis, M. Cowan, G. Hanson, E. S. Smotkin, J. Phys. Chem. C 113 (2009) 18730–18739.

(d). S.I. Gorelsky, E.I. Solomon, Theor. Chem. Acc. 119 (2008) 57–65.

(e). S.I. Gorelsky, A.B.P. Lever, J. Organomet. Chem. 635 (2001) 187−196.

[31]. (a). S.I. Gorelsky, S. Ghosh, E.I. Solomon, J. Am. Chem. Soc. 128 (2006) 278−290.

(b). S.I. Gorelsky, L. Basumallick, J. Vura-Weis, R. Sarangi, K.O. Hodgson, B. Hedman, K. Fujisawa, E.I. Solomon, Inorg. Chem. 44 (2005) 4947−4960.

Figure 1. The nickel complexes of 1,2,4-triazole derived amido-functionalized N-heterocyclic carbene Ligands.

Highlights

- Ni complexes of the 1,2,4-triazole based NHC ligands were synthesized.
- The Ni–NHC interaction was probed by DFT studies
- The Ni–NHC complexes exhibited moderate activity in borylation of aryl bromides.

Supporting Information

Nickel Complexes of 1,2,4-Triazole Derived Amido-functionalized N-heterocyclic Carbene Ligands: Synthesis, Theoretical Studies and Catalytic Application

Anuj Kumar,[†] Linus Paulin Bheeter,[‡] Manoj Kumar Gangwar,[†] Jean-Baptiste Sortais,[‡] Christophe Darcel*,[‡] and Prasenjit Ghosh*,[†]

[†]Department of Chemistry

Indian Institute of Technology Bombay,

Powai, Mumbai 400 076.

[‡]Université de Rennes 1,

UMR CNRS-UR1 6226 Institut des Sciences chimiques de Rennes,

Team "Organometallics: Matrials and Catalysis" - Centre for Catalysis and Green Chemistry

Campus de Beaulieu, 35042 – Rennes, France

Email: pghosh@chem.iitb.ac.in, christophe.darcel@univ-rennes1.fr,

Fax: +91 22 2572 3480, +33 2 23 23 69 39

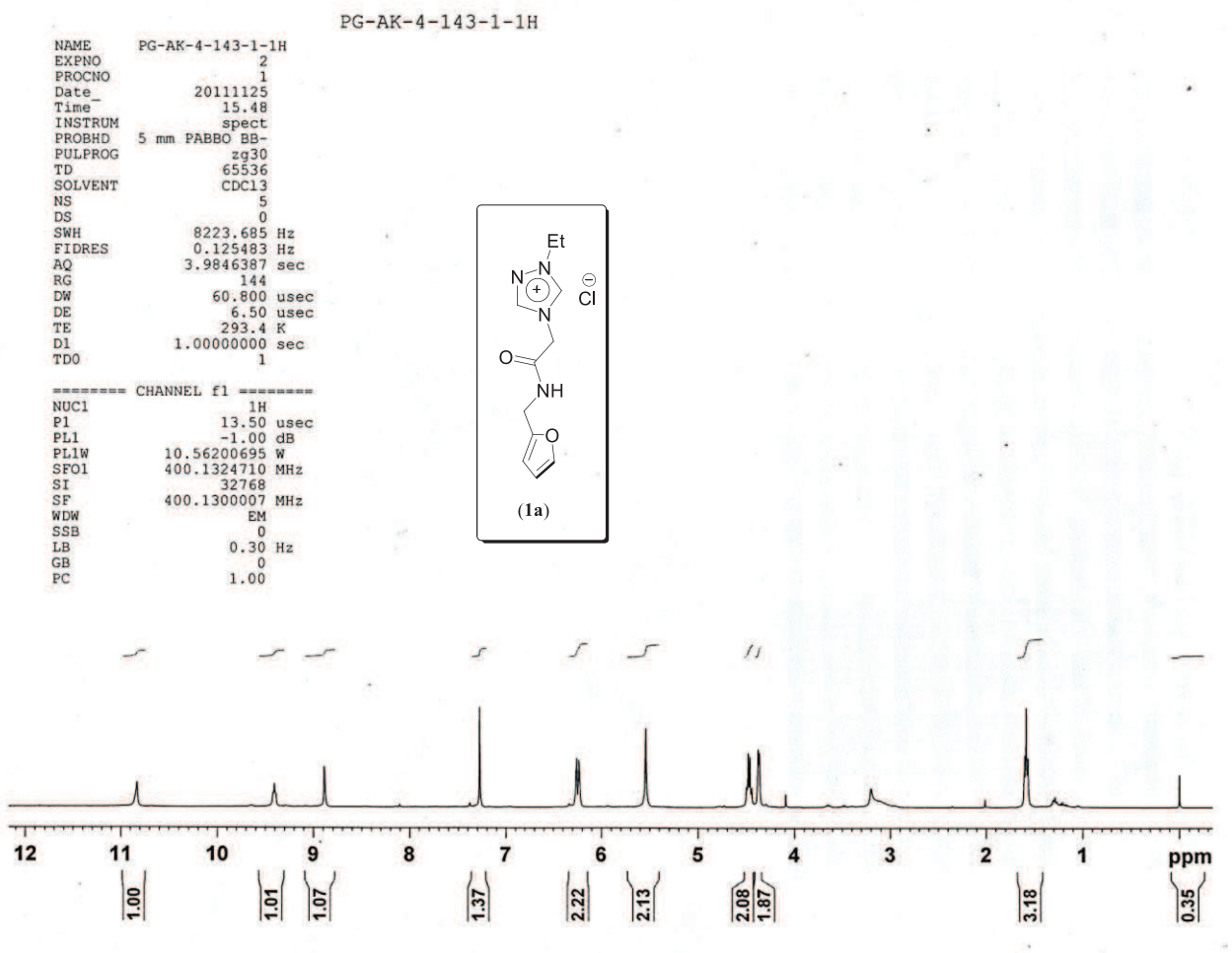

Figure S1. ^{1}H NMR spectrum of **1a** in $CDCl_3$.

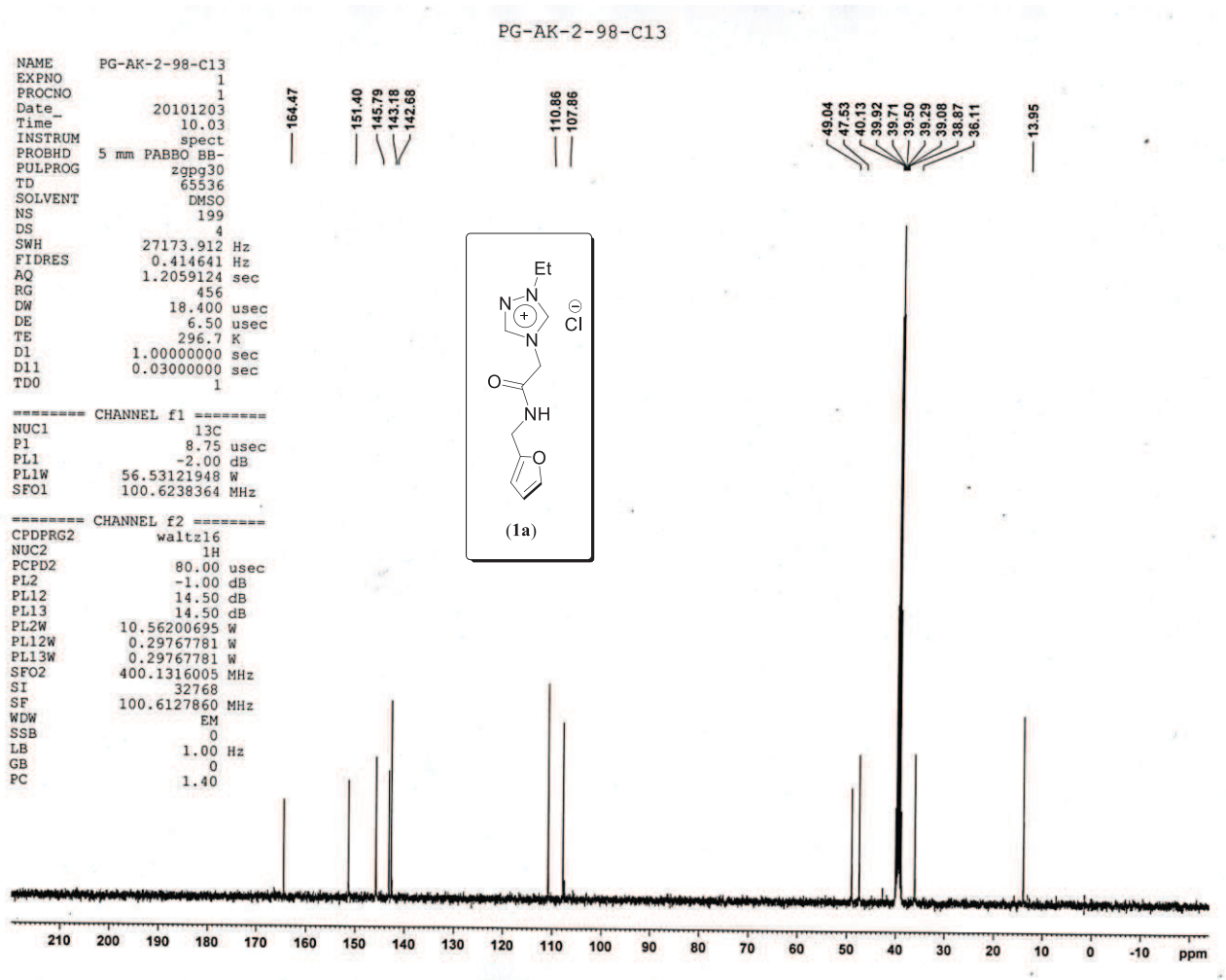

Figure S2. $^{13}C\{^{1}H\}$ NMR spectrum of **1a** in DMSO-d_6.

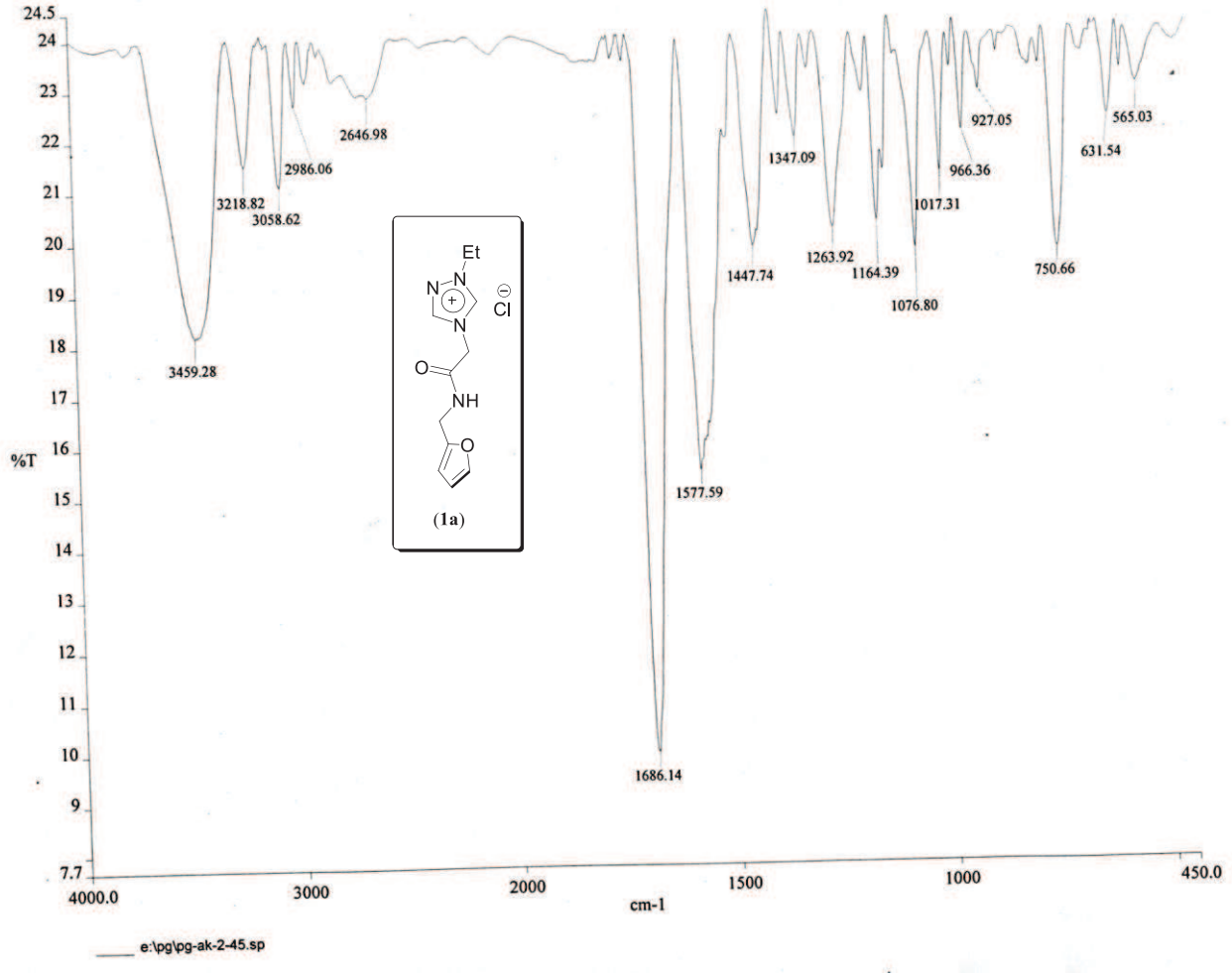

Figure S3. Infrared spectrum of **1a** in KBr.

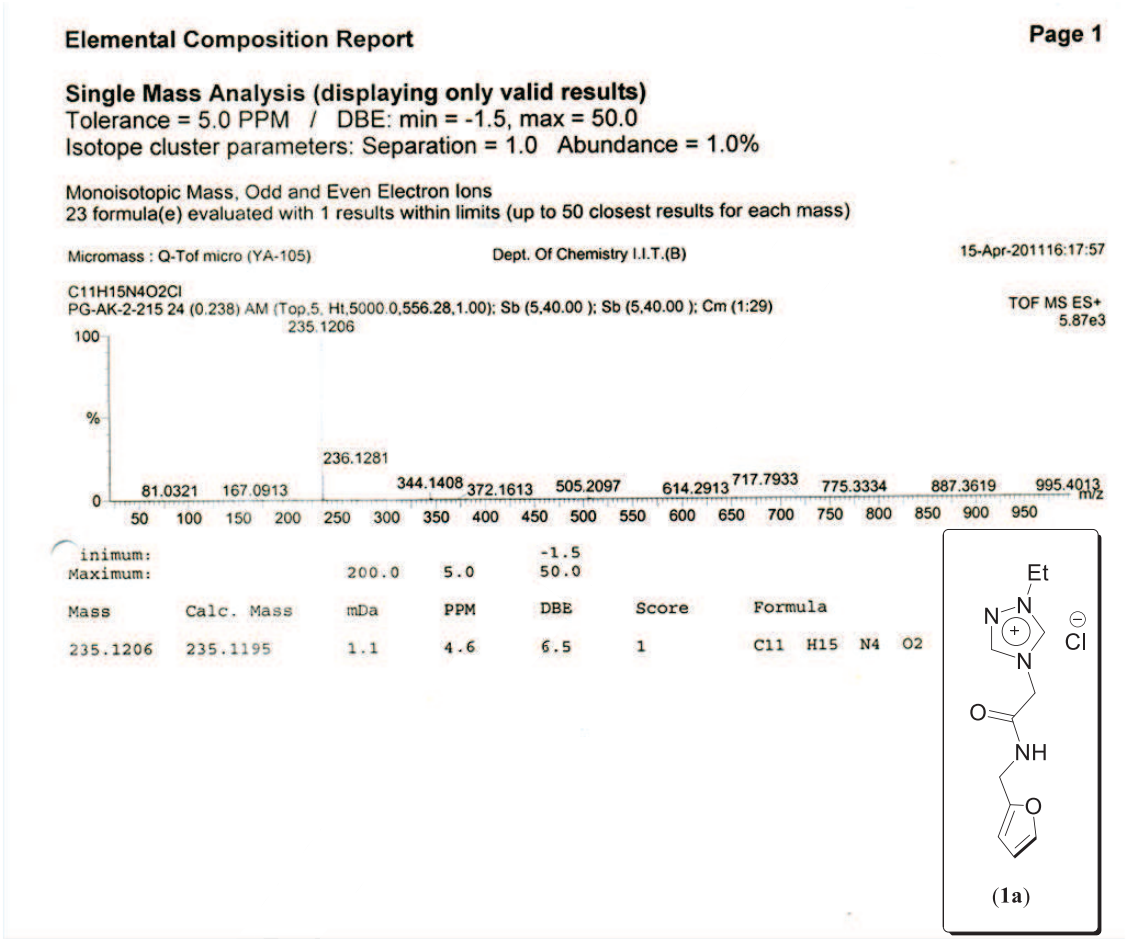

Figure S4. High Resolution Mass Spectrometry (HRMS) data of **1a.**

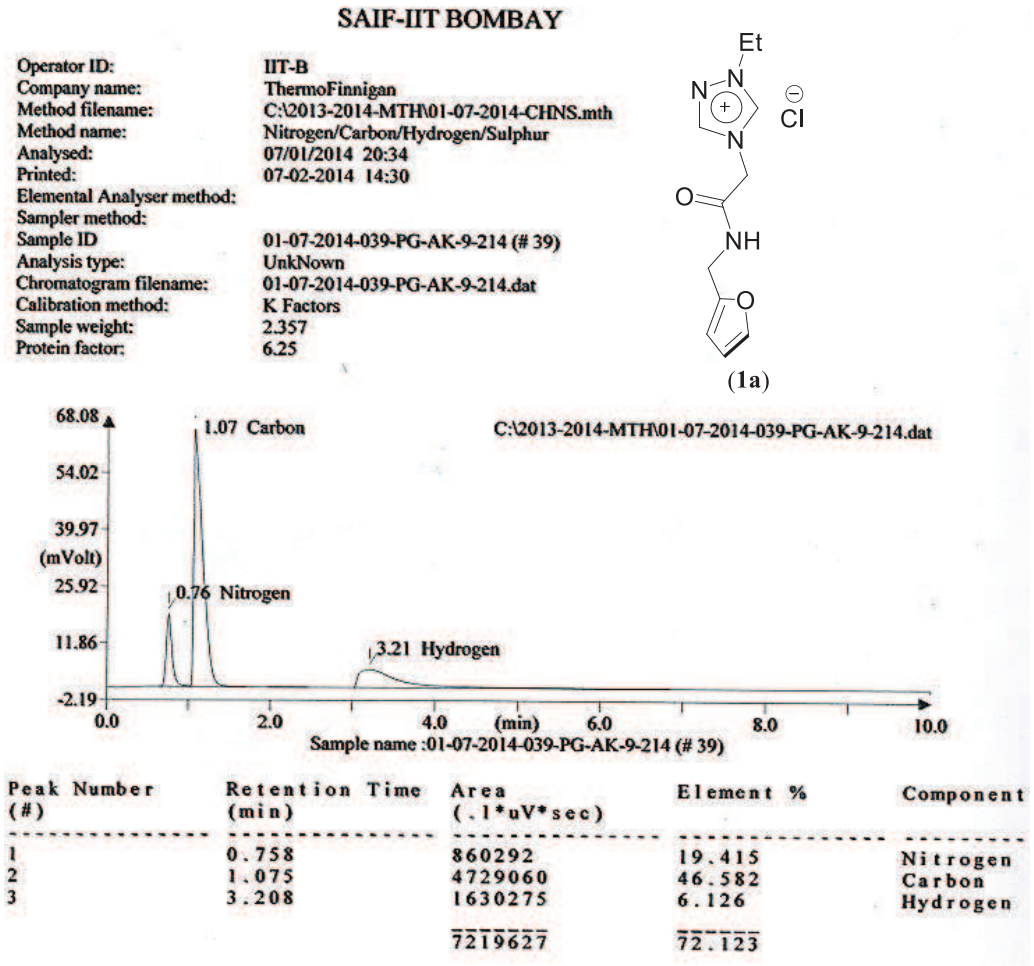

Figure S5. Elemental analysis data of **1a**.

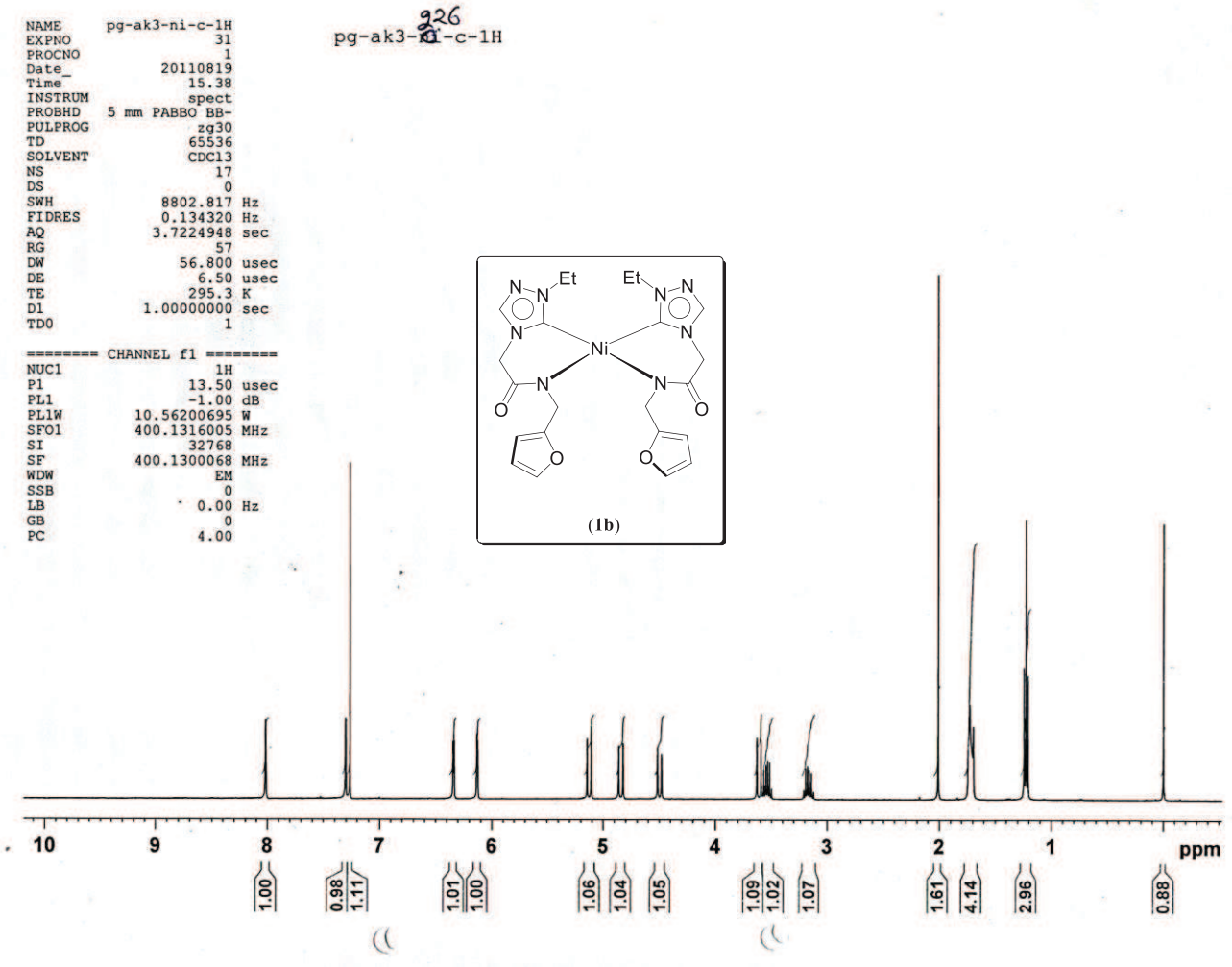

Figure S6. ^{1}H NMR spectrum of **1b** in $CDCl_3$.

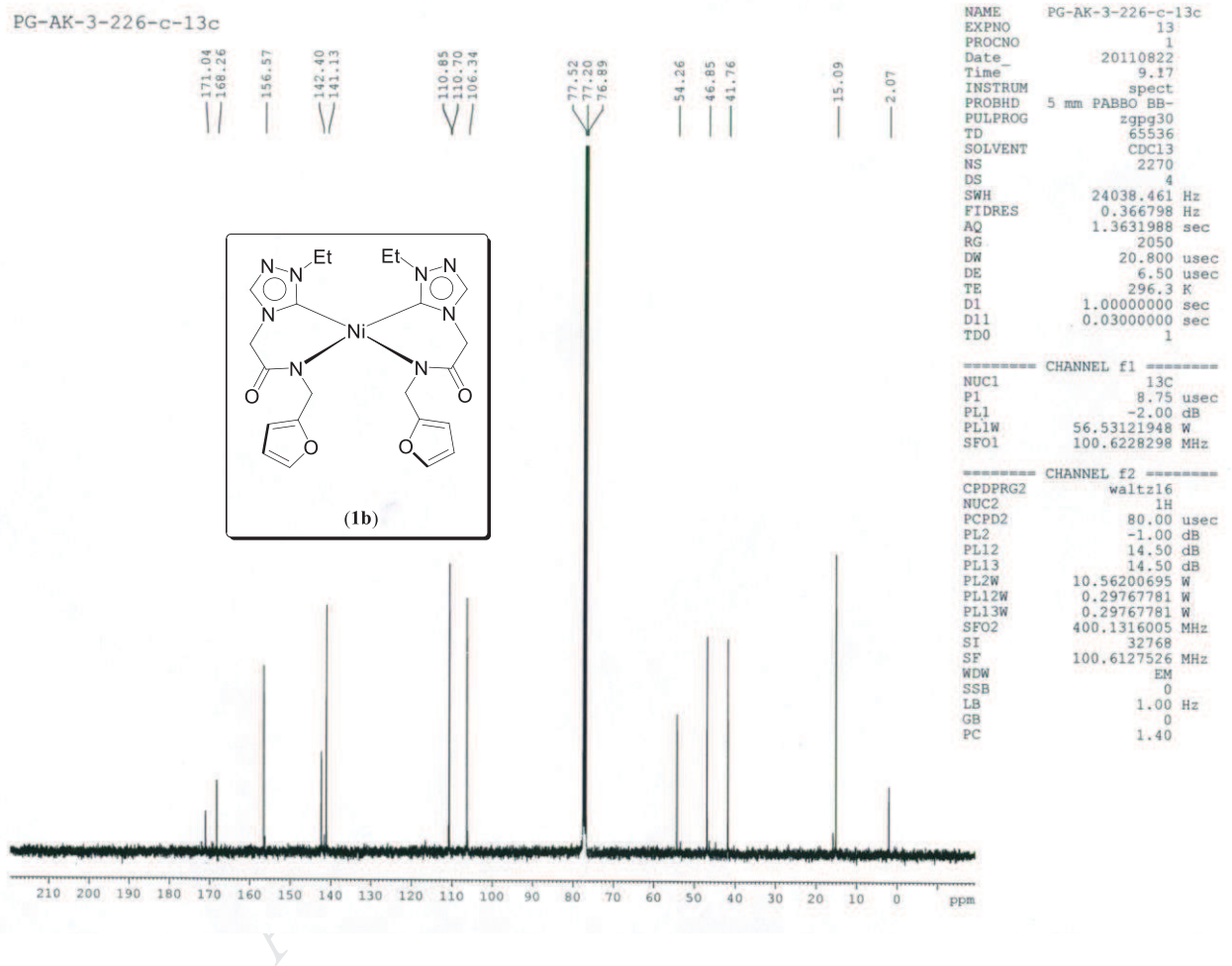

Figure S7. $^{13}C\{^{1}H\}$ NMR spectrum of **1b** in $CDCl_3$.

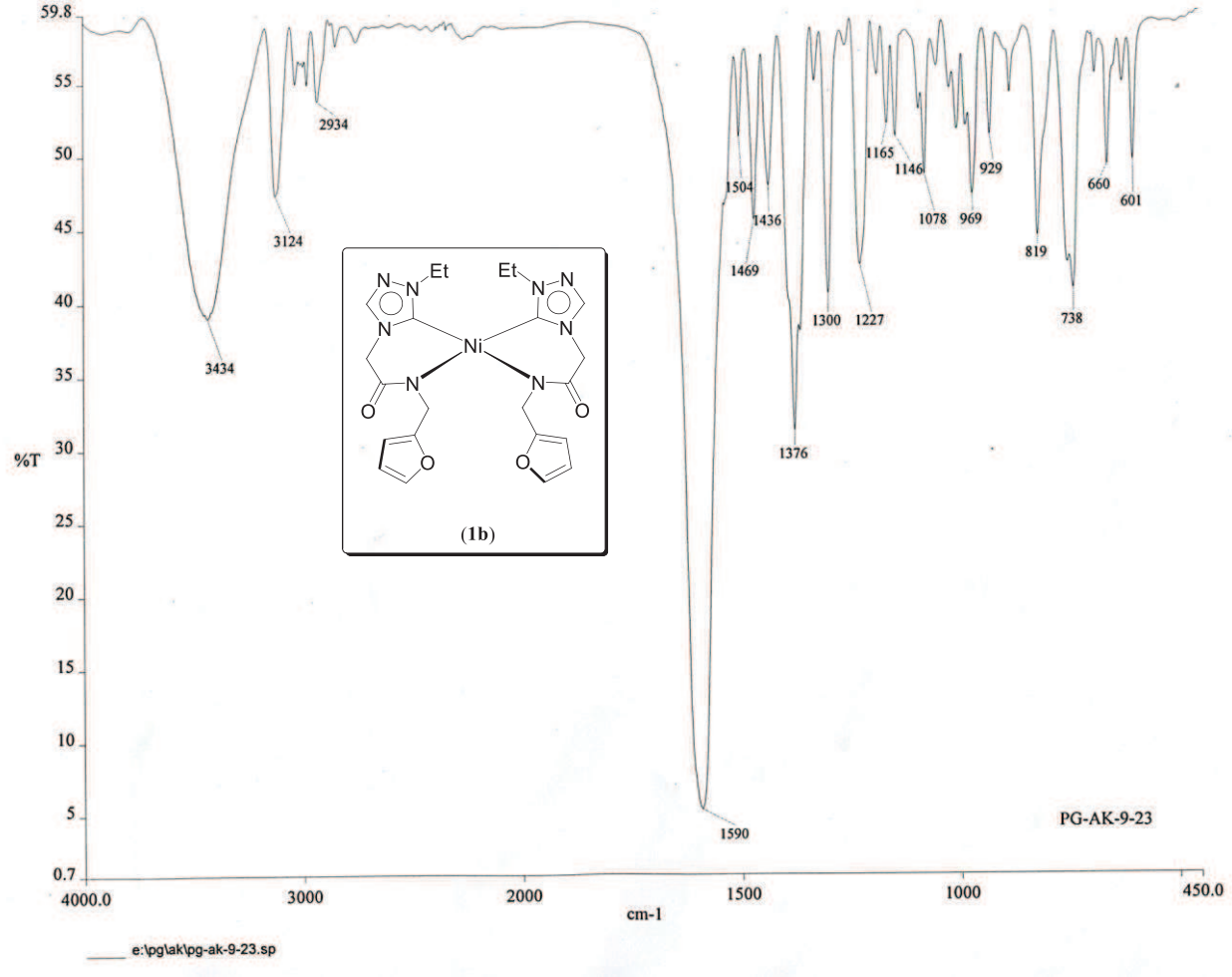

Figure S8. Infrared spectrum of **1b** in KBr.

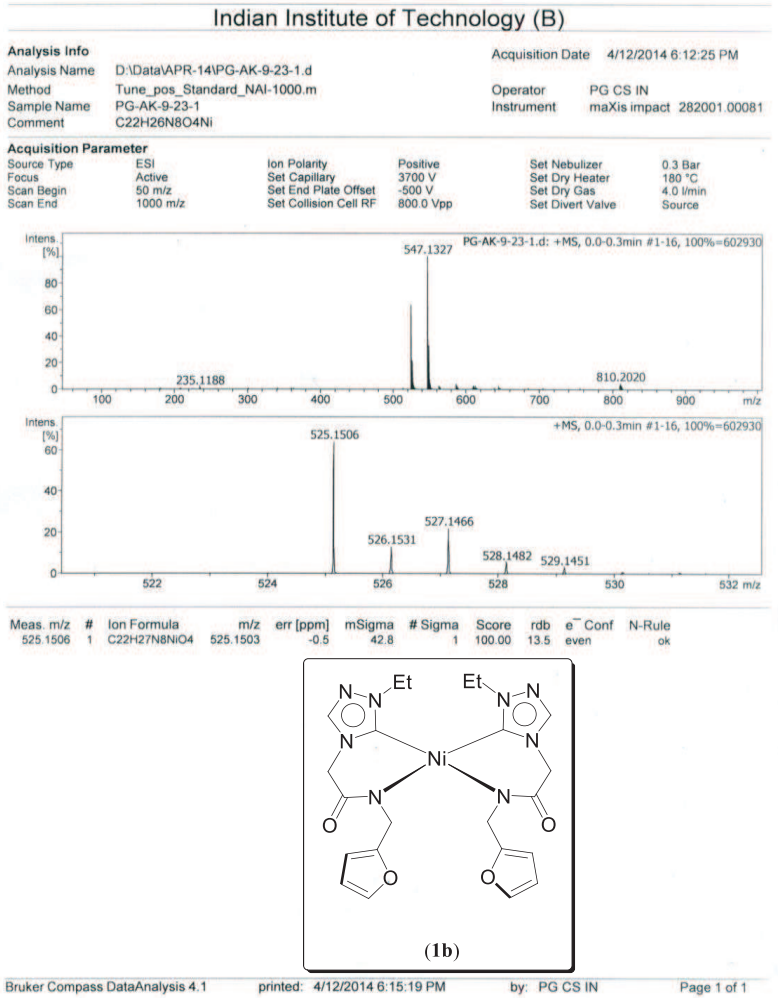

Figure S9. High Resolution Mass Spectrometry (HRMS) data of **1b.**

SAIF-IIT BOMBAY

rator ID:	pradnya
mpany name:	ThermoFinnigan
Method filename:	C:\chns-o analyser\methods\17-10-2011-chns-mth.mth
Method name:	Nitrogen/Carbon/Hydrogen/Sulphur
Analysed:	10/17/2011 19:08
Printed:	10-18-2011 14:52
Elemental Analyser method:	
Sampler method:	
Sample ID	17-10-2011040-PG-AK-4-77-IN (# 40)
Analysis type:	UnkNown
Chromatogram filename:	17-10-2011040-PG-AK-4-77-IN.dat
Calibration method:	K Factors
Sample weight:	2.428
Protein factor:	6.25

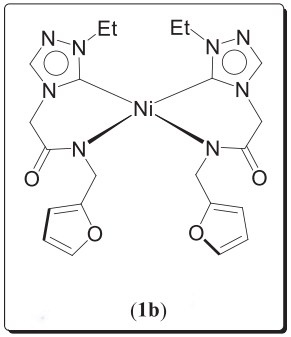

(1b)

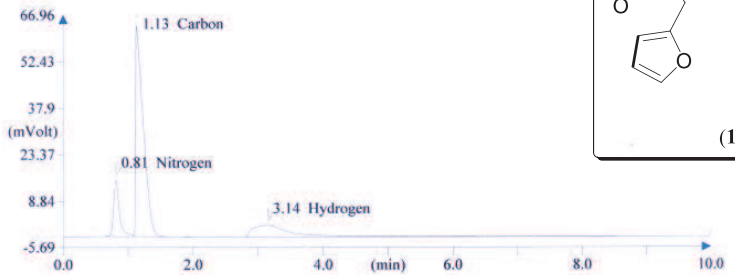

Peak Number (#)	Retention Time (min)	Area (.1*uV*sec)	Element %	Component
1	0.808	1099861	20.297	Nitrogen
2	1.133	5381218	48.422	Carbon
3	3.142	1618790	5.447	Hydrogen
		8099869	74.166	

Figure S10. Elemental analysis data of **1b**.

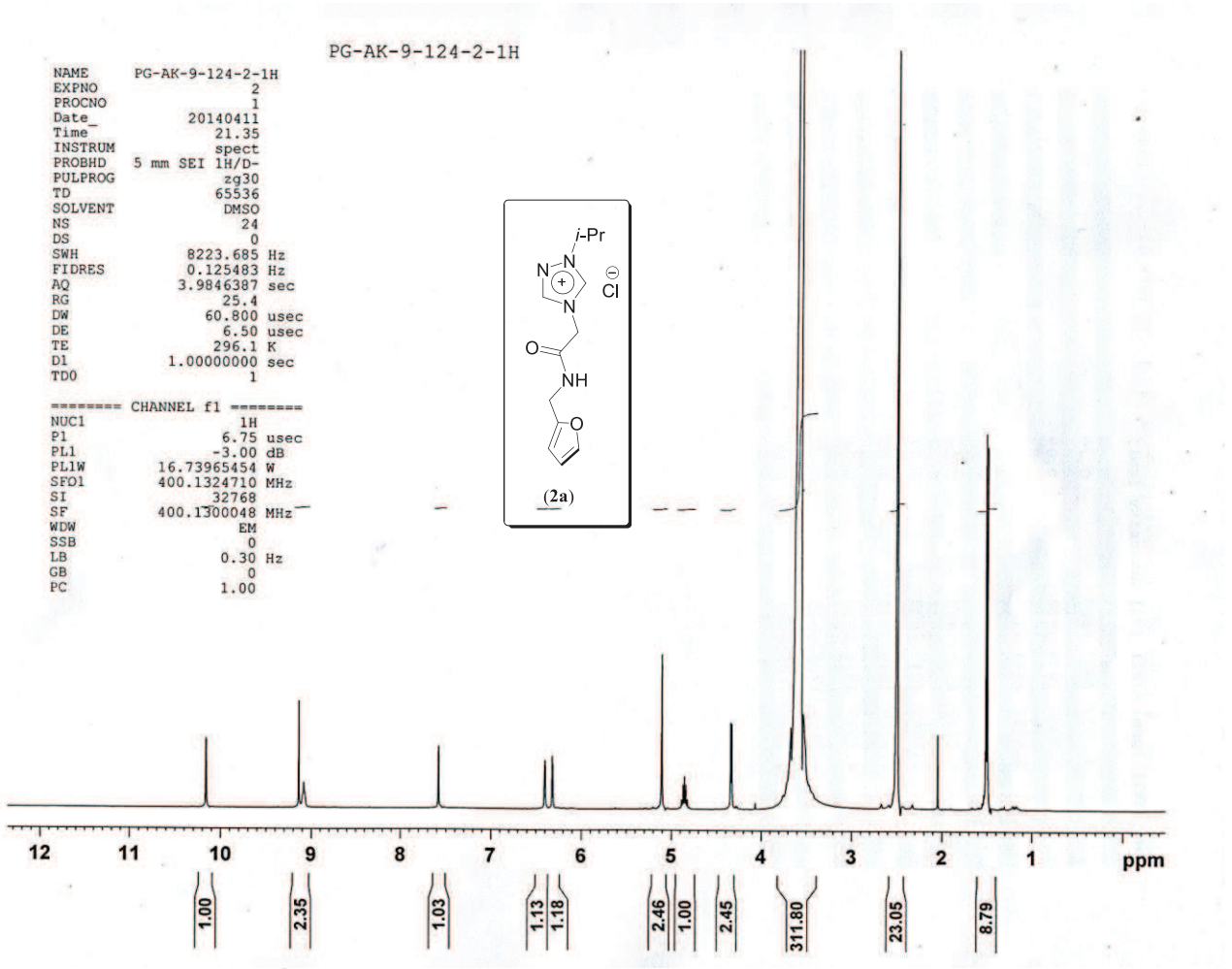

Figure S11. ^{1}H NMR spectrum of **2a** in DMSO-d_6.

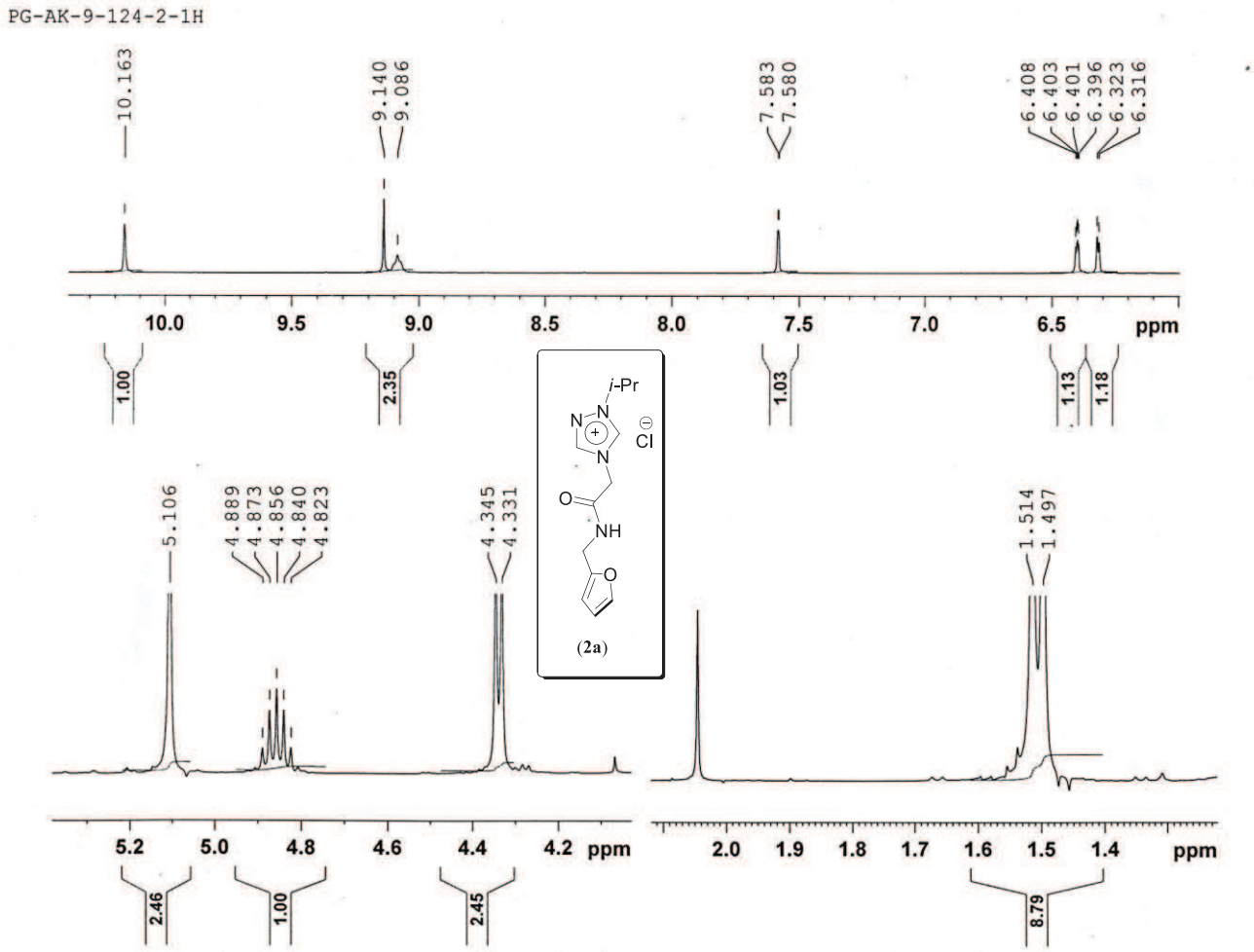

Figure S12. Expanded ^{1}H NMR spectrum of **2a** in DMSO-d_6.

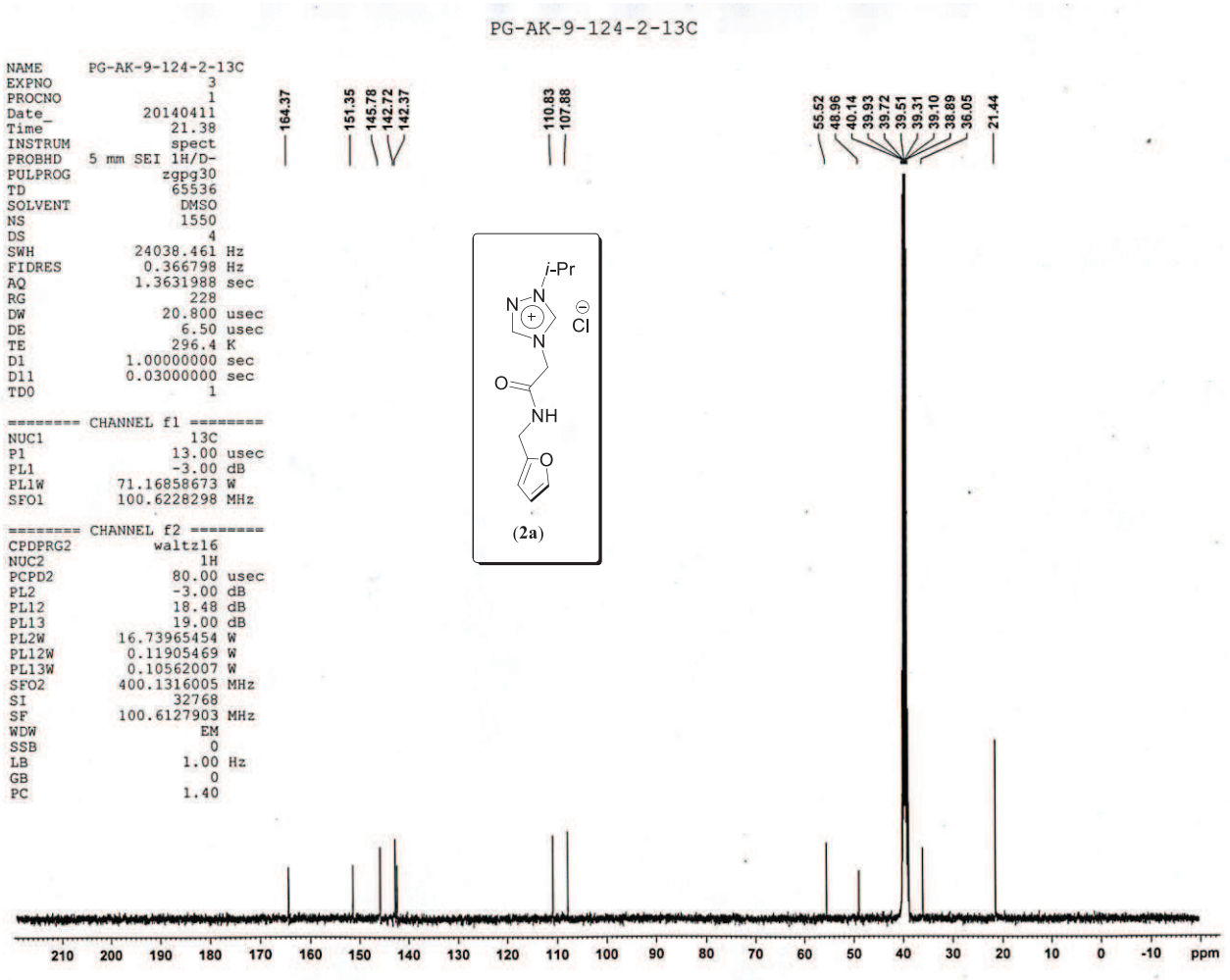

Figure S13. $^{13}C\{^{1}H\}$ NMR spectrum of **2a** in DMSO-d_6.

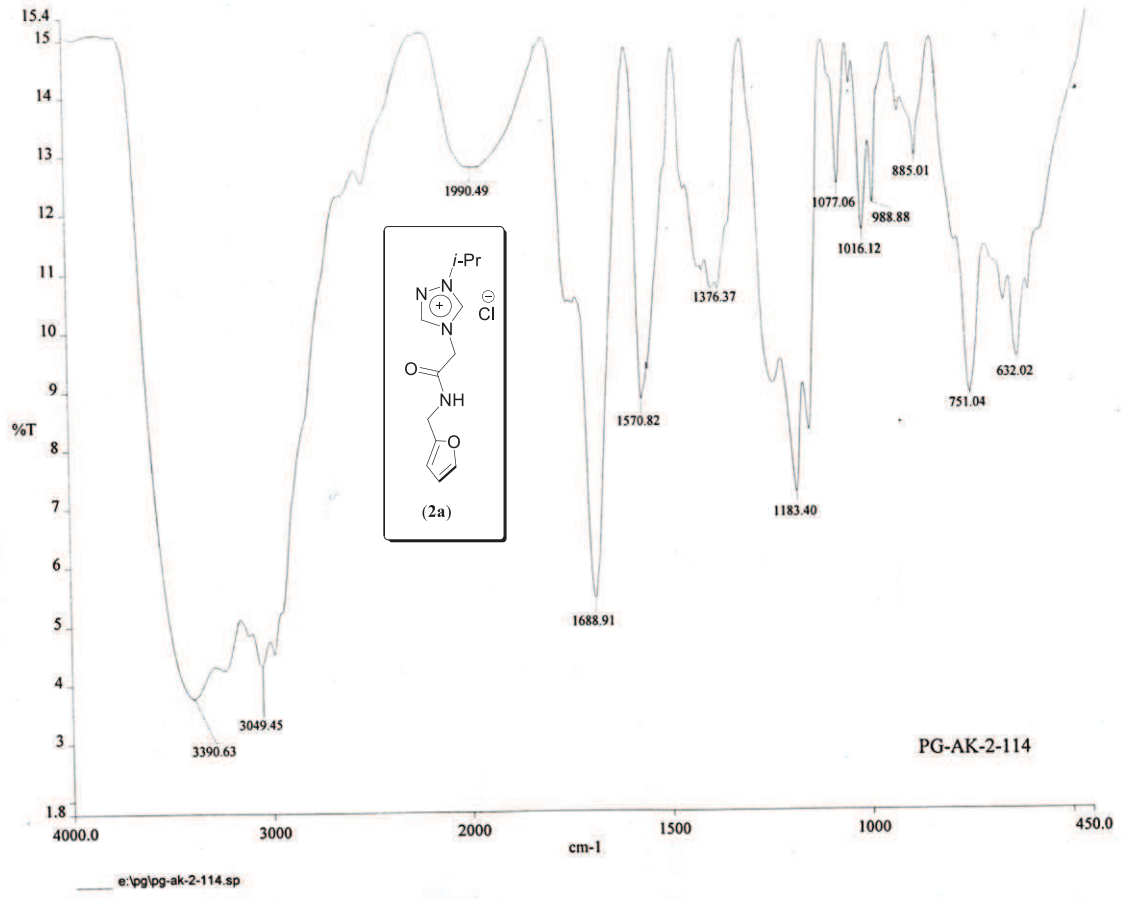

Figure S14. Infrared spectrum of **2a** in KBr.

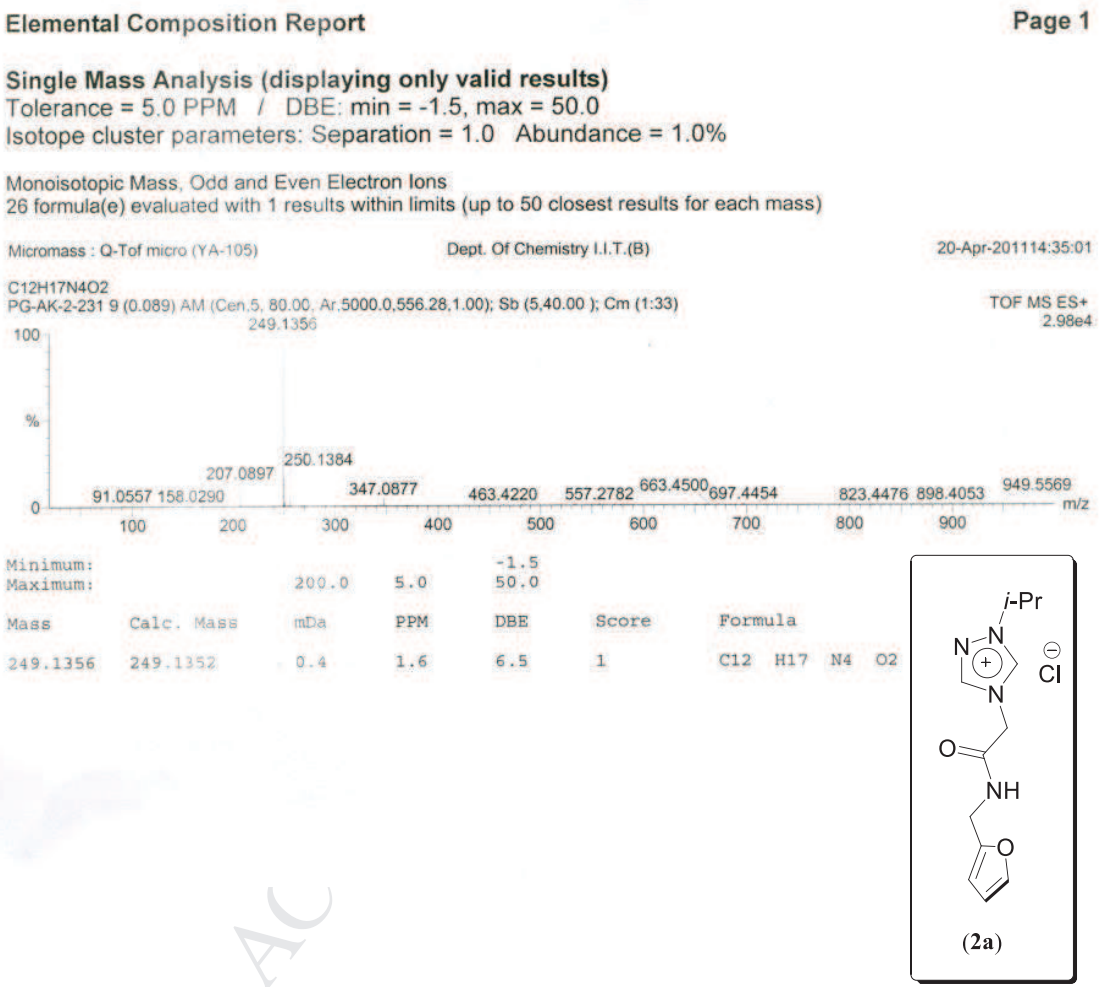

Figure S15. High Resolution Mass Spectrometry (HRMS) data of **2a.**

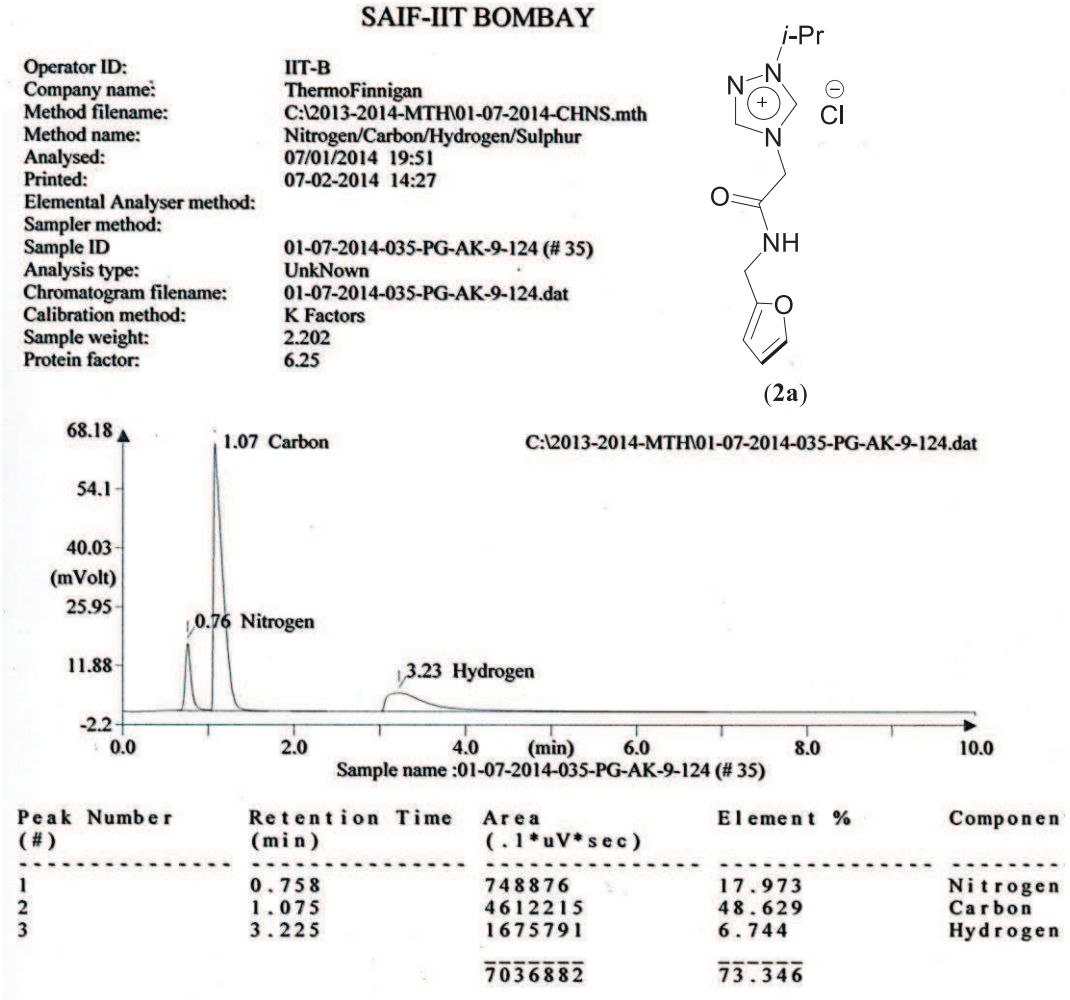

Peak Number (#)	Retention Time (min)	Area (.1*uV*sec)	Element %	Componen
1	0.758	748876	17.973	Nitrogen
2	1.075	4612215	48.629	Carbon
3	3.225	1675791	6.744	Hydrogen
		7036882	73.346	

Figure S16. Elemental analysis data of **2a**.

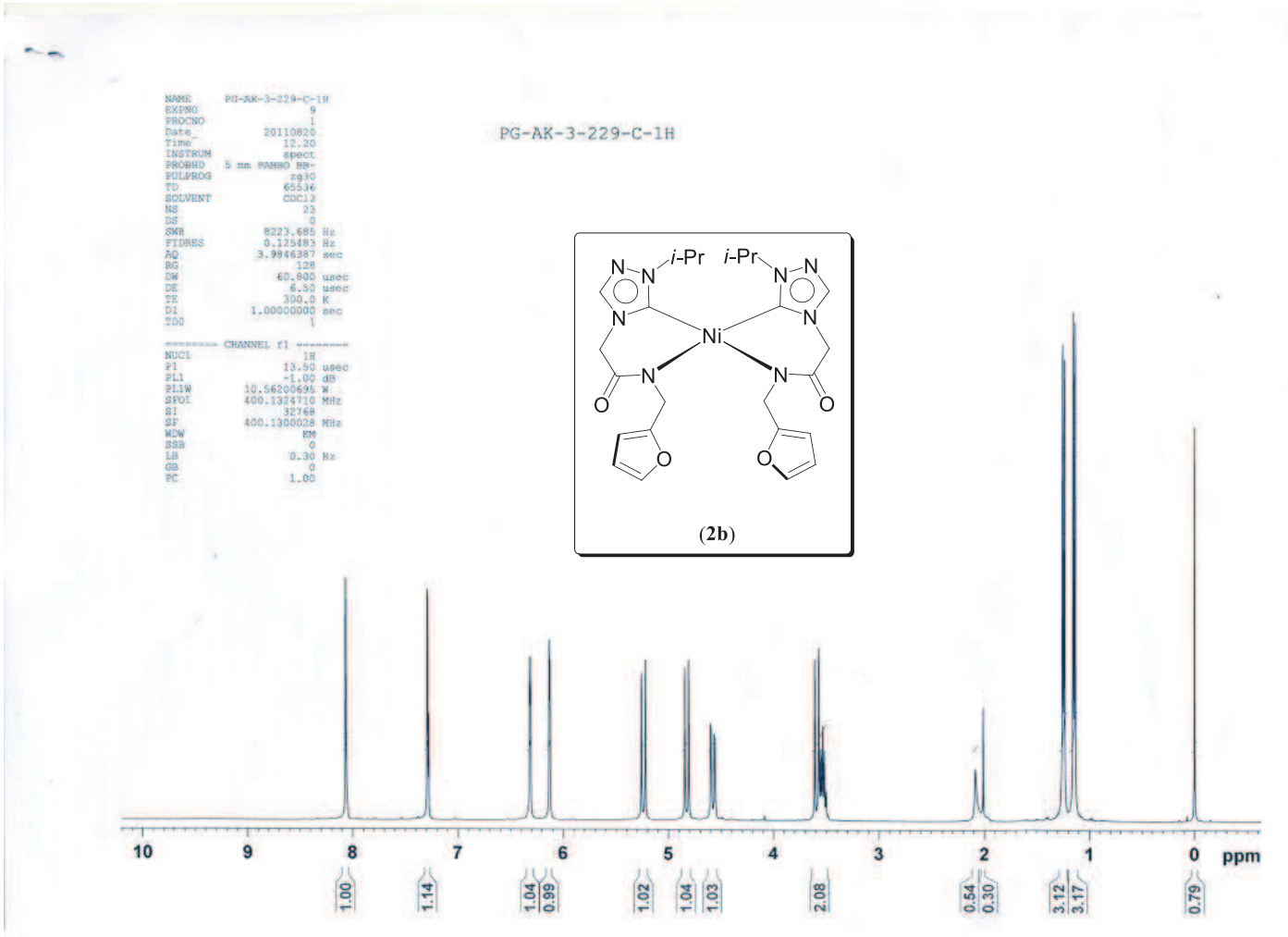

Figure S17. ^{1}H NMR spectrum of **2b** in $CDCl_3$.

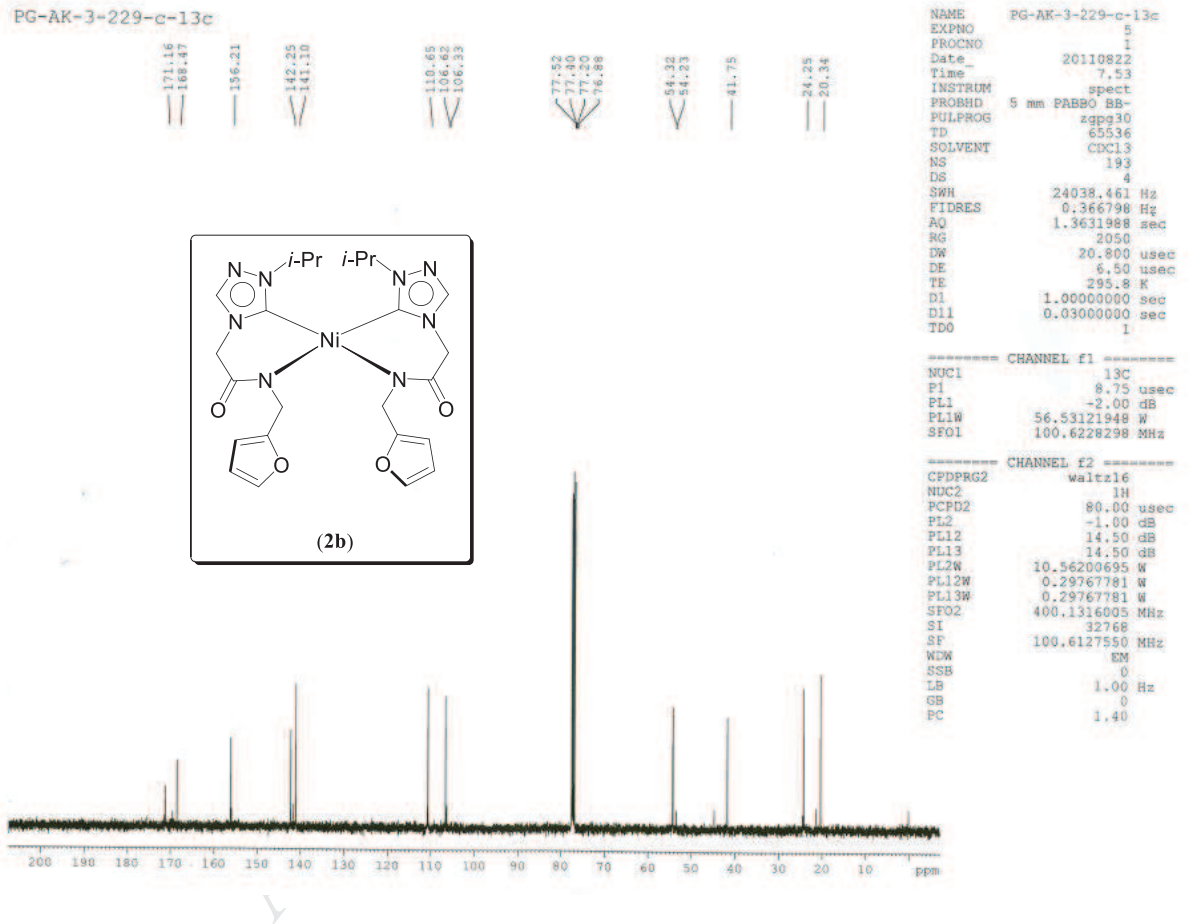

Figure S18. $^{13}C\{^{1}H\}$ NMR spectrum of **2b** in $CDCl_3$.

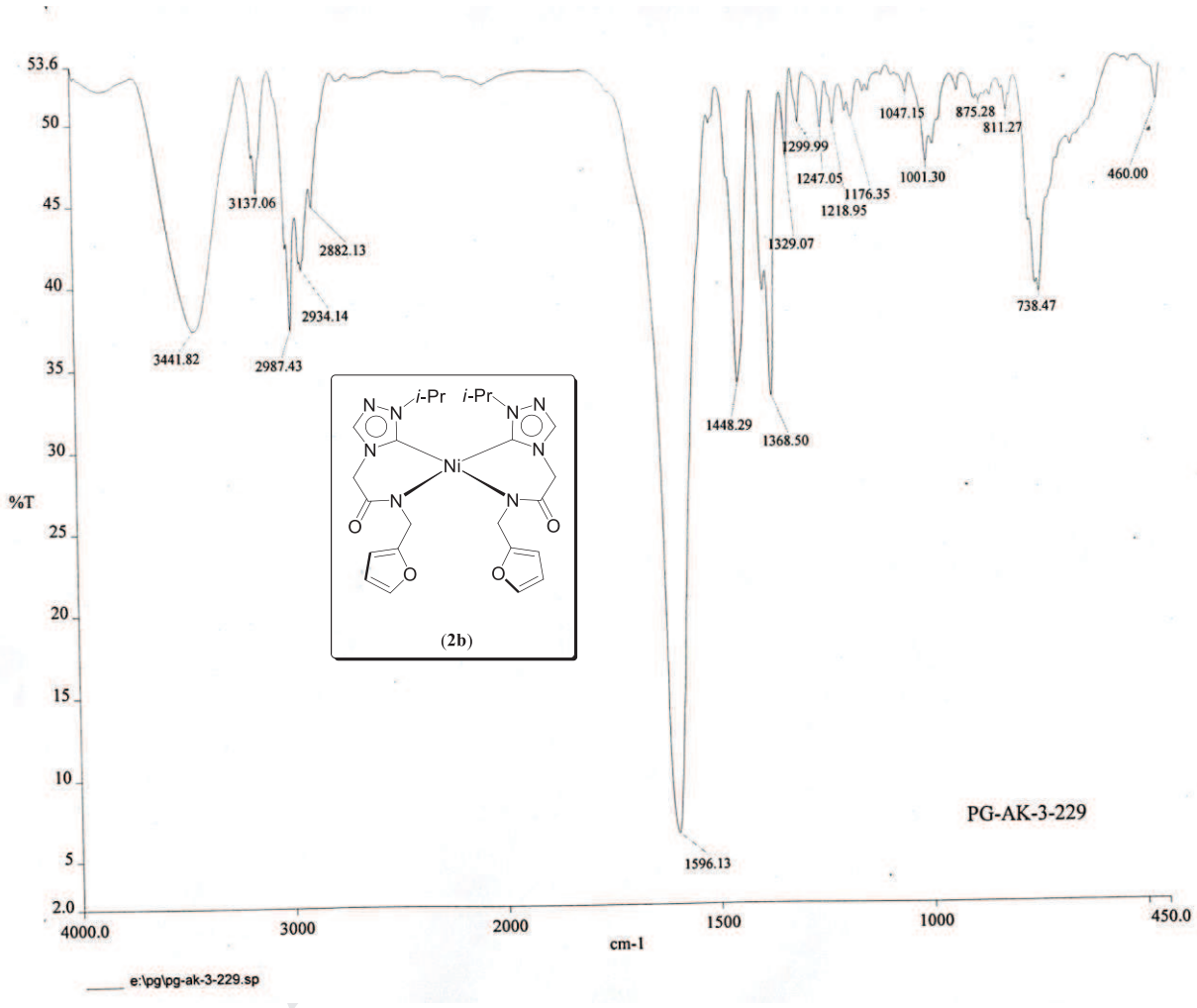

Figure S19. Infrared spectrum of **2b** in KBr.

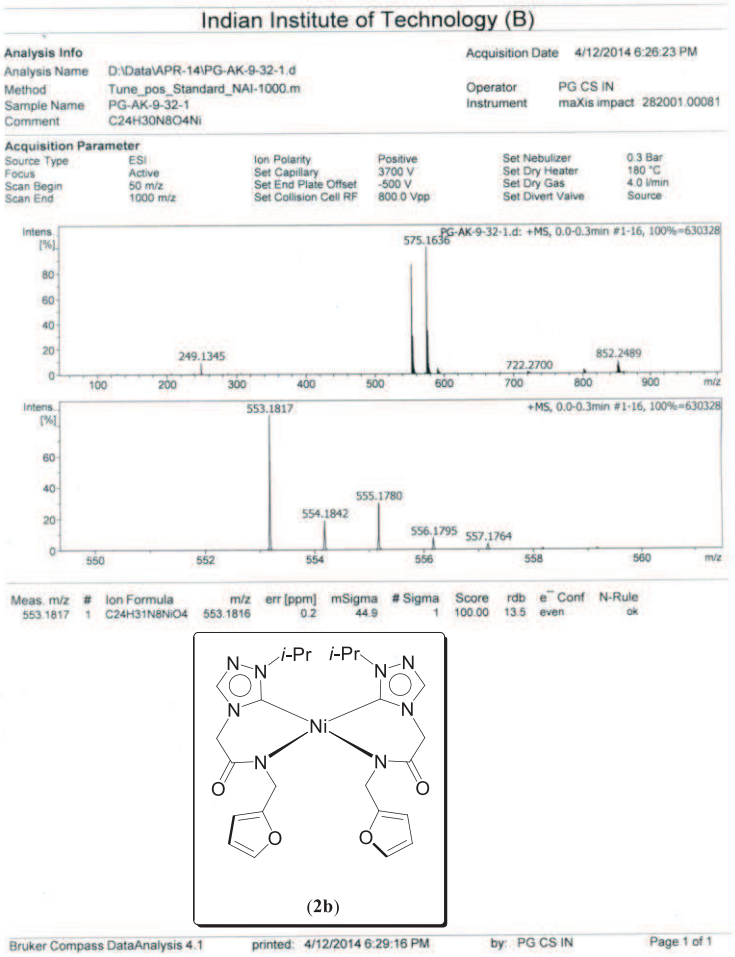

Figure S20. High Resolution Mass Spectrometry (HRMS) data of **2b.**

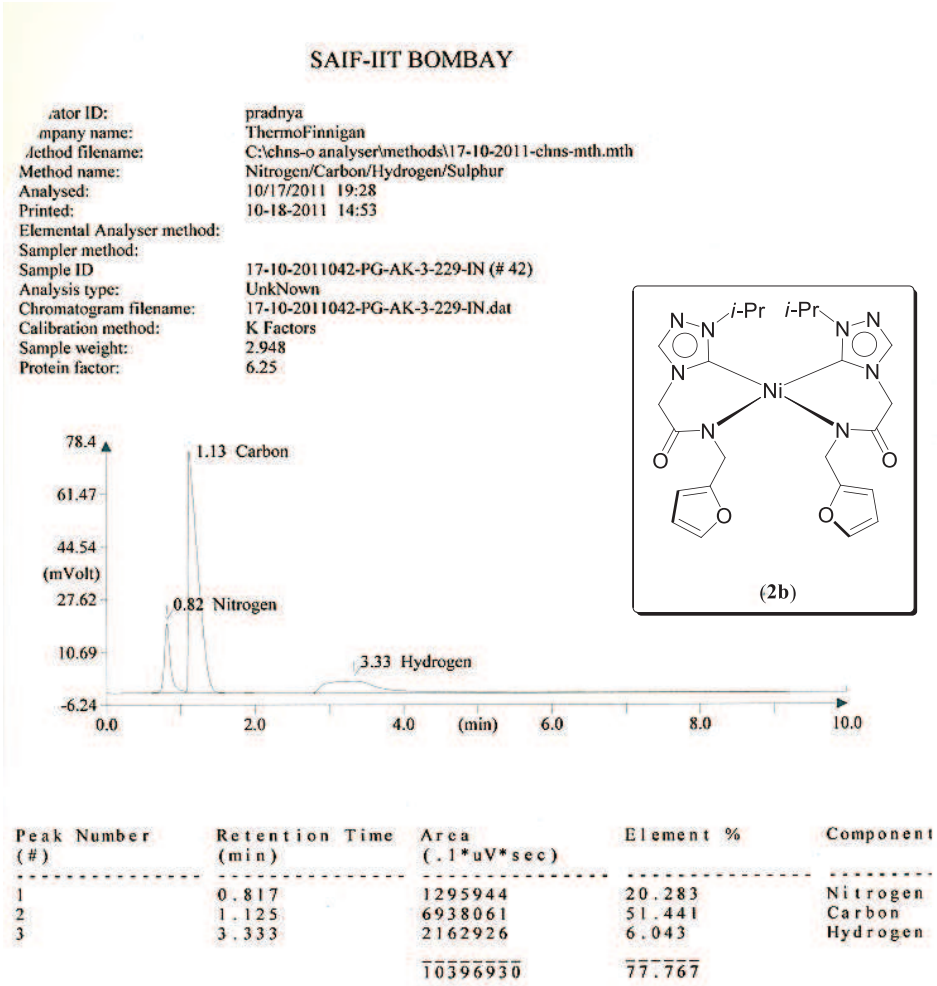

Figure S21. Elemental analysis data of **2b**.

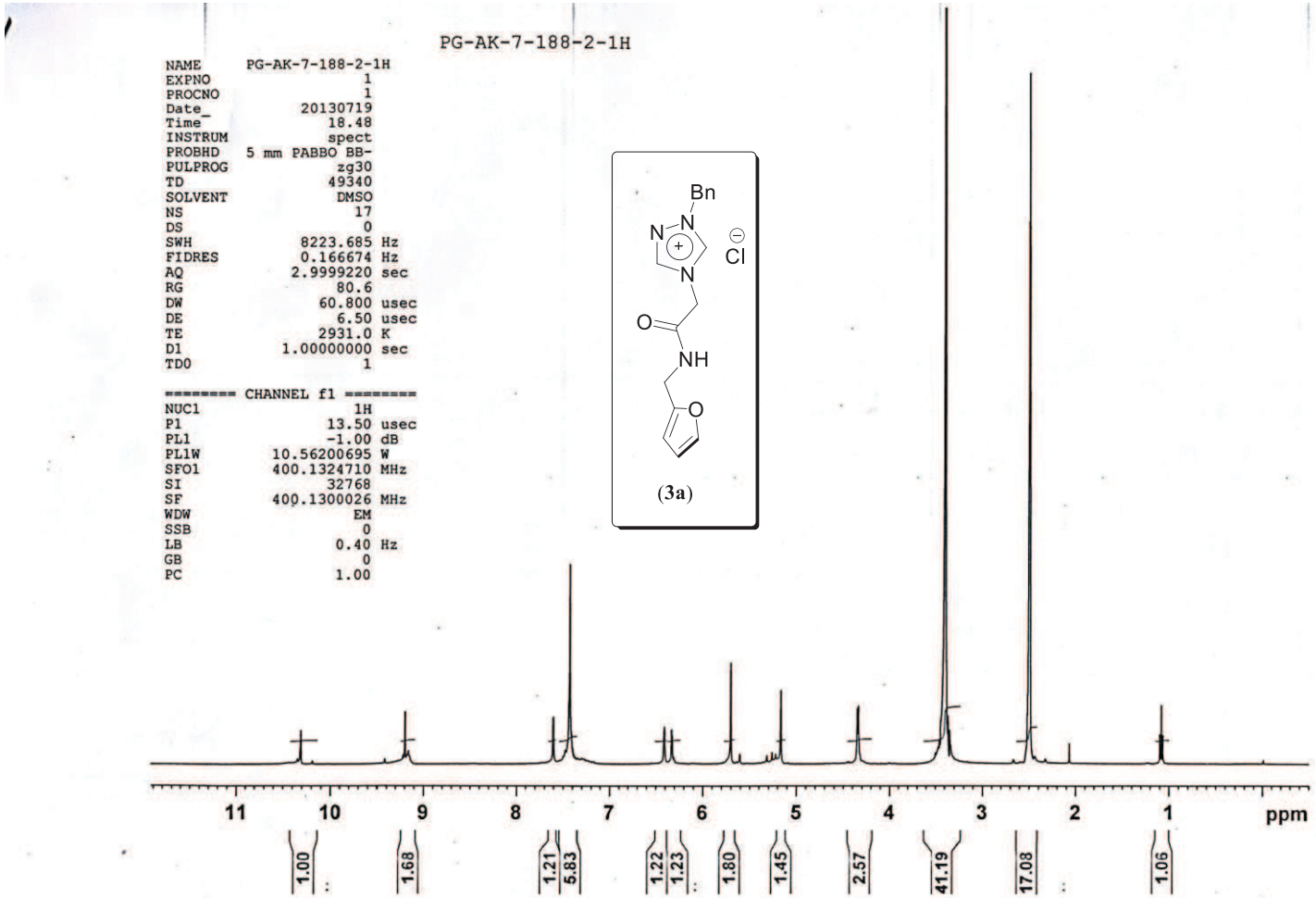

Figure S22. ^{1}H NMR spectrum of **3a** in DMSO-d_6.

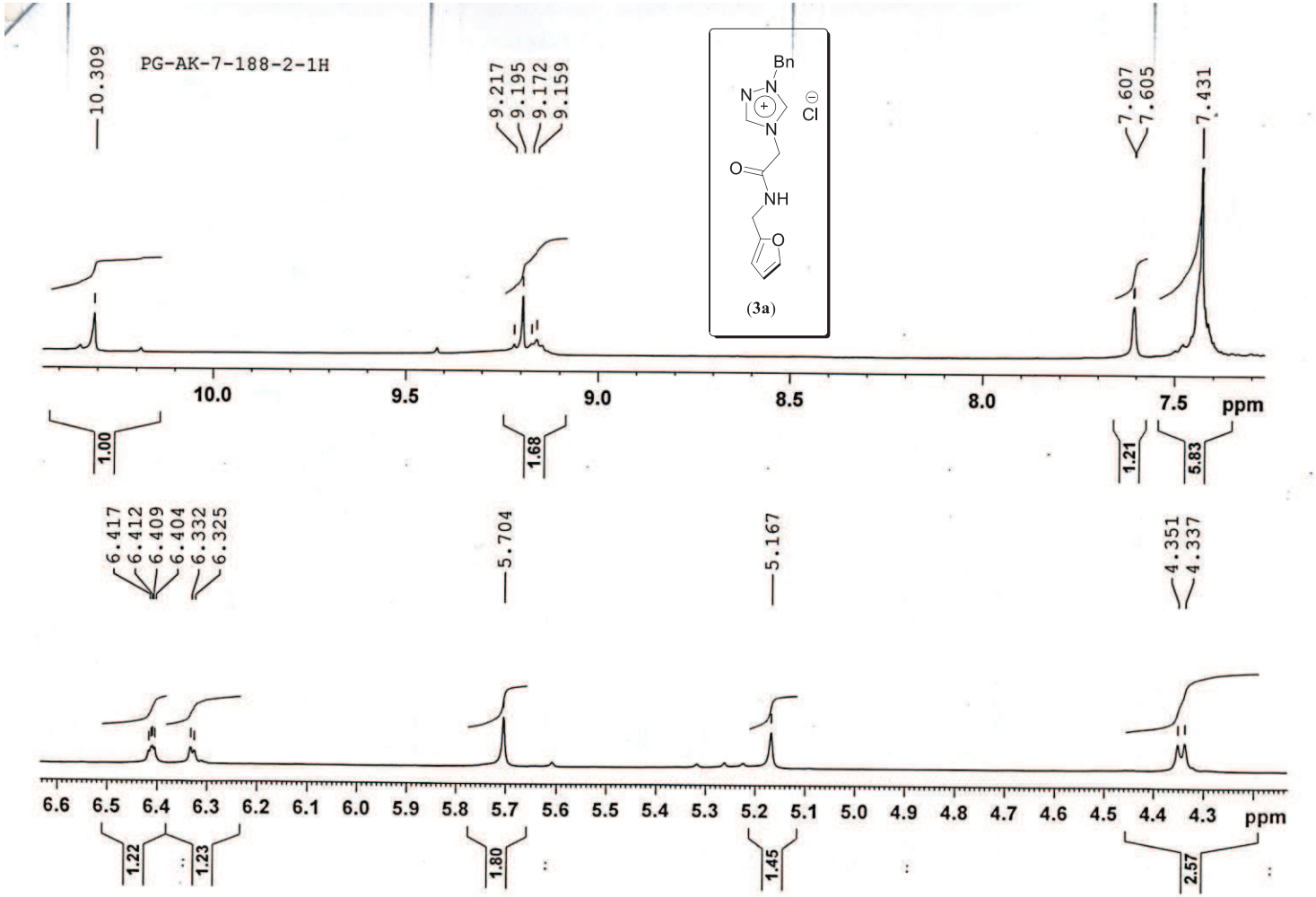

Figure S23. Expanded ^{1}H NMR spectrum of **3a** in DMSO-d_6.

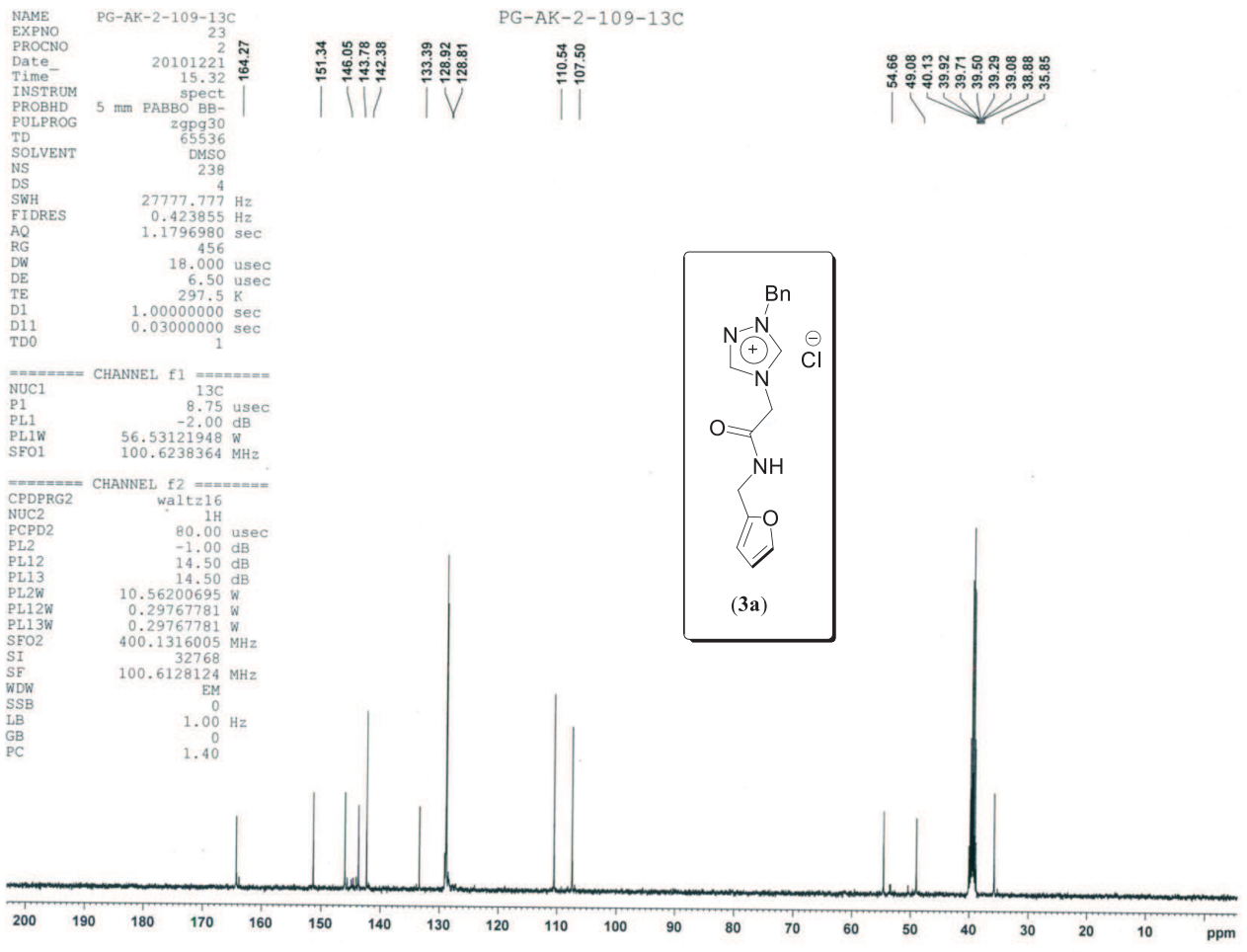

Figure S24. $^{13}C\{^{1}H\}$ NMR spectrum of **3a** in DMSO-d_6.

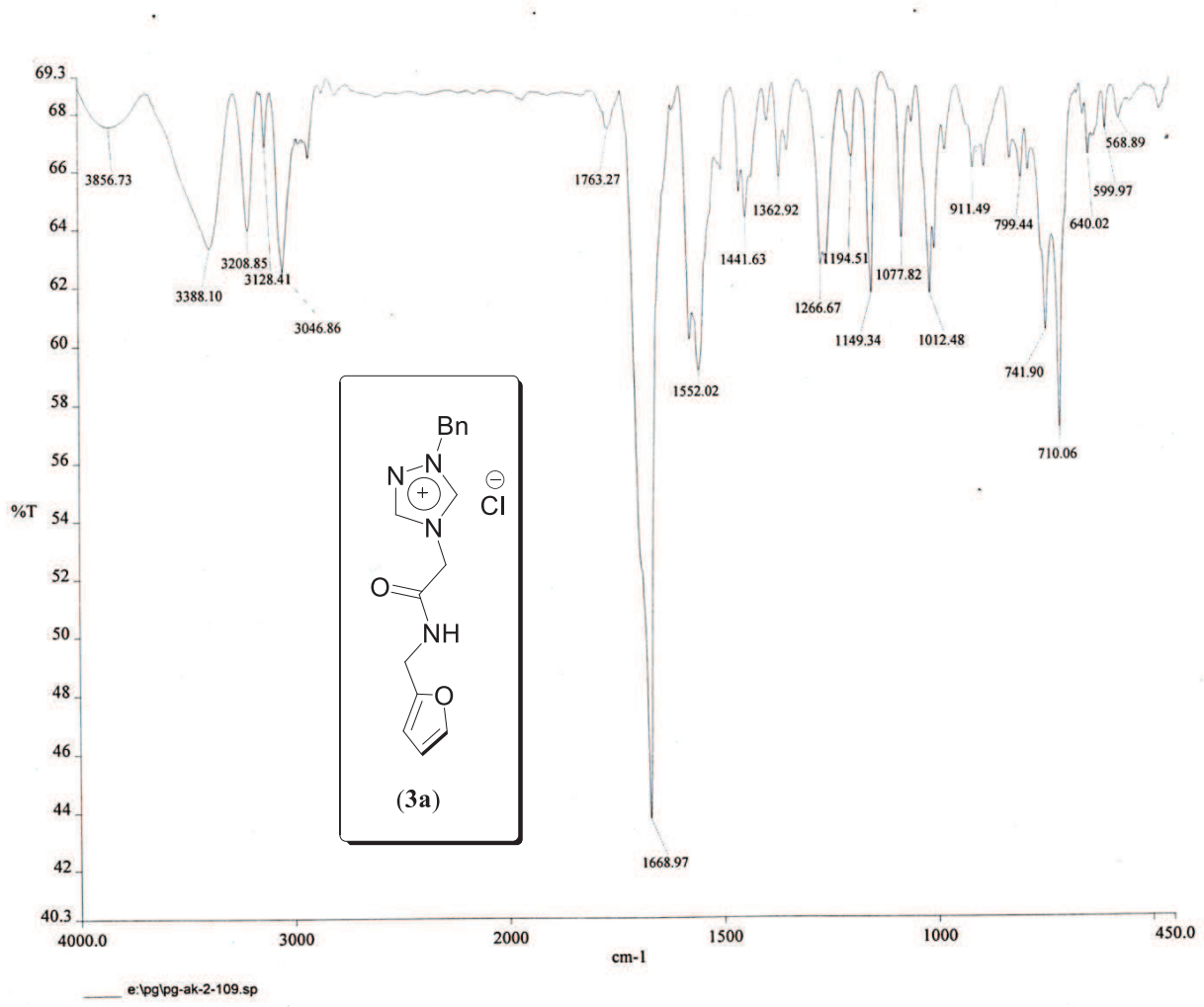

Figure S25. Infrared spectrum of **3a** in KBr.

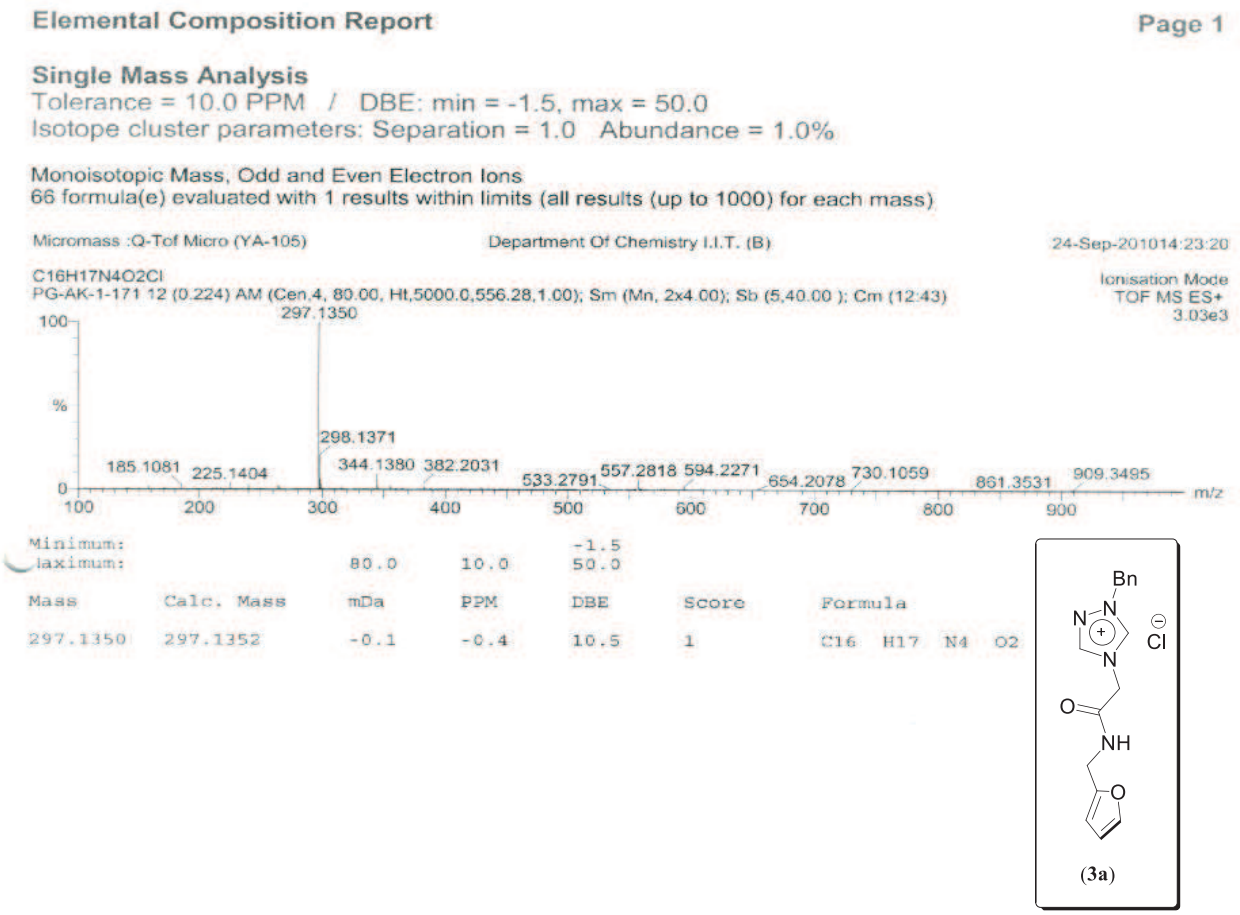

Figure S26. High Resolution Mass Spectrometry (HRMS) data of **3a.**

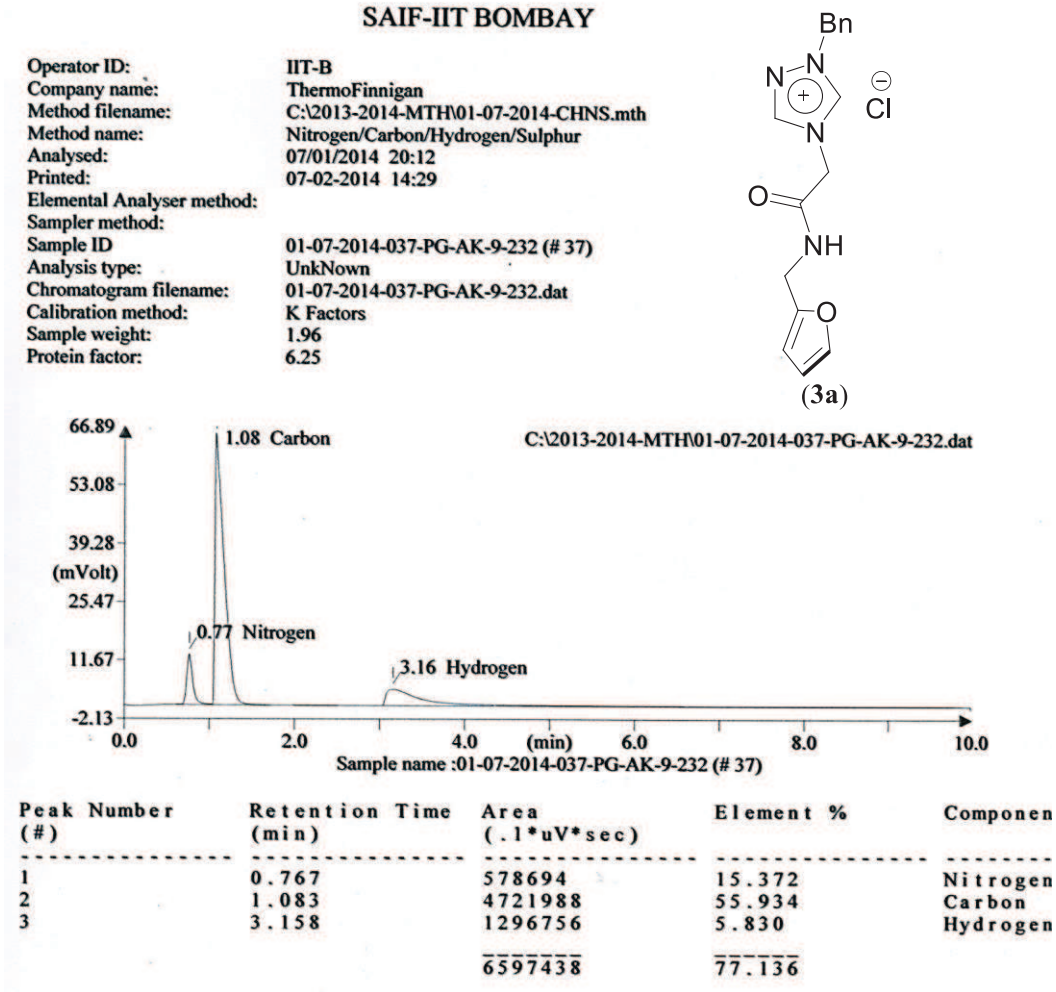

Peak Number (#)	Retention Time (min)	Area (.1*uV*sec)	Element %	Componen
1	0.767	578694	15.372	Nitrogen
2	1.083	4721988	55.934	Carbon
3	3.158	1296756	5.830	Hydrogen
		6597438	77.136	

Figure S27. Elemental analysis data of **3a**.

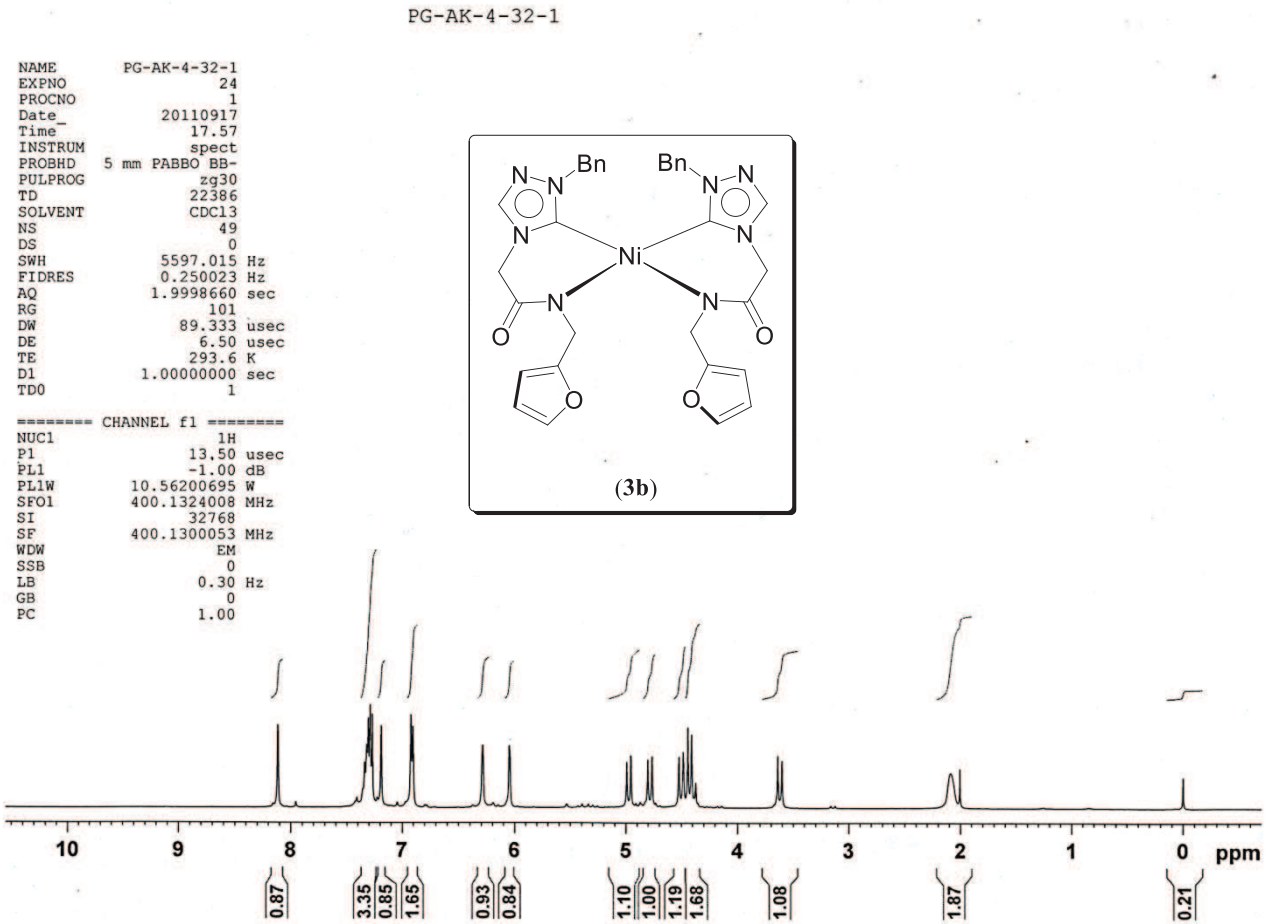

Figure S28. ^{1}H NMR spectrum of **3b** in $CDCl_3$.

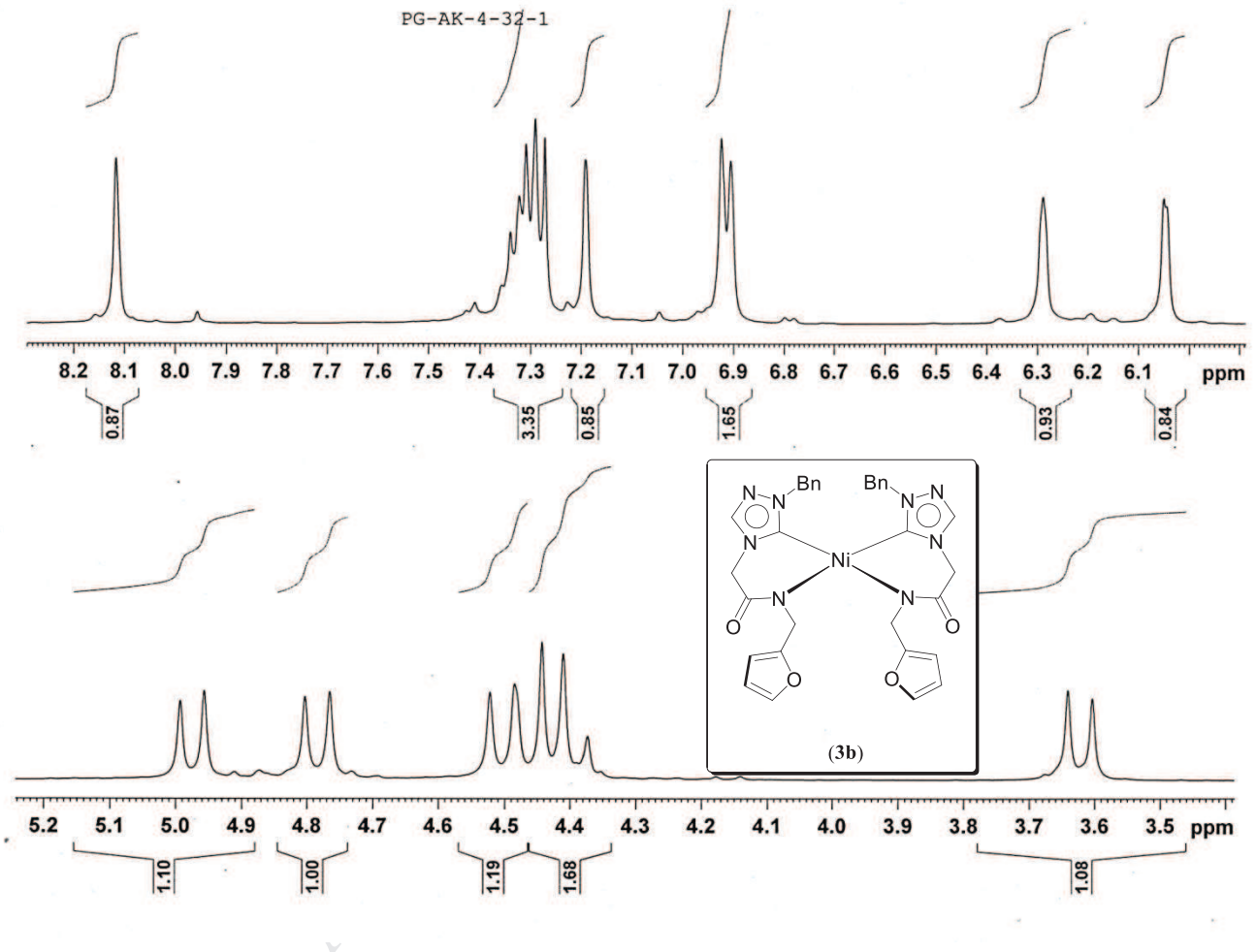

Figure S29. Expanded ^{1}H NMR spectrum of **3b** in $CDCl_3$.

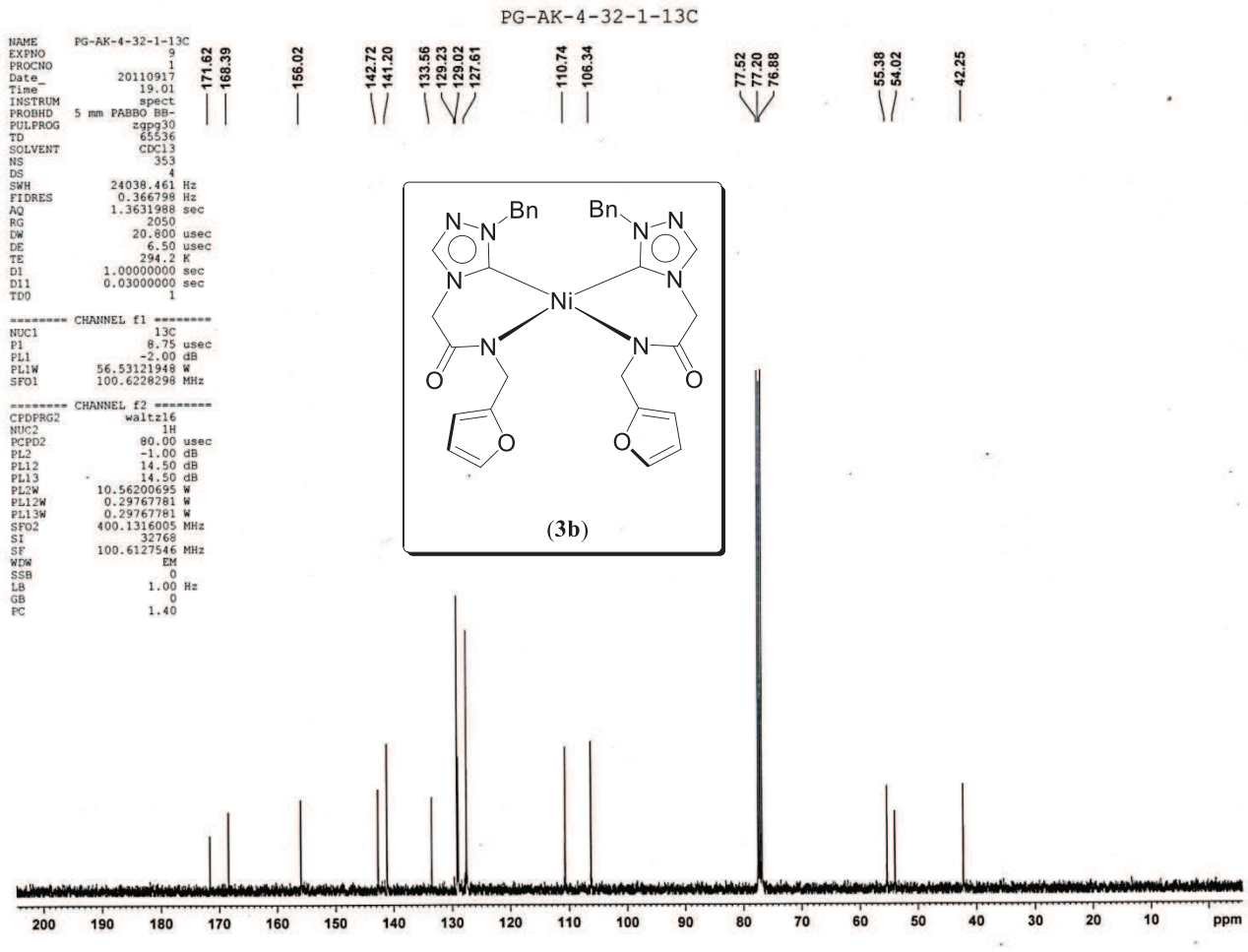

Figure S30. $^{13}C\{^{1}H\}$ NMR spectrum of **3b** in $CDCl_3$.

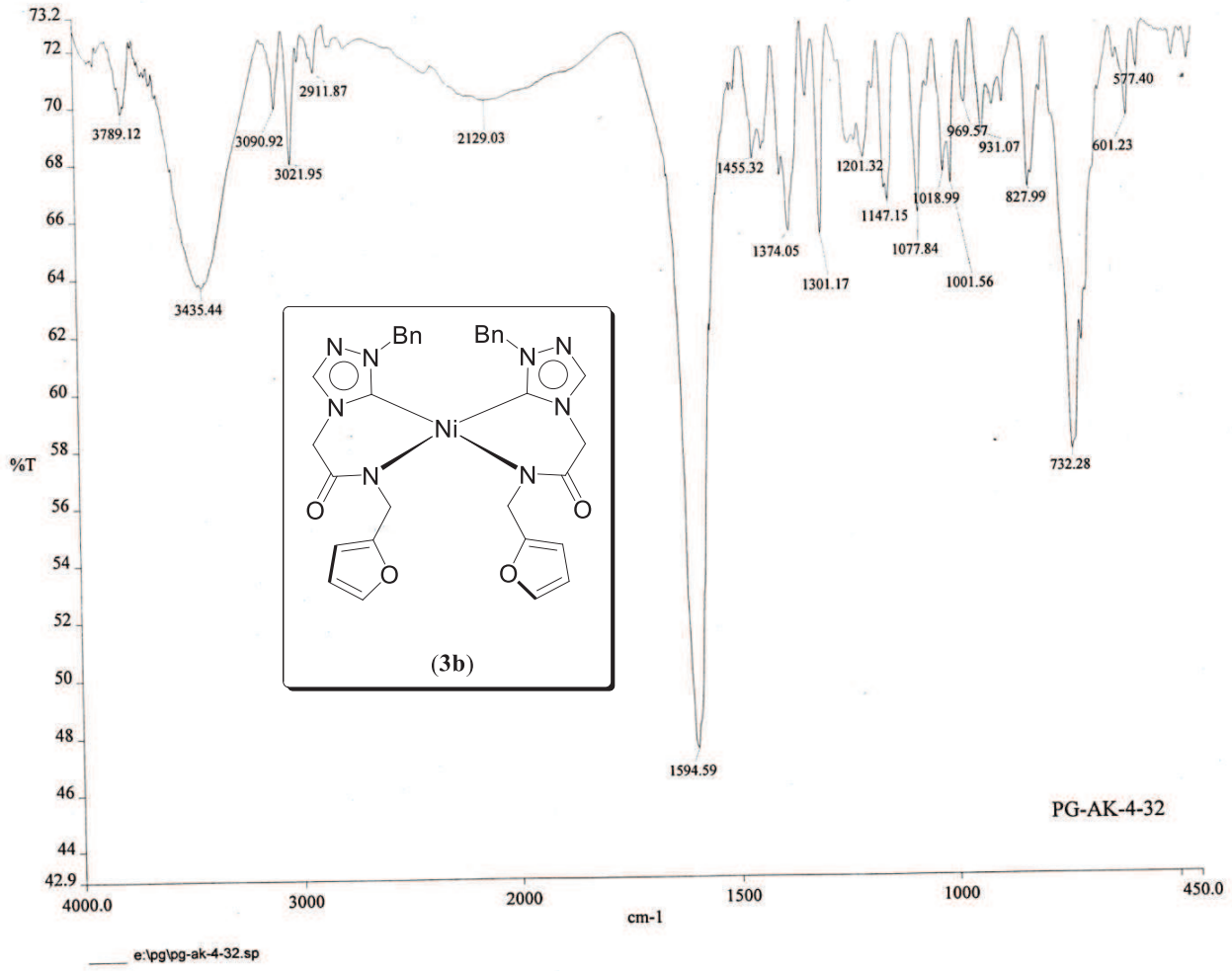

Figure S31. Infrared spectrum of **3b** in KBr.

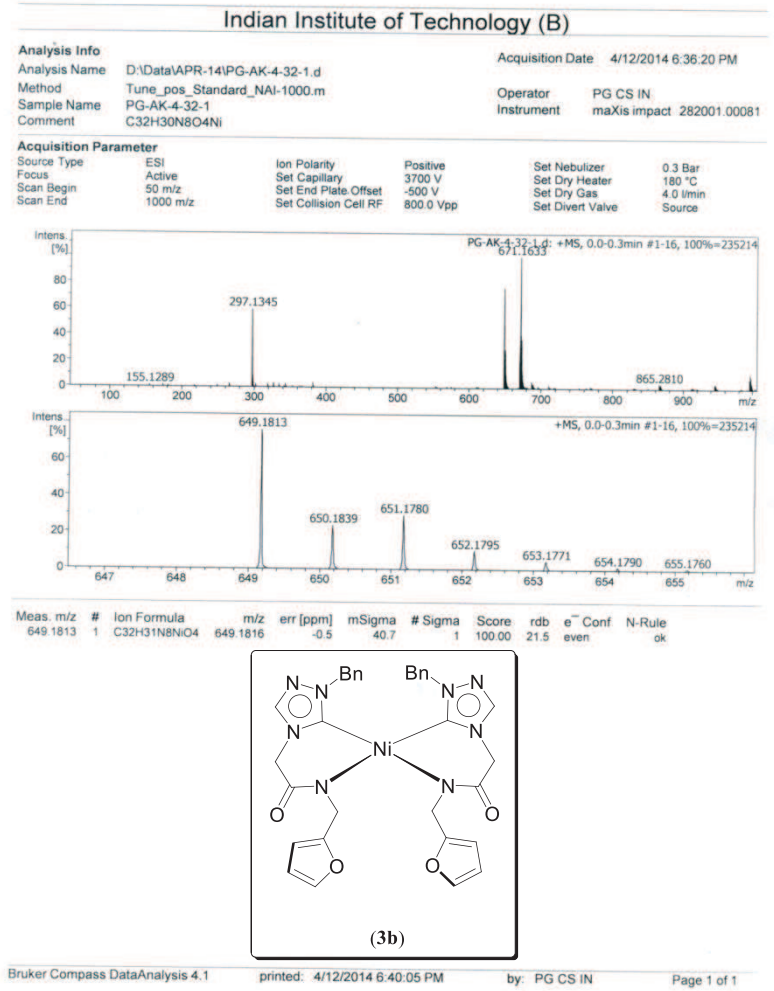

Figure S32. High Resolution Mass Spectrometry (HRMS) data of **3b.**

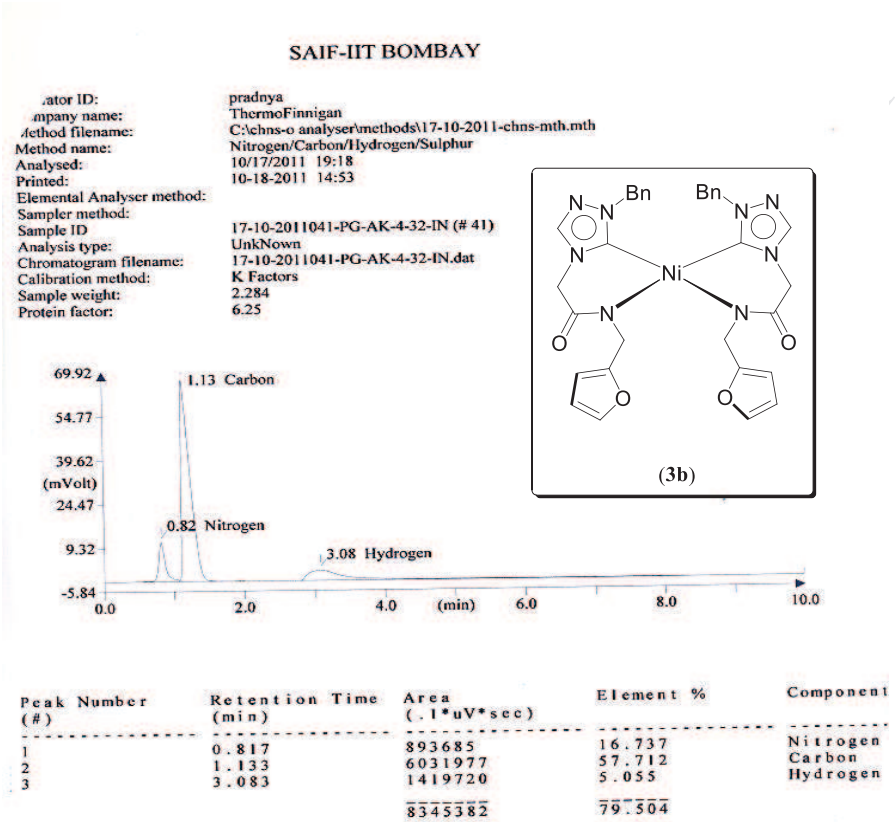

Figure S33. Elemental analysis data of **3b**.

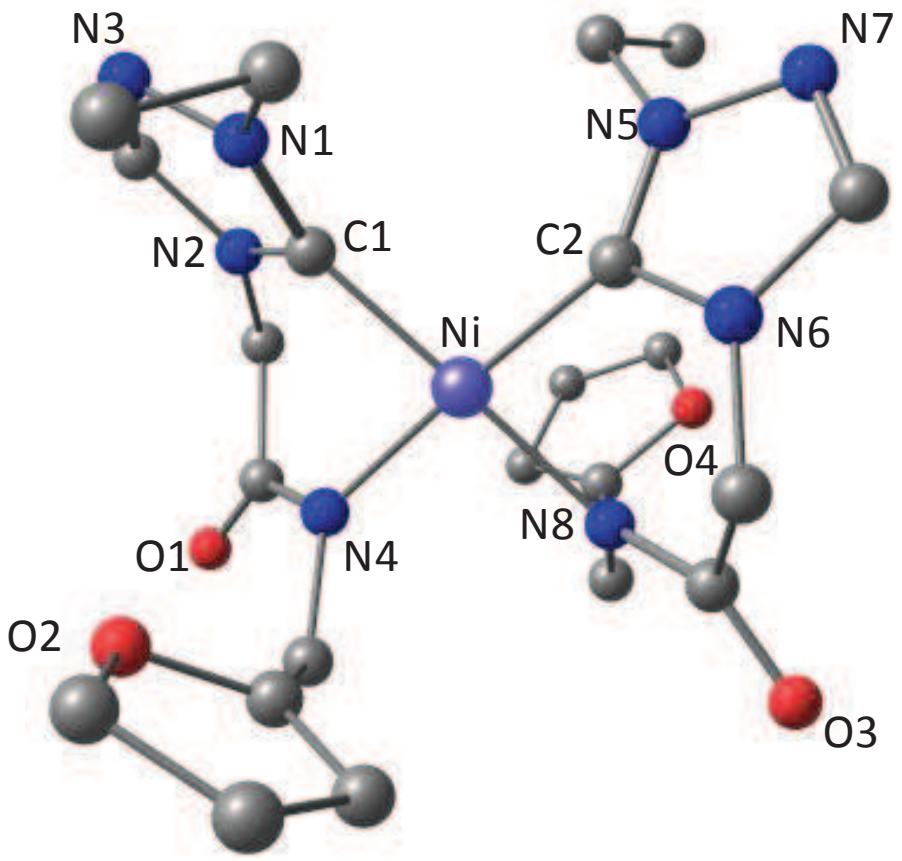

Figure S34. Computed structure of **1b**. Selected bond lengths (Å), bond angles (°); Ni−C1 1.907, Ni−C2 1.908, Ni−N4 1.941, Ni−N8 1.941, C1−N1 1.346, C1−N2 1.364, C2−N5 1.346, C2−N6 1.364, C1−Ni−C2 97.1, N4−Ni−N8 92.3, C1−Ni−N8 175.8, C2−Ni−N4 175.6.

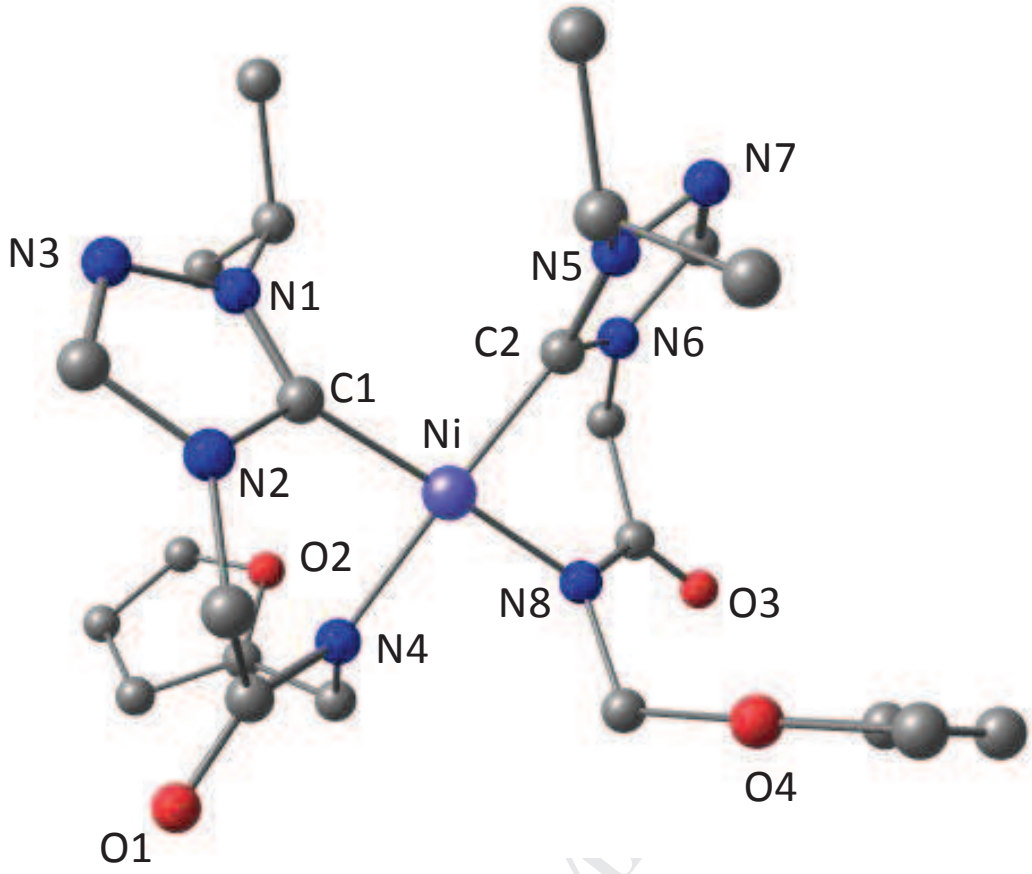

Figure S35. Computed structure of **2b**. Selected bond lengths (Å), bond angles (°); Ni−C1 1.908, Ni−C2 1.909, Ni−N4 1.942, Ni−N8 1.942, C1−N1 1.346, C1−N2 1.364, C2−N5 1.347, C2−N6 1.364, C1−Ni−C2 96.3, N4−Ni−N8 92.2, C1−Ni−N8 177.9, C2−Ni−N4 177.9.

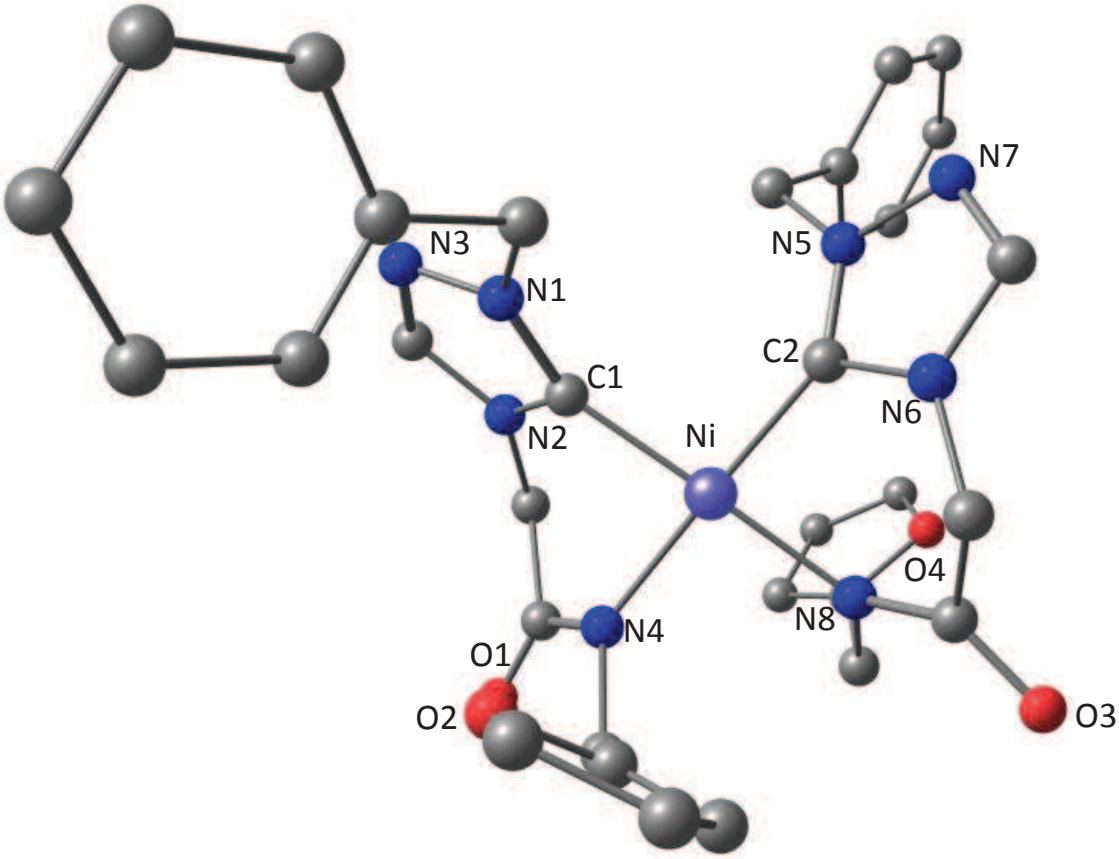

Figure S36. Computed structure of **3b.** Selected bond lengths (Å), bond angles (°); Ni−C1 1.910, Ni−C2 1.911, Ni−N4 1.943, Ni−N8 1.941, C1−N1 1.347, C1−N2 1.363, C2−N5 1.348, C2−N6 1.363, C1−Ni−C2 96.6, N4−Ni−N8 92.5, C1−Ni−N8 174.2, C2−Ni−N4 175.7.

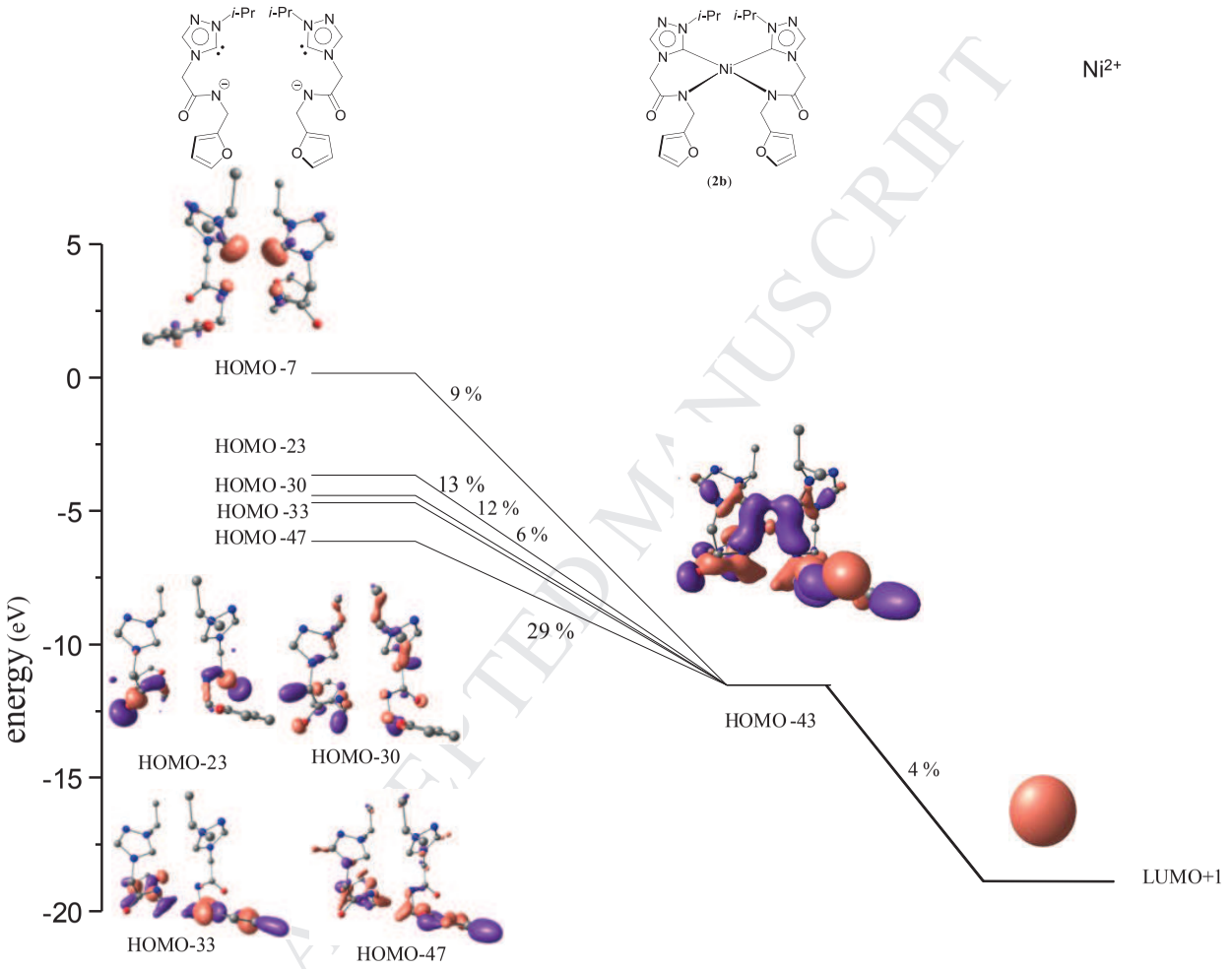

Figure S37. Simplified orbital interaction diagram showing the major contributions of the NHC–Ni bond in **2b**.

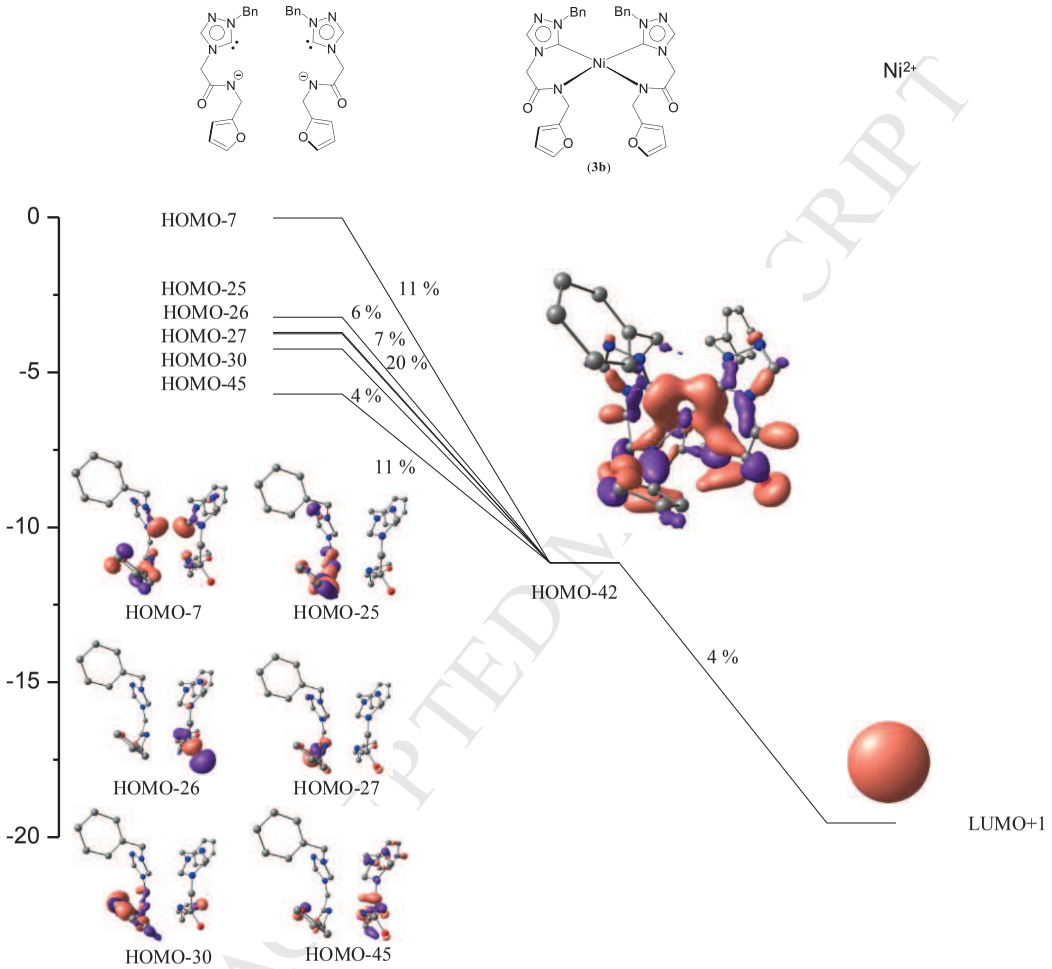

Figure S38. Simplified orbital interaction diagram showing the major contributions of the NHC–Ni bond in **3b**.

Table S1. Natural and Mulliken charge data for **1b,** its NHC ligand fragment and Ni.

specie/compound	Natural charge			Mulliken charge		
	$C_{carbene}$	$-CON^-$	Ni	$C_{carbene}$	$-CON^-$	Ni
Ni^{2+}			2.000			2.000
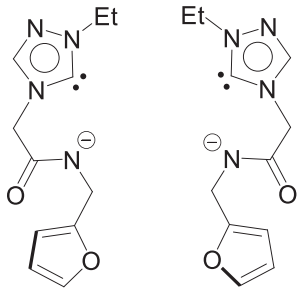	0.224 0.224	-0.639 -0.639		0.228 0.229	-0.397 -0.396	
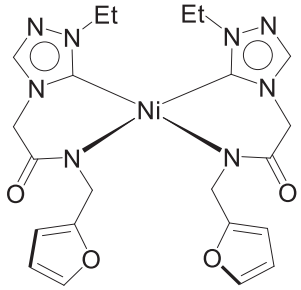 **1b**	0.259 0.259	-0.646 -0.646	0.340	0.342 0.342	-0.495 -0.495	0.133

Table S2. Natural and Mulliken charge data for **2b**, its NHC ligand fragment and Ni.

Compound	Natural charge			Mulliken charge		
	$C_{carbene}$	$-CON^-$	Ni	$C_{carbene}$	$-CON^-$	Ni
Ni^{2+}			2.000			2.000
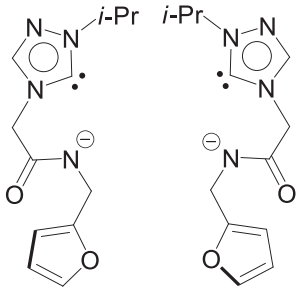	0.224 0.224	-0.629 -0.630		0.228 0.228	-0.393 -0.394	
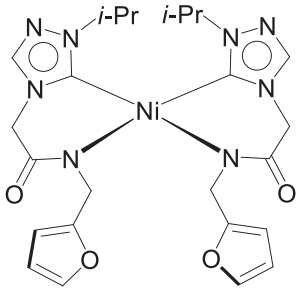	0.261 0.261	-0.648 -0.648	0.335	0.334 0.334	-0.494 -0.495	0.123
2b						

Table S3. Natural and Mulliken charge data for **3b**, its NHC ligand fragment and Ni.

Compound	Natural charge			Mulliken charge		
	$C_{carbene}$	$-CON^-$	Ni	$C_{carbene}$	$-CON^-$	Ni
Ni^{2+}			2.000			2.000
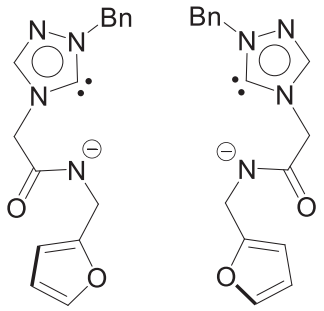	0.225 0.226	-0.638 -0.640		0.228 0.223	-0.400 -0.402	
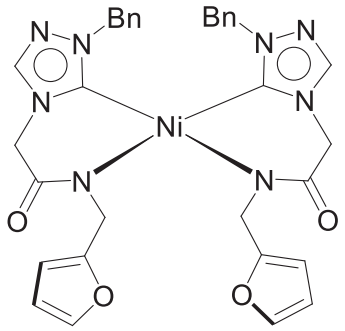 **3b**	0.257 0.257	-0.646 -0.645	0.343	0.332 0.341	-0.496 -0.496	0.148

Table S4. Electronic configuration of Ni^{2+}, **1b**, **2b** and **3b**.

compounds	*4s*	*3d*	*5p*
Ni^{2+}	0.00	8.00	0.00
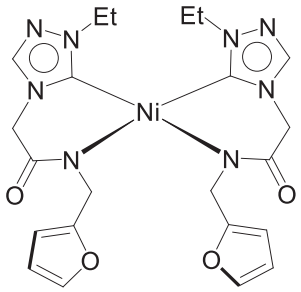 **1b**	0.38	8.89	0.01
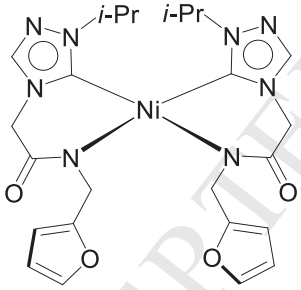 **2b**	0.39	8.89	0.01
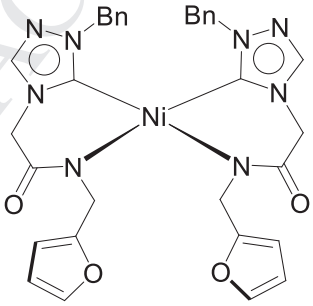 **3b**	0.38	8.89	0.01

Table S5. Hybrid Orbitals of (**1**–**3**)**b**.

specie/compound	hybrid orbitals of $C_{carbene}$–Ni bond	$C_{carbene}$ *s* (%)	$C_{carbene}$ *p* (%)	Ni *s* (%)	Ni *p*(%)	Ni *d* (%)
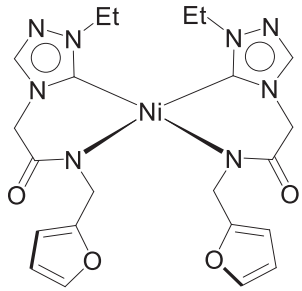 **1b**	[C($sp^{1.37}$)Ni($sp^{2.09}d^{0.99}$)]	42.11	57.89	24.48	51.23	24.29
	[C($sp^{1.37}$)Ni($sp^{2.10}d^{0.99}$)]	42.11	57.89	24.46	51.23	24.30
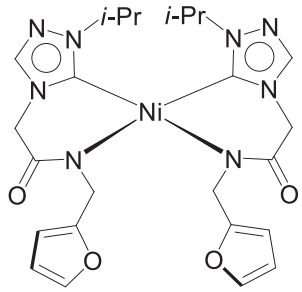 **2b**	[C($sp^{1.39}$)Ni($sp^{2.10}d^{1.00}$)]	41.81	58.18	24.38	51.17	24.44
	[C($sp^{1.39}$)Ni($sp^{2.10}d^{1.00}$)]	41.81	58.18	24.38	51.15	24.47
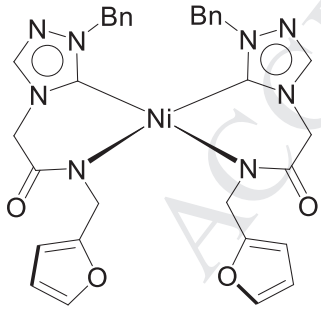 **3b**	[C($sp^{1.37}$)Ni($sp^{1.90}d^{0.85}$)]	42.17	57.82	26.69	50.64	22.67
	[C($sp^{1.38}$)Ni($sp^{1.92}d^{0.85}$)]	42.02	57.98	26.53	50.87	22.60

Table S6. Charge decomposition analysis (CDA) of (**1**–**3**)**b** results showing the [NHC]→[Ni] fragment σ-donation (*d*), the [NHC]←[Ni] fragment π-back donation (*b*), *d*/*b* ratio and the [NHC]→[Ni] repulsive polarization (*r*) for the complexes.

Complex	2[NHC]$^{-}$→[Ni] (*d*)	2[NHC]$^{-}$←[Ni] (*b*)	*d*/*b* ratio	Repulsive polarization (*r*)
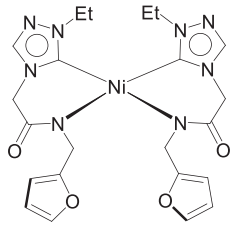 **1b**	0.657	0.060	10.95	0.026
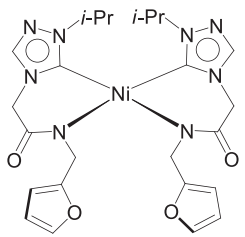 **2b**	0.644	0.057	11.30	0.049
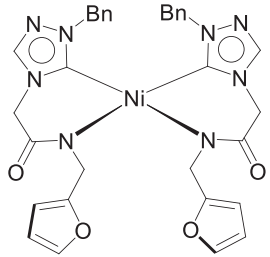 **3b**	0.644	0.059	11.25	0.025

Table S7. B3LYP/6-31G*, LANL2DZ level optimized coordinates of **1b**.

Ground state electronic energy =-1762.1629142 Hartree/Particle.

Ni	6.615628000	8.324206000	3.135501000
O	5.610616000	4.889824000	5.114982000
O	9.468045000	6.888036000	5.381643000
O	8.581309000	7.276072000	-0.290246000
O	4.212487000	7.484412000	0.225537000
N	6.446842000	10.039648000	5.643320000
N	5.787852000	10.033404000	6.851905000
N	5.170397000	8.344542000	5.570067000
N	6.738727000	6.611913000	4.041305000
N	5.842891000	11.069519000	2.070132000
N	6.314119000	11.989456000	1.160757000
N	7.658860000	10.247028000	1.339675000
N	7.024254000	7.529600000	1.412721000
C	6.103945000	9.016931000	4.837542000
C	5.019848000	8.981672000	6.772098000
H	4.345282000	8.652686000	7.548973000
C	7.474901000	11.058785000	5.425471000
H	7.012417000	12.032319000	5.615924000
H	7.746161000	11.002471000	4.370756000
C	8.693629000	10.847355000	6.322131000
H	8.403783000	10.866780000	7.376624000
H	9.420199000	11.648226000	6.147256000
H	9.173703000	9.888199000	6.104547000
C	4.615809000	7.054802000	5.147858000
H	3.930342000	7.212477000	4.309109000
H	4.066990000	6.621673000	5.984495000
C	5.738661000	6.066377000	4.750664000
C	7.918927000	5.765688000	3.844712000
H	7.972749000	5.377515000	2.821309000
H	7.824926000	4.900043000	4.511609000
C	9.206048000	6.479071000	4.099405000
C	10.269038000	6.788211000	3.297048000
H	10.340247000	6.578095000	2.237928000
C	11.246835000	7.426961000	4.131672000
H	12.220348000	7.796684000	3.839677000
C	10.707805000	7.460389000	5.381615000
H	11.059652000	7.816063000	6.338424000
C	6.632149000	9.986602000	2.198781000
C	7.422759000	11.450915000	0.732643000
H	8.077870000	11.894517000	-0.002772000
C	4.538709000	11.317591000	2.687216000
H	4.577794000	12.312075000	3.142598000
H	4.426316000	10.575627000	3.478577000
C	3.397994000	11.224180000	1.675244000
H	3.541575000	11.945689000	0.865882000

H	2.447701000	11.445292000	2.173083000
H	3.341690000	10.218592000	1.247435000
C	8.695546000	9.257829000	1.029789000
H	9.361674000	9.150110000	1.891690000
H	9.269785000	9.611861000	0.173197000
C	8.069985000	7.892469000	0.654136000
C	6.272214000	6.361655000	0.946586000
H	6.515823000	5.463866000	1.526507000
H	6.572265000	6.161935000	-0.089381000
C	4.792083000	6.539259000	1.033098000
C	3.821002000	5.890757000	1.743768000
H	3.988915000	5.096266000	2.458918000
C	2.566009000	6.468883000	1.354736000
H	1.579625000	6.195865000	1.704323000
C	2.864297000	7.427284000	0.434770000
H	2.269412000	8.109070000	-0.154300000

Table S8. B3LYP/6-31G*, LANL2DZ level optimized coordinates of **2b**.

Ground state electronic energy =-1840.7924673 Hartree/Particle.

Ni	7.191189000	6.791227000	0.133428000
O	9.778939000	6.752433000	3.335727000
O	7.591890000	3.170954000	1.629734000
O	8.722956000	5.192387000	-3.337491000
O	9.751144000	9.242077000	-1.571140000
N	4.843618000	6.914459000	2.045013000
N	6.601885000	7.928565000	2.676696000
N	4.562559000	7.371995000	3.312788000
N	8.525208000	6.274214000	1.446882000
N	5.188960000	8.378965000	-1.493813000
N	5.699992000	6.466886000	-2.269050000
N	4.529519000	8.288471000	-2.699048000
N	8.356768000	6.319543000	-1.346255000
C	6.087532000	7.221083000	1.630515000
C	5.658365000	7.983714000	3.667555000
H	5.808442000	8.476601000	4.616970000
C	3.881011000	6.004031000	1.392032000
H	4.229817000	5.934938000	0.358728000
C	3.957017000	4.619505000	2.046614000
H	4.971858000	4.214169000	1.990519000
H	3.277113000	3.930625000	1.533431000
H	3.660601000	4.676724000	3.098977000
C	2.470572000	6.595111000	1.424505000
H	2.121117000	6.710644000	2.454063000
H	1.783905000	5.925114000	0.897096000
H	2.436387000	7.573841000	0.935684000
C	8.025239000	8.270401000	2.752485000
H	8.240893000	8.654284000	3.749623000

H	8.250665000	9.041359000	2.008868000
C	8.876309000	6.995774000	2.524382000
C	9.219404000	4.979835000	1.332338000
H	10.263894000	5.104097000	1.636727000
H	9.189149000	4.668662000	0.286522000
C	8.612061000	3.909535000	2.182978000
C	8.834244000	3.490318000	3.462579000
H	9.569762000	3.907952000	4.134810000
C	7.904716000	2.428537000	3.719571000
H	7.799926000	1.852604000	4.629040000
C	7.179732000	2.276244000	2.577880000
H	6.390546000	1.603758000	2.276935000
C	5.928822000	7.291465000	-1.207079000
C	4.866546000	7.110004000	-3.144674000
H	4.532061000	6.686893000	-4.080609000
C	5.180812000	9.670583000	-0.777599000
H	5.603752000	9.440020000	0.203376000
C	3.750729000	10.189352000	-0.616973000
H	3.297064000	10.387162000	-1.591967000
H	3.764623000	11.122222000	-0.044156000
H	3.122771000	9.469142000	-0.083068000
C	6.094221000	10.666168000	-1.501992000
H	7.112196000	10.273647000	-1.586016000
H	6.128402000	11.609047000	-0.945165000
H	5.714174000	10.872896000	-2.507725000
C	6.488325000	5.250290000	-2.485720000
H	6.266877000	4.860837000	-3.479414000
H	6.214531000	4.504804000	-1.732412000
C	7.997366000	5.595049000	-2.419114000
C	9.750132000	6.797186000	-1.375174000
H	10.390196000	6.013036000	-1.792857000
H	10.062167000	7.000509000	-0.349071000
C	9.932431000	8.032012000	-2.200205000
C	10.231051000	8.243772000	-3.514890000
H	10.407620000	7.467196000	-4.245101000
C	10.241840000	9.663999000	-3.715480000
H	10.450691000	10.196569000	-4.633387000
C	9.947014000	10.218446000	-2.508048000
H	9.860388000	11.234133000	-2.152397000

Table S9. B3LYP/6-31G*, LANL2DZ level optimized coordinates of **3b**.

Ground state electronic energy =-2145.6187651 Hartree/Particle.

Ni	-0.217899000	0.576260000	12.884264000
C	-2.184900000	2.082601000	15.974939000
H	-3.050806000	2.463308000	15.450058000
O	-1.822302000	1.661775000	9.367438000
O	-4.189654000	1.562038000	12.866267000

O	1.940354000	4.030750000	13.147252000
N	2.117903000	-1.150443000	13.830172000
N	3.492842000	-1.139701000	13.759141000
N	2.600529000	0.604381000	12.737719000
N	0.490937000	2.263223000	13.537248000
N	-1.920366000	1.378145000	12.409318000
N	-2.258878000	-1.383112000	12.783760000
N	-1.654299000	-3.118562000	11.559953000
N	-0.667106000	-2.163631000	11.616757000
C	1.536834000	-0.101161000	13.216363000
C	3.751180000	-0.050474000	13.090721000
H	4.743274000	0.297162000	12.842166000
C	1.465657000	-2.217412000	14.593396000
H	1.644684000	-3.166693000	14.077921000
H	0.395615000	-2.000128000	14.545395000
C	1.951370000	-2.303925000	16.027015000
C	2.303854000	-3.545135000	16.564720000
H	2.261217000	-4.434947000	15.940492000
C	2.715994000	-3.651375000	17.895040000
H	2.987786000	-4.622369000	18.299892000
C	2.790920000	-2.510752000	18.694351000
H	3.120140000	-2.588383000	19.726941000
C	2.447354000	-1.265930000	18.159110000
H	2.512567000	-0.372255000	18.774238000
C	2.024338000	-1.160920000	16.834219000
H	1.754109000	-0.189608000	16.429140000
C	-2.170349000	1.270010000	17.158440000
H	-3.021652000	0.930145000	17.732392000
C	-0.859912000	1.018974000	17.425873000
H	-0.347245000	0.458742000	18.192766000
O	-0.060229000	1.620851000	16.495953000
C	-0.883175000	2.268015000	15.605128000
C	-0.248237000	3.067504000	14.516407000
H	0.449021000	3.800602000	14.941073000
H	-1.050691000	3.648075000	14.043417000
C	1.575123000	2.855164000	13.012936000
C	2.457308000	1.934033000	12.135543000
H	2.027385000	1.834004000	11.133671000
H	3.445527000	2.388245000	12.058419000
C	-0.998642000	-1.086175000	12.356482000
C	-2.613698000	-2.604699000	12.278610000
H	-3.568282000	-3.077153000	12.458324000
C	0.577069000	-2.409105000	10.871045000
H	1.044209000	-3.299629000	11.304153000
H	1.217400000	-1.550058000	11.070039000
C	0.366781000	-2.593583000	9.383440000
C	0.424154000	-1.493824000	8.519359000
H	0.601983000	-0.497023000	8.915339000
C	0.248152000	-1.667461000	7.145737000
H	0.301447000	-0.807106000	6.484283000

C	0.012325000	-2.941071000	6.624497000
H	-0.121023000	-3.076160000	5.554543000
C	-0.048140000	-4.041837000	7.481851000
H	-0.230779000	-5.035539000	7.082134000
C	0.130522000	-3.868328000	8.854475000
H	0.079793000	-4.724707000	9.521398000
C	-1.083770000	1.772766000	8.226447000
H	-1.415130000	1.168497000	7.395775000
C	-0.065613000	2.660021000	8.402958000
H	0.668993000	2.954415000	7.665734000
C	-0.185204000	3.133237000	9.753740000
H	0.435684000	3.864411000	10.254558000
C	-1.267161000	2.499234000	10.299193000
C	-1.950482000	2.614405000	11.621896000
H	-1.466073000	3.439391000	12.153845000
H	-3.001882000	2.891014000	11.478791000
C	-3.106464000	0.961062000	12.879596000
C	-3.093446000	-0.439028000	13.533284000
H	-2.729825000	-0.371365000	14.563579000
H	-4.117117000	-0.814297000	13.539432000

Table S10. Comparison between selected bond distances [Å] and selected bond angles [°] in X-ray structure and computed structure for complex **1b**.

Parameter	Experimental	Calculated	Parameter	Experimental	Calculated
Ni(2)−C(12)	1.859(3)	1.908	N(3) −C(5)	1.463(4)	1.466
Ni(2)−C(1)	1.860(3)	1.908	N(4) −C(6)	1.325(3)	1.342
Ni(2)−N(8)	1.9211(18)	1.941	N(5)−C(13)	1.334(4)	1.346
Ni(2) −N(4)	1.922(2)	1.941	N(5) −N(6)	1.460(4)	1.377
N(1) −C(1)	1.332(4)	1.346	N(5) −C(14)	1.469(3)	1.464
N(1) −N(2)	1.376(3)	1.378	N(6) −C(13)	1.295(5)	1.305
N(1) −C(3)	1.459(4)	1.464	N(7) −C(16)	1.466(4)	1.466
N(2) −C(2)	1.299(4)	1.305	N(7) −C(12)	1.360(3)	1.364
N(3) −C(2)	1.359(3)	1.369	N(7) −C(13)	1.363(4)	1.369
N(3) −C(1)	1.366(3)	1.364	N(8) −C(17)	1.322(4)	1.342
C(12)−Ni(2)−C(1)	94.64(11)	97.12	N(1)−C(1)−N(2)	103.1(2)	103.14
C(12)−Ni(2)−N(8)	85.82(10)	85.36	N(1)−C(1)−Ni(2)	137.5(2)	137.86
C(1)−Ni(2)−N(8)	174.229(11)	85.47	N(3)−C(1)−Ni(2)	119.32(19)	118.93
C(12)−Ni(2)−N(4)	175.26(11)	175.59	C(6)−N(4)−Ni(2)	124.72(18)	123.92
C(1)−Ni(2)−N(4)	87.54(10)	85.47	C(12)−N(5)−N(6)	113.2(3)	113.58
N(8)−Ni(2)−N(4)	92.43(9)	92.28	C(12)−N(5)−C(14)	128.8(3)	128.20
C(1)−N(1)−N(2)	113.6(2)	113.58	N(6)−N(5)−C(14)	118.0(3)	118.04
C(1)−N(1)−C(3)	128.8(2)	128.21	C(12)−N(7)−C(13)	108.9(3)	108.51
C(1)−N(3)−C(2)	108.6(2)	108.51	C(17)−N(8)−Ni(2)	124.9(2)	123.72
C(1)−N(3)−C(5)	123.2(2)	122.55	C(18)−N(8)−Ni(2)	118.79(18)	120.05

Table S11. Comparison between selected bond distances [Å] and selected bond angles [°] in X-ray structure and computed structure for complex **2b**.

Parameter	Experimental	Calculated	Parameter	Experimental	Calculated
Ni(1)−C(13)	1.853(2)	1.908	N(3)−C(2)	1.291(3)	1.304
Ni(1)−C(1)	1.853(2)	1.909	N(4)−C(7)	1.327(3)	1.343
Ni(1)−N(8)	1.9211(18)	1.942	N(5)−C(13)	1.333(3)	1.346
Ni(1)−N(4)	1.9260(18)	1.942	N(5)−N(7)	1.382(3)	1.377
N(1)−C(1)	1.335(3)	1.346	N(5)−C(15)	1.469(3)	1.477
N(1)−N(3)	1.387(3)	1.377	N(6)−C(13)	1.350(3)	1.364
N(1)−C(3)	1.470(3)	1.477	N(6)−C(14)	1.366(3)	1.369
N(2)−C(1)	1.354(3)	1.364	N(6)−C(18)	1.457(3)	1.466
N(2)−C(2)	1.359(3)	1.370	N(7)−C(14)	1.291(3)	1.369
N(2)−C(6)	1.452(3)	1.466	N(8)−C(19)	1.318(3)	1.344
C(13)−Ni(1)−C(1)	92.83(8)	96.28	N(1)−C(1)−N(2)	104.06(17)	103.32
C(13)−Ni(1)−N(8)	86.21(9)	85.79	N(1)−C(1)−Ni(1)	135.16(17)	136.47
C(1)−Ni(1)−N(8)	175.96(9)	177.90	N(2)−C(1)−Ni(1)	120.69(15)	119.97
C(13)−Ni(1)−N(4)	175.28(10)	177.93	C(7)−N(4)−Ni(1)	122.34(16)	125.37
C(1)−Ni(1)−N(4)	86.67(8)	85.80	C(13)−N(5)−N(7)	112.52(19)	113.35
N(8)−Ni(1)−N(4)	94.61(7)	92.20	C(13)−N(5)−C(15)	128.13(19)	127.32
C(1)−N(1)−N(3)	112.45(18)	113.36	N(7)−N(5)−C(15)	118.99(19)	118.61
C(1)−N(1)−C(3)	126.99(18)	127.32	C(13)−N(6)−C(14)	108.6(2)	108.43
C(1)−N(2)−C(2)	108.24((18)	108.43	C(19)−N(8)−Ni(1)	124.22(15)	125.38
C(1)−N(2)−C(6)	121.55(18)	121.78	C(20)−N(8)−Ni(1)	121.63(15)	120.33

Table S12. Comparison between selected bond distances [Å] and selected bond angles [°] in X-ray structure and computed structure for complex **3b**.

Parameter	Experimental	Calculated	Parameter	Experimental	Calculated
Ni(1)−C(17)	1.871(4)	1.911	N(3)−C(1)	1.358(5)	1.363
Ni(1)−C(1)	1.871(4)	1.910	N(4)−C(15)	1.342(5)	1.344
Ni(1)−N(4)	1.927(3)	1.942	N(8)−C(17)	1.343(3)	1.348
Ni(1)−N(5)	1.931(3)	1.937	N(8)−N(7)	1.380(4)	1.376
N(1)−C(1)	1.343(5)	1.348	N(8)−C(19)	1.463(5)	1.467
N(1)−N(2)	1.370(4)	1.377	N(6)−C(18)	1.368(5)	1.370
N(1)−C(3)	1.469(5)	1.465	N(6)−C(17)	1.364(4)	1.363
N(2)−C(2)	1.314(5)	1.304	N(7)−C(18)	1.308(3)	1.304
N(3)−C(2)	1.377(5)	1.370	N(6)−C(32)	1.469(5)	1.466
N(3)−C(16)	1.462(5)	1.467	N(5)−C(30)	1.469(5)	1.472
C(17)−Ni(1)−C(1)	94.40(15)	96.11	N(1)−C(1)−N(3)	103.6(3)	103.07
C(17)−Ni(1)−N(5)	88.09(14)	86.20	N(1)−C(1)−Ni(1)	137.8(3)	138.08
C(1)−Ni(1)−N(5)	175.22(15)	175.30	N(3)−C(1)−Ni(1)	118.6(3)	118.85
C(17)−Ni(1)−N(4)	175.66(15)	176.04	C(15)−N(4)−Ni(1)	124.2(3)	124.73
C(1)−Ni(1)−N(4)	86.25(14)	85.62	C(17)−N(8)−N(7)	113.5(3)	113.65
N(5)−Ni(1)−N(4)	91.57(13)	92.34	C(17)−N(8)−C(19)	128.8(3)	128.02
C(1)−N(1)−N(2)	113.9(3)	113.65	N(7)−N(8)−C(19)	116.9(3)	118.11
C(1)−N(1)−C(3)	128.7(3)	108.53	C(17)−N(6)−C(32)	124.0(3)	122.80
C(1)−N(3)−C(2)	108.3(3)	122.45	C(31)−N(5)−Ni(1)	125.1(2)	125.13
C(1)−N(3)−C(16)	122.7(3)	122.45	C(30)−N(5)−Ni(1)	120.3(2)	120.30